Mononuclear and Multinuclear Salicylaldimine Metal Complexes as Catalysts Precursors in the Oxidation of Phenol and Cyclohexene

Juanita Lizélle van Wyk

A dissertation submitted in partial fulfilment of the requirement for the degree
Doctor of Philosophy

Department of Chemistry,

University of the Western Cape,

Supervisor: S. F. Mapolie

ABSTRACT

In this thesis typical homogeneous and dendritic immobilized catalysts derived from salicylaldimines were investigated as catalysts for the oxidation of hydrocarbons using hydrogen peroxide as oxidant under aerobic conditions. This research work thus describes the synthesis of several new *N*-(aryl)salicylaldimines as well as peripheral functionalised salicylaldimine poly(propyleneimine) dendrimers. The dendritic ligands were obtained by modifying the peripheral groups of Generation 1 and Generation 2 poly(propyleneimine) dendrimer, (DAB-$(NH_2)_n$) which are commercially available. Both types of ligands were utilized to synthesize Cu(II) and Co(II) complexes using appropriate acetate salts. The ligands systems and metal complexes prepared were fully characterized using a range of physical techniques.
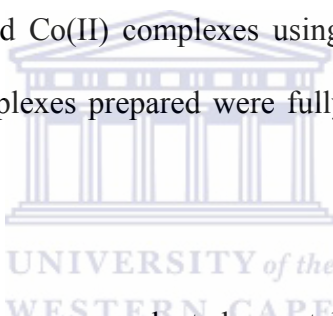
The Cu(II) and Co(II) complexes were evaluated as catalysts for the oxidation of phenol and cyclohexene using hydrogen peroxide as oxidant under an oxygen atmosphere. The catalytic oxidation of phenol to the dihydroxybenzenes, catechol (CT) and hydroquinone (HQ), was investigated in aqueous media at various pH values. All the complexes investigated were active for the hydroxylation process producing CT as major product. The pH of the reaction medium was found to have much more of an influence on the activity and product selectivity of the Co(II) complexes as compared to the case for the Cu(II) complexes.

All the catalysts investigated were also found to exhibit good activity for the oxidation of cyclohexene producing predominantly the allylic oxidation products 2-cyclohexene-1-one

and 2-cyclohexene-1-ol. However the formation of the epoxide, cyclohexene oxide was also observed as minor product or in trace quantities. It was found that the cobalt catalysts produced 2-cyclohexene-1-one as major product, however higher levels of 2-cyclohexene-1-ol was produced by all catalysts in catalytic runs where the oxidant to substrate ratio was reduced and when the metal loading was increased. In the case of the copper catalysts 2-cyclohexene-1-ol was produce in slightly higher levels than 2-cyclohexene-1-one.

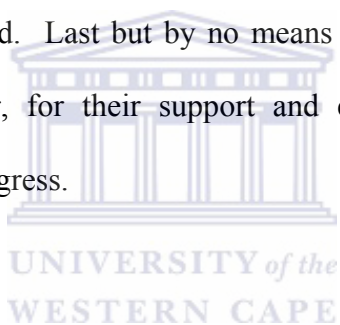UNIVERSITY of the
WESTERN CAPE

DECLARATION

I declare that the thesis "*Mononuclear and multinuclear salicylaldimine metal complexes as catalysts precursors in the oxidation of phenol and cyclohexene*" is my own work, that it has not been submitted before for any degree or examination in any other university, and that all the sources I have used or quoted have been indicated and acknowledged as complete references.

....

Juanita L. van Wyk

ACKNOWLEDGEMENTS

PUBLICATIONS

JOURNAL ARTICLES:

J. L. van Wyk, S. Mapolie, A. Lennartson, M. Håkansson and S. Jagner
The Synthesis of Copper(II) Salicylaldiminato Complexes and their Catalytic Activity in the Hydroxylation of Phenol
Z. Naturforsch **2007**, *62b*, 331.

J. L. van Wyk, S. Mapolie, A. Lennartson, M. Håkansson and S. Jagner
The Catalytic Oxidation of Phenol in Aqueous Media Using Cobalt(II) Complexes Derived from N-(Aryl)salicylaldimines
Inorganica Chimica Acta **2008***, 361,* 2094.

J. Martinovic, A. Chiorcea-Paquim, V. C. Diculescu, J. van Wyk, E. Iwuoha, P. Baker, S. Mapolie, A. Oliveira-Brett
Metallo-Functionalized First Generation Salicylaldimine Poly(Propyleneimine) Tetraamine Dendrimers: Electrochemical Study and Atomic Force Microscopy Imaging
Electrochimica Acta **2008***, 53,* 4907.

CONFERENCE CONTRIBUTIONS:

J. L. van Wyk and S. F. Mapolie
Preparation and Characterization of Some Salicylaldimine Metal Complexes and a Preliminary Evaluation as Catalyst Precursors
37th Convention of the South African Chemical Institute
Pretoria, South Africa, 2004

J. L. van Wyk and S. F. Mapolie

Preparation and Characterization of Some Salicylaldimine Metal Complexes and a Preliminary Evaluation as Catalyst Precursors

Cape Organometallic Symposium, Cape Town, South Africa, 2004

J. L. van Wyk and S. F. Mapolie

(p-Cymene) Ruthenium(II) Salicylaldiminato Complexes as Catalyst Precursors in Transfer Hydrogenation of Acetophenone

CATSA Catalysis Conference, Potchefstroom, South Africa, 2004

J. L. van Wyk and S. F. Mapolie

The Synthesis of Copper(II) Complexes Derived from Mono- and Multifunctional Salicylaldimines

SACI Inorganic, Pietermarizburg, South Africa, 2005

S. F. Mapolie, G. S. Smith, S. Ray, S.O. Ojwach, J. L. Van Wyk, and R. Malgas,

Catalyst Precursors Based on Peripherally Modified Dendrimeric Ligands

SACI Inorganic, Pietermarizburg, South Africa, 2005

S F. Mapolie, G S. Smith, S. Ray, S. Ojwach, J. L. Van Wyk and R. Malgas

Salicylaldimine Functionalized Dendrimers as Synthons for Catalytic Complexes.

XVI th FECHEM Conference on Organometallic Chemistry, Budapest, September 2005

J. L. van Wyk and S. F. Mapolie

The Hydroxylation of Phenol Using Copper(II) Complexes Derived from Both Mono- and Multi-Functional Salicylaldimines

Cape Organometallic Symposium, Cape Town, South Africa, 2005

J. L. van Wyk and S. F. Mapolie

The Catalytic Oxidation of Phenol Using Copper(II) Complexes Derived from both Mono- and Multifunctional Salicylaldimines

CATSA Catalysis Conference, Midrand, South Africa, 2005

J. L. van Wyk and S. F. Mapolie

Phenol Oxidation Mediated by Catalysts Based on Mono- and Multinuclear Salicylaldimine Copper(II) Complexes

Cape Organometallic Symposium: Organometallics and their Applications Cape Town, South Africa, 2006

J. L. van Wyk and S. F. Mapolie

The Synthesis of Mono- and Multinuclear Salicylaldimine Copper(II) and Cobalt(II) Complexes

37th International Conference on Coordination Chemistry, Cape Town, South Africa, 2006

J. L. van Wyk and S. F. Mapolie

Phenol Oxidation Mediated by Catalysts Based on Mono- and Multinuclear Salicylaldimine Copper(II) Complexes

15th International Symposium on Homogenous Catalysis, Sun City, South Africa, 2006

J. L. van Wyk and S. F. Mapolie

Phenol Oxidation Mediated by Catalysts Based on Mono- and Multinuclear Salicylaldimine Metal Complexes

SACI Inorganic, Langebaan, South Africa, 2007

TABLE OF CONTENT

LIST OF FIGURES

Chapter 1

Chapter 2

Chapter 3

Chapter 4

Chapter 5

UNIVERSITY *of the*
WESTERN CAPE

LIST OF SCHEMES

Chapter 1

Chapter 2

Chapter 3

Chapter 4

Chapter 5

LIST OF TABLES

Chapter 4

Chapter 5

ABBREVIATIONS

°	degrees
Å	Ångstrom
atm	atmosphere
AIBN	azobisisobutyronitrile
BQ	benzoquinone
br	broad
calcd.	calculated
COD	cyclooctadiene
CT	catechol
CWAO	catalytic wet air oxidation
°C	degrees Celsius
δ	chemical shift
d	doublet
dd	doublet of doublets
DFT	density functional theory
DIPEA	N,N-diisopropylethylamine
DMF	dimethylformamide
DMAP	4-dimethylaminopyridine
ESI-MS	electrospray ionization mass spectrometry
eV	electron volt
FT-IR	fourier transform infrared spectroscopy
g	gram(s)
GC	gas chromatography
GC-MS	gas chromatography mass spectroscopy
h	hour(s)
HPLC	high performance liquid chromatography
HQ	hydroquinone
Hz	hertz
i-Pr	isopropyl

IR	infrared
J	coupling constant
m	multiplet
mp	melting point
m/z	mass to charge ratio
MAO	methylaluminoxane
MHz	megahertz
min	minute(s)
ml	millilitres
mmol	millimoles
M_n	number average molecular weight.
NMR	nuclear magnetic resonance
nd	not determinded
OTs	tosyl
PDI	polydispersity index
pH	hydrogen ion concentration in aqueous solution
PhOH	phenol
ppm	parts per million
s	singlet
sh	shoulder
t	triplet
t-Bu	tertiary-butyl
TGA	thermogravimetric analysis
THF	tetrahydrofuran
TOF	turn over frequency
UV-Vis	ultraviolet-visible
w/w	weight per weight

CHAPTER 1

LITERATURE REVIEW: SALICYLALDIMINE METAL COMPLEXES AS HOMOGENEOUS AND HETEROGENISED CATALYSTS

CONTENT

1.1 INTRODUCTION

Catalysis is a key factor in the development of industrial chemical processes, which are environmentally and economically sustainable. As a result there has been intensive research by academia and industry to develop catalyst technologies which can be utilized for sustainable and *green* chemical processes. Various parameters such as atom economy (a parameter of the synthetic efficiency), *E* factor (defined as the ratio of by-product to product (kg/kg) produced) and *'The Twelve Principles of Green Chemistry'* have been introduced in order to evaluate the sustainability of an industrial process [1, 2]. The desire to develop catalysts which meet the requirements of the above mentioned parameters has pushed heterogeneous catalysis to the fore front. The primary reason for this is the ease of separation of the catalyst from the products which allows for catalyst recycling. Homogeneous catalysts also already possess several qualities, which meet the requirement for achieving this goal. These qualities include good selectivity, high activity and the requirement of mild process conditions. Since homogeneous catalysts typically consist of transition metal complexes, the molecular structures are known, which allow for the fine-tuning of the catalysts for process optimization. However industrial implementation of homogeneous catalysts has been hampered by the difficulty in catalyst-product separation and thus also catalyst recycling. Nevertheless several industrial processes have been developed which utilizes homogeneous catalysts, however the catalysts are used in very low concentrations thus eliminating the need to recover the catalyst from the product stream [3].

In recent times the problem of catalyst-product separation for homogeneous catalysts have been circumvented by utilizing novel strategies such as the liquid-liquid biphasic system employed by Ruhrchemie/Rhône-Poulenc for the hydroformylation of olefins.

In this process a water soluble catalyst which is retained in the aqueous phase is used, while the products and reactants are retained in an organic solvent system. Recovery of the catalyst is thus achieved by separation of the two solvent phases [4]. This method serves as a means of '*immobilizing*' the homogeneous catalyst since the catalyst is retained in the aqueous layer of the biphasic system. However successful implementation of aqueous-organic biphasic systems requires suitable water soluble catalysts. There have thus been extensive investigations conducted into designing suitable ligands for water soluble catalysis [5].

Table 1.1: Advantages of homogeneous and heterogeneous catalysts.

Homogeneous catalysts	Heterogeneous catalyst
Good activity	Catalyst-product separation easy
Good selectivity	Recyclable
High atom efficiency	Low quantities of catalyst utilised
Require mild process conditions	High total turnover numbers achieved
Molecular structure of catalysts is known which allows fine-tuning of catalysts	

Various other solvents such as ionic liquids, fluorinated hydrocarbons and supercritical carbon dioxide have also been investigated as suitable systems for multiphase catalysis [6-8]. Phase tag methodologies for multiphase catalysis have also been developed to effect strategic separation and recovery of reagents and catalysts [9]. In addition other strategies have also been developed to facilitate immobilization of transition metal catalysts, which involve the anchoring of the catalyst on an organic or inorganic support. This often requires the incorporation of functional groups onto the ligand of

the metal complex which can facilitate the anchoring of the catalyst onto the support material. Catalyst immobilization serves as a convenient method of heterogenizing homogeneous catalysts thus potentially producing systems which possesses the advantages of both homogeneous and heterogeneous catalysts (Table 1.1) [3].

Various coordination systems have been investigated as suitable immobilized catalysts [10-13]. Among these coordination systems, salicylaldimine metal complexes have been extensively investigated as both homogeneous catalysts and heterogenised catalysts. Salicylaldimines are N,O-donor ligands and the coordination systems based on this class of ligands have been widely investigated [14]. Typical salicylaldimine metal complexes found in literature are of the type **I** and **II** shown in Figure 1.1. However type **II** complexes, which are generally referred to as the salen type complexes, are perhaps the most extensively studied class of salicylaldimine metal complexes. The current significance of salicylaldimine coordination systems is due to the ease of synthesis of the ligand systems and the fact that the properties of the metal complexes are very dependent on the detailed framework structure of the ligand system. This allows for the synthesis of metal complexes of which the steric and electronic properties can readily be controlled. The ease in modifying the ligand backbone allows for the incorporation of various functional groups which in turn facilitate the immobilization of the ligand or metal complex onto supports.

M = metal
B = alkyl, aryl bridging group
X = electon donating, electron withdrawing group
R = alkyl, aryl group
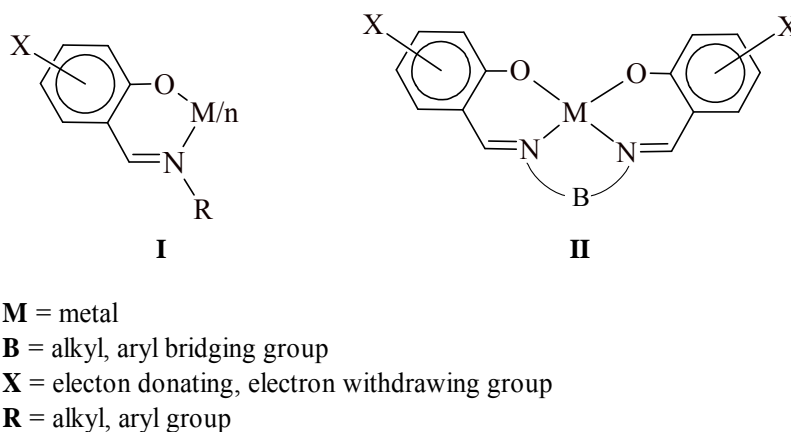
Figure 1.1: *General structures of known salicylaldimine metal complexes.*

The synthesis of new catalysts based on salicylaldimine coordination systems, which potentially allows for the development of *greener* and improved catalytic processes have been demonstrated by a number of research groups. The objective of this chapter is to give a brief survey of some of the work published in recent years in the areas of homogeneous catalysis and immobilized catalyst which are based on salicylaldimine coordination systems.

1.2 SALICYLALDIMINE METAL COMPLEXES IN HOMOGENEOUS CATALYTIC PROCESSES

The most common processes where salicylaldimine metal complexes have been investigated are in the areas of polymerization, asymmetric catalysis and oxidation processes. The synthetic flexibility of the ligand system has played a prominent role in generating interest in these metal complexes for catalytic purposes. There are numerous examples of catalysts within the literature, which show improved activity and enhanced selectivity of the metal complex by simply changing the structural properties of the ligand system. The purpose of this section is to highlight some of the activity

surrounding the development of homogeneous catalysts in the three above mentioned processes.

1.2.1 Polymerization

The dominant catalyst technologies used in industry for the polymerization of α-olefins are those based on Ziegler catalysts and metallocenes. However both these catalysts are limited by the fact that they require activators such as alkylaluminiums, air-free handling and moisture free conditions. Another disadvantage of these catalysts is the requirement of hyper purification of the monomer feed due to the sensitivity of the both the catalyst and activator to heteroatoms. The discovery of late transition metal catalysts which are more tolerant to functional groups because of their less oxophilic nature has represented a major advance in developing catalysts which are more economical. However these systems usually yield dimers and oligomers due to the propensity of the late transition metal alkyl complexes to undergo chain transfer by β-hydride elimination.

Recently a new class of polymerization catalysts was reported by Grubbs et al. [15, 16] which are based on neutral nickel(II) salicylaldiminato complexes. These complexes produced high molecular weight polyethylene under mild conditions with co-catalysts such as $Ni(COD)_2$ and $B(C_6F_5)_3$. The complexes were found to be tolerant to functionalised monomers and also produced high molecular weight polymers in the homopolymerization of ethylene in the presence of polar reagents such as ethers, ethyl acetates, acetone and water [17]. These nickel catalyst were also shown to be active in the copolymerization of ethylene with monomers such as esters, alcohols, anhydrides and amides producing linear functionalised polyethylene in a single step in the absence

of any cocatalyst [18]. These nickel complexes thus potentially provide highly active polymerization catalysts which do not exhibit typical problems associated with industrial olefin polymerization catalysts and would possibly allow access to new polymers.

The complexes synthesised by Grubbs (Fig 1.2) were shown to be strongly affected by the framework structure of the ligand system [15]. It was found that the bulkiness of the ortho-phenoxy substituent (R_1) enhances the catalytic activity of the metal complex and also reduces branching in the polyethylene. In addition the presence of an electron-withdrawing group in the para position (R_2) on the salicylaldiminato ring was shown to enhance catalytic activity of the metal complex.

R_1 = H, t-Bu, Ph, 9-phenanthreyl, 9-anthraceryl
R_2 = H, OMe, NO_2
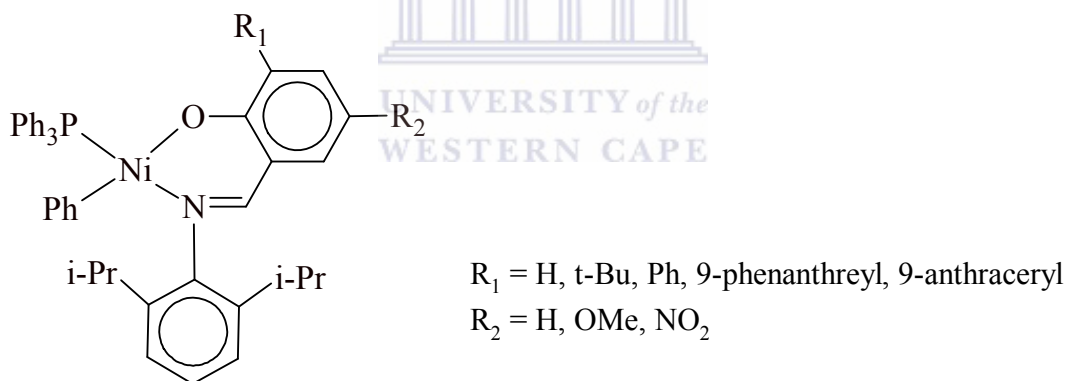
Figure 1.2: *Neutral nickel(II) salicylaldiminato complexes synthesised by Grubbs et al. [15].*

A similar structure activity relationship was observed by Sun et al. for neutral Ni(II) salicylaldiminato complexes (Figure 1.3) which are structurally related to the Grubbs nickel complexes [19]. The polymerization activity of these nickel(II) systems was investigated in the vinyl polymerization of norbornene. The activity of the complexes were shown to be dependent on the electron withdrawing ability of the ring substituents

7

on the salicylaldimine backbone. It was found that complexes containing chlorine substituents on the phenolic aromatic ring were more active than analogues containing iodine. Although there was no clear relationship observed between the steric factors of the ligand environment, it was shown that the naphthyl group directly coordinated to the nickel centre produced a catalyst with higher activity than analogous Grubbs systems containing a phenyl substituent on the nickel atom. However unlike the Grubbs complexes, which did not required a co-catalyst, polymerization was only observed to proceed using methylaluminoxane (MAO) as co-catalyst.
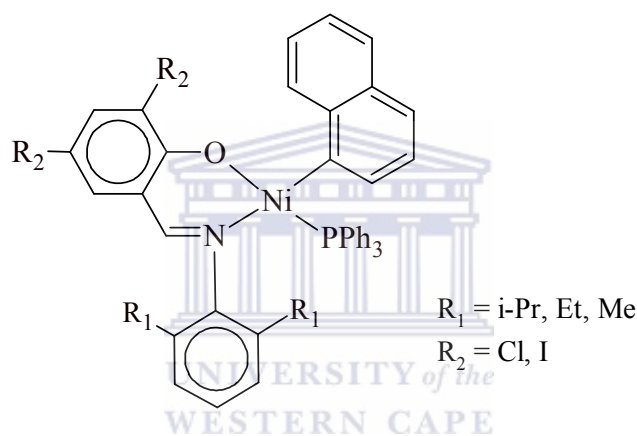
Figure 1.3: Neutral Ni(II) salicylaldiminato complexes synthesised by Sun et al. [19].

The Grubbs systems inspired the development of a number of related nickel complexes based on salicylaldimines such as the novel Ziegler-Natta type Ni(II) catalyst precursors developed by Carlini et al. [20] (Figure 1.4). These systems were shown to be active for the polymerization of ethylene requiring stoichiometric amounts of MAO as co-catalyst. As was the case for the Grubbs catalysts, substituents on the phenolic fragment of the ligand were also shown to have an effect on the activity of the catalysts. It was found that electron-withdrawing substituents on the salicylaldiminato ring gave systems with higher activity. However systems containing electron-withdrawing groups in both the ortho- and para-positions were much more active than mono-substituted complexes.

R = 2,6-diisopropylphenyl, phenyl

$R_1 = R_2 = H$, NO_2, Ph
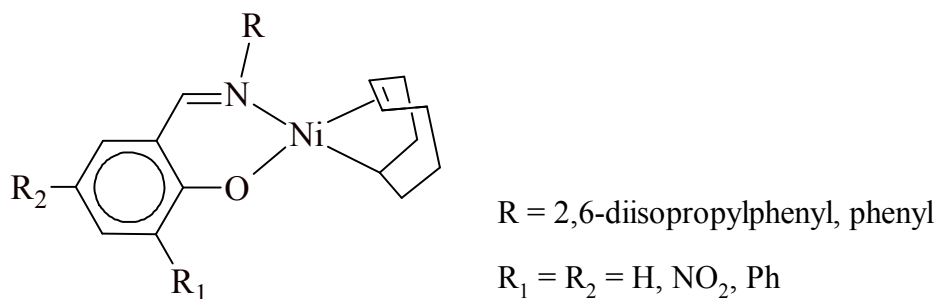
Figure 1.4: *Nickel(II) salicylaldiminato complexes synthesised by Carlini et al. [20].*

A ligand library consisting of various bidentate and tridentate salicylaldimine ligands was recently utilised by Gibson et al. [21] to develop a new class of chromium catalysts (Figure 1.5). The catalysts were developed by screening a ligand library consisting of various salicylaldimine systems which demonstrates the ease in the synthetic method of these Schiff bases. The catalysts developed were shown to be active for the polymerization of ethylene using MAO as co-catalyst. This group found that for the bidentate system with small substituents on the imino nitrogen highly active ethylene polymerization catalyst were obtained which produced high molecular weight polymers. In the same study tridentate systems were also found to be very active, however low molecular weight polymers were obtained [21].
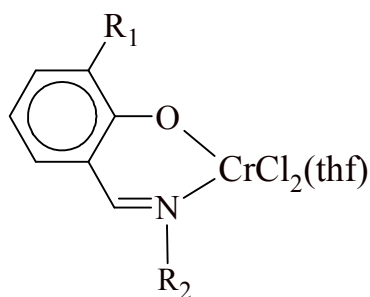
R_1 = Anthracenyl; R_2 = 2,6-(i-Pr)$_2$C$_6$H$_3$, Ph, i-Pr

Figure 1.5: *Bidentate chromium catalysts developed by Gibson et al. [21].*

Efforts by the group of Fujita [22] to develop single site olefin polymerization catalysts have led to the discovery of Group 4 non-metallocence catalyst based on bis(phenoxyimine) ligand systems. These catalysts were shown to have activities comparable or exceeding that of metallocene catalysts in the polymerization of ethylene using MAO as activator. Catalyst containing fluorinated aromatic groups on the imino nitrogen were also shown to behave as living polymerization catalysts. An added advantage of these bidentate phenoxyimine Group 4 catalysts is the fact that stereochemical aspects of the polymers obtained with these catalysts can be controlled [23, 24].
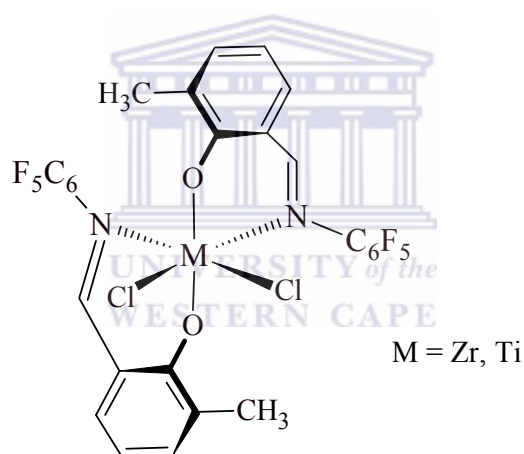
Figure 1.6: *Group four bis(phenoxyimine) metal complexes [22].*

Titanium complexes containing both salicylaldimine and pyrrolylaldimine ligands in the same system have been synthesized by Lancaster et al. [25] (Figure 1.7). These complexes were shown to be very active for the polymerization of ethene producing moderately high molecular weight, high density polyethylene. The properties of the catalysts were found to be intermediate between the properties of complexes which contain either of the two ligands coordinated to Ti.

R = C$_6$H$_5$, C$_6$F$_5$
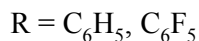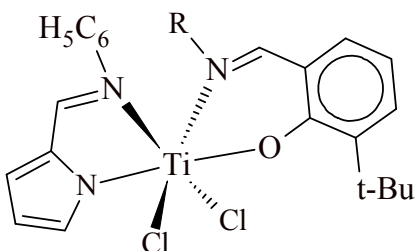
Figure 1.7: Hybrid titanium coordination systems developed by Lancaster et al. for the polymerization of ethene [25].

Bidentate-(salicylaldiminato) neutral palladium(II) complexes have been synthesized by Sen et al. [26] (Figure 1.8). These complexes exhibit moderate activity for the polymerization of methyl acrylate at ambient temperature. The poly(methyl acrylate) obtained had high (M_n>2.11×10^5) to ultrahigh (M_n>1.6×10^6) molecular weight with high polydispersities. However higher polymer yields with narrower PDI's were obtained by decreasing the monomer concentration. In this investigation it was found that polymerization of methyl acrylate operates via a radical rather than a vinyl pathway. However the complexes showed no activity for styrene and methyl methacrylate polymerization, which are known to operate via a radical mechanism. The complexes were also found to be inactive for the polymerization of non-polar monomers such as ethene, propene and norbornene. Inactivity was ascribed to the failure of the imine to dissociate since CO insertion was shown to proceed without dissociation of the imine. This hypothesis was supported by mechanistic studies which consisted of NMR studies which probed the insertion of [13]CO into the Pd-Me bond. These studies showed insertion of CO into the Pd-Me bond to proceed via a five coordinate intermediate thus indicating that imine dissociation does not occur.
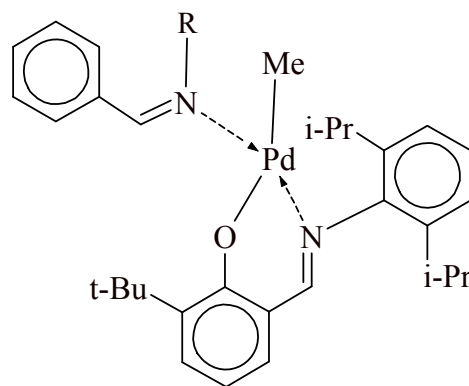
R = CH$_3$, n-Pr, t-Bu, Ph, Benzyl

Figure 1.8: Neutral palladium catalyst synthesised by Sen et al. investigated in the polymerization of methyl acrylate [26].

1.2.2 Oxidation

The coordination sphere of tetradentate salicylaldimine metal complexes resembles those of porphyrins and phthalocyanines. These two latter coordination systems have been extensively utilized as model compounds to study oxygen binding of peroxidases, which are enzymes capable of oxidising various substrates using hydrogen peroxide as oxidant. Due to the similarity of the coordination sphere of salicylaldimine metal complexes to the two above mentioned coordination systems, they have also been extensively employed as model compounds to study oxygen binding of enzymes. Over the last couple of years the interest in the application of these complexes as oxidation catalysts has increased significantly as demonstrated by the review of Venkataramanan et al. [27] which discusses the utilization of metal salen complexes in oxidation processes for sulfides, sulfoxides and aromatic amines. One of the most active areas of research both industrially and academically is the development of catalysts which are able to utilise molecular oxygen and hydrogen peroxide as oxidants in various oxidation processes.

M = MnCl
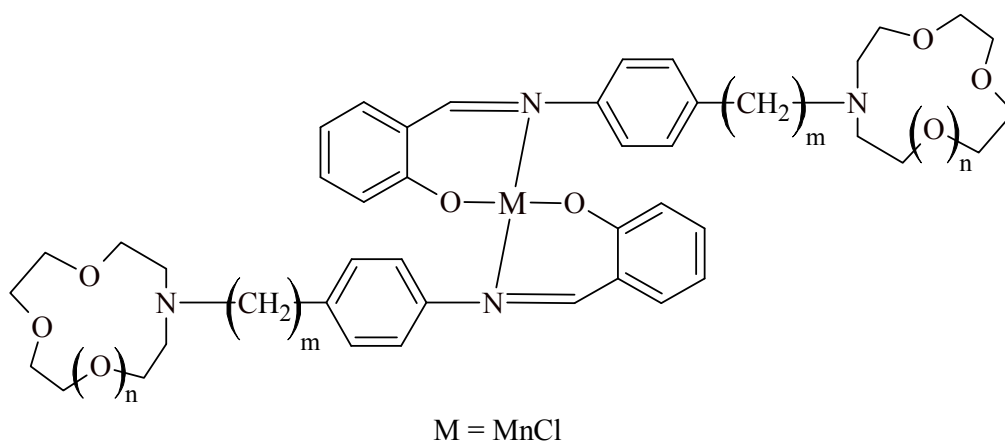
Figure 1.9*: Crown ether functionalised Mn(III) salicylaldimine complexes [28].*

The salicylaldimine framework has been extensively utilized to design catalysts which exhibit enhanced oxygen binding affinities. This was demonstrated by Zeng et al. who synthesised manganese(III) salicylaldimine systems bearing aza crown pendants on the ligand backbone [28] (Figure 1.9). The crown functionalities were shown to significantly improve dioxygen affinities compared to uncrowned analogues. The systems were found to be highly selective for the oxidation of styrene to benzaldehyde. The presence of metal salts such as $NaNO_3$ were shown to improve conversion as well as the TOF of styrene oxidation.

The oxidation of veratryl alcohol using molecular oxygen in aqueous media was investigated by Kervine et al. using salen-type cobalt complexes shown in Figure 1.10 [29]. It was shown that subtituents on the ligand backbone plays an important role in the oxidation process. In all experiments the oxidation occurred exclusively at the benzylic position producing only veratraldehyde. The reaction was also shown to be pH and temperature dependant. In addition catalytic activity was found to be enhanced by increasing the oxygen pressure and by increasing the ratio of catalyst to substrate.
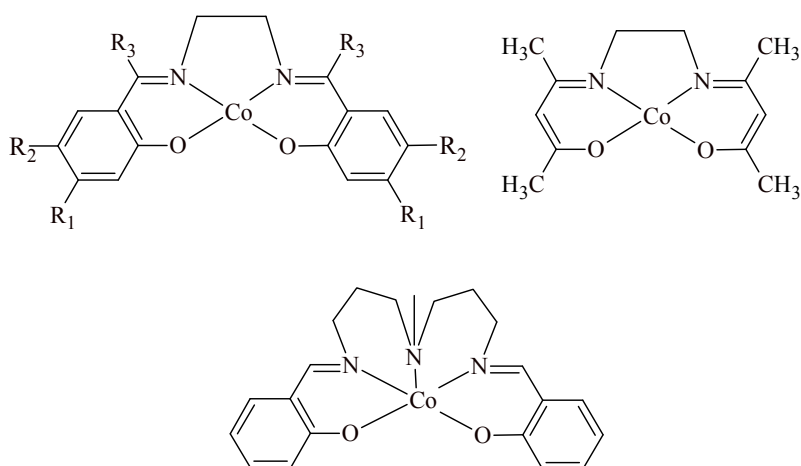
Figure 1.10: *Co(II) salen complexes investigated in the oxidation of veratryl alcohol by Kervine et al. [29].*

Lee et al. investigated the catalytic activity of several manganese(III) catalysts in the oxidation of olefins to the corresponding alcohol using molecular oxygen as oxidant in the presence of NaBH₄ [30]. The systems were found to oxidise only conjugated vinyl arenes with high efficiency. Very low reactivity was observed with non-conjugated vinyl or non vinylic olefins. This phenomenon was investigated by developing several manganese salen systems which were evaluated in the oxidation of *trans*-β-methylstyrene and allyl benzene. Bulky electron rich groups were shown to reduce activity whereas ligands containing electron withdrawing substituents showed comparable, but not better activity than unsubstituted analogues. The oxidation process was also shown to be very regioselective producing only compounds oxidised in the benzylic position with *trans*-β-methylstyrene.
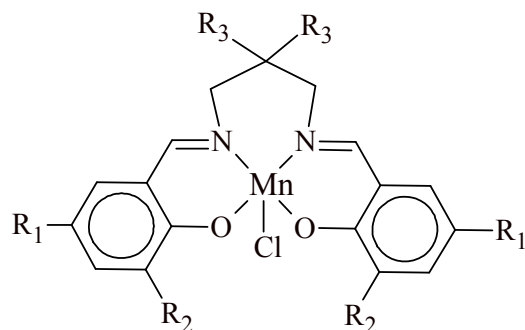
Figure 1.11*: Mn(III) salen complexes investigated by Lee et al. in the oxidation of olefins to alcohols [30].*

1.2.3   Asymmetric catalysis

Over the last decade a wide variety of highly selective asymmetric catalysts based on chiral salen ligand systems have been developed which have been shown to be active catalysts for a range of process, e.g. olefin epoxidation, hydrolytic kinetic resolution (HKR) of epoxides, cyclopropanation, Diels-Alder reactions, cyanohydrin formation, Baeyer-Villiger oxidation, cyclopropanation, etc. Despite a wide variety of accessible structures, the most active catalysts for a variety of asymmetric catalytic processes have often been found to be based on salen ligands of the type shown in Figure 1.12. As a result this ligand is currently commercially available and is industrially synthesised utilizing relatively inexpensive raw materials. The variety of process for which salen metal complexes are active has resulted in the application of these chiral salen complexes in both the pharmaceutical and fine chemical industries [31]. The structural features, mechanistic aspects and applications of salen metal complexes as catalyst for asymmetric transformations have been extensively reviewed [32-34].
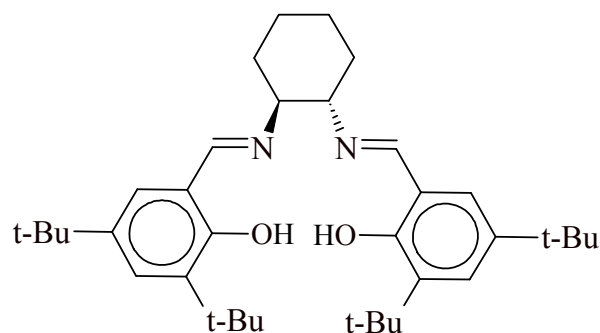
Figure 1.12: *Chiral salen type ligand which has been utilised to synthesise a variety of metal complexes which are active for asymmetric processes [31].*

Jacobsen et al. was the first to report the enantioselective epoxidation of unfunctionalised olefins using salen complex (**i**) (Scheme 1.1) as catalyst [31]. Although a variety of ligand designs and metal centres have been screened, this complex still remains the most selective and efficient catalyst to date for the epoxidation of unfunctionalised olefins. The epoxidation of olefin substrates using catalyst (**i**) is typically conducted in organic solvents using either an aqueous oxidant such as sodium hypochlorite or an organic peracid such as m-chloroperbenzoic acid as shown in Scheme 1.1. Under both conditions the presence of an additive such as 4-phenylpyridine N-oxide (aqueous) or N-methylmorpholine (organic) has a significant effect on the yield, enantioselectivity and catalytic rate of the epoxidation process. The Mn(III) salen complex (**i**) is prone to deactivation due to dimerization during the oxidation process and thus the primary role of the additive is to prevent this catalyst deactivation.
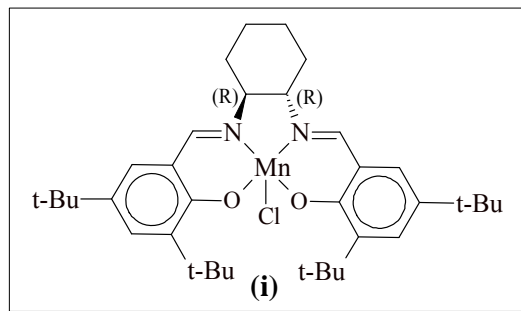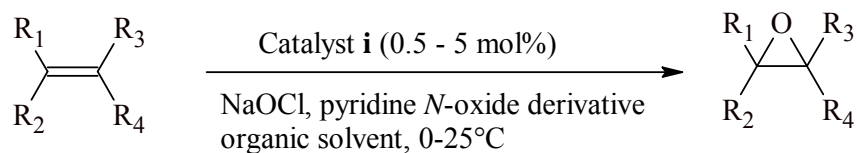
Scheme 1.1: *Epoxidation reaction catalysed by Mn(III) salen complex (**i**).*

Although Mn-salen catalysts are highly active for olefin epoxidation, the requirement of conjugated olefins presents a significant limitation since access to terminal epoxides is not possible. This substrate limitation problem was overcome by the development of hydrolytic kinetic resolution of terminal epoxides. This process utilizes Co-salen complexes such as (**ii**) (Scheme 1.2) and water in the absence of an organic solvent to produce highly enantioselective terminal epoxides and 1,2-diols [31].
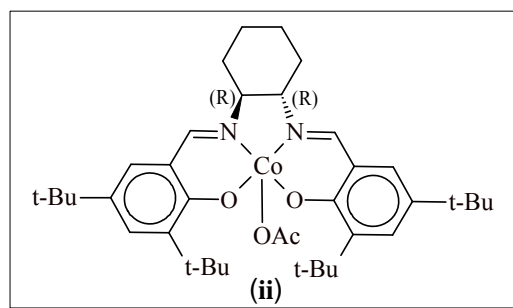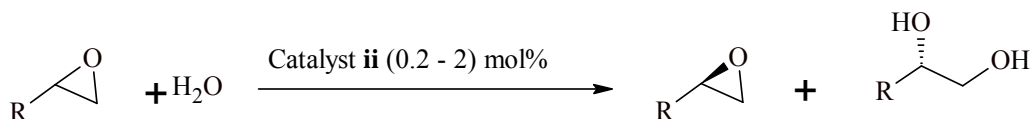
Scheme1.2: *Epoxide ring opening reaction catalysed by Co(II) salen complex (**ii**).*

Following investigations which showed that epoxidation and epoxide ring opening proceeds via two different mechanisms, Jacobsen et al. developed an oligomeric cobalt coordination system (Fig. 1.13) [35, 36]. These coordination systems were designed based on the dual function of the metal centre during the epoxide ring opening mechanism. The cyclic oligomeric complexes displayed dramatically enhanced activities and enantioselectivities compared to the monomeric analogues because the dual function of the metal centre was reinforced by the covalent assembly of the multinuclear metal complex. The oligomeric Co-salen complex (**iii**) was shown to be much more efficient in the hydrolytic kinetic resolution of cyclohexene oxide (Fig. 1.13), a reaction which is very difficult to catalyze with mononuclear salen analogues [37].
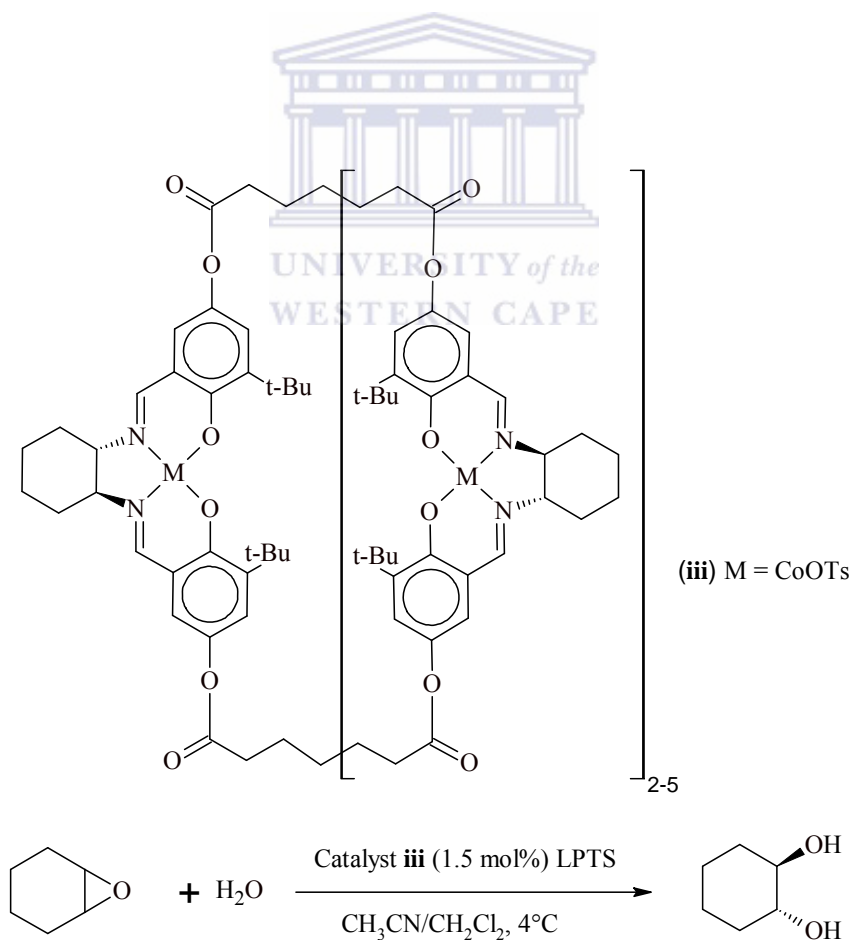
Figure 1.13: Oligomeric Co(III) salen complexes developed by Jacobsen et al. which show good activity for the HKR of cyclohexene oxide.

Research on asymmetric processes catalysed by salen metal complexes continue to be an active research topic and as a result asymmetric processes for which these catalysts show good activity continue to be found. Recently the group of Skarzewski investigated the activity of chromium complexes based on salen type ligands in the asymmetric nitroaldol reaction (Scheme 1.3) [39]. The chromium catalyst (**iv**) was shown to be a very efficient catalyst for this process. Previously this reaction was shown to be effectively catalysed by cobalt salen complexes, however a long reaction period was required.
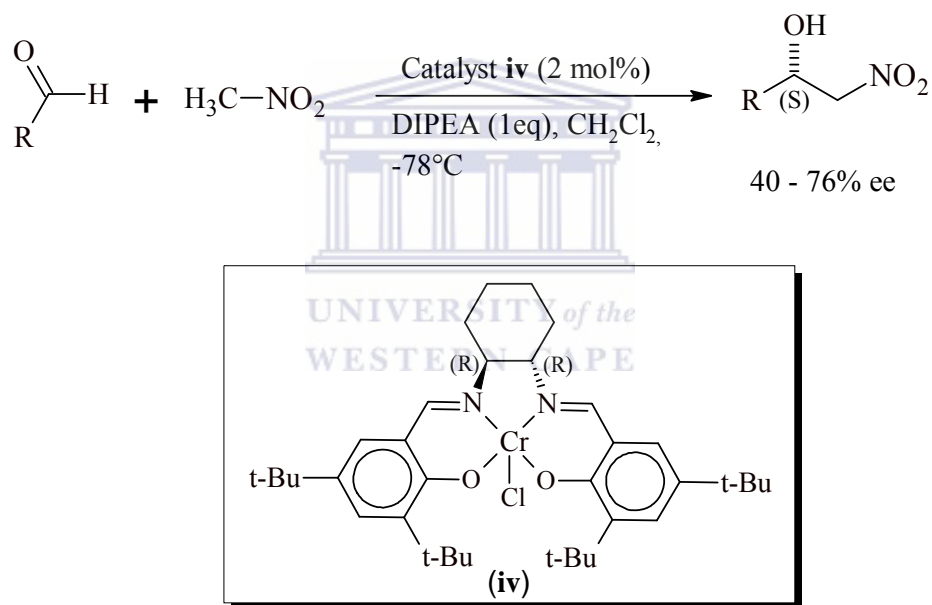
Scheme 1.3: *Asymmetric nitroaldol reaction catalysed by Cr(II) salen complex (**iv**)* [39].

Structural variants of salen ligands continue to be investigated and as a result Hutson et al. developed the new coordination systems (**v**) shown in Scheme 1.4 which has been shown to be active for the carbonyl-ene reaction of a number of 1,1-disubtituted and trisubstituted alkenes with ethyl glyoxylate [40]. Catalysts based on this ligand have

19

been shown to be very active under mild conditions such as room temperature with catalyst loading as low as 0.1 mol%. Under these conditions the conversion to the homoallylic alcohols are obtained in high yields with very good enantiomeric excesses and diastereoselectivities.
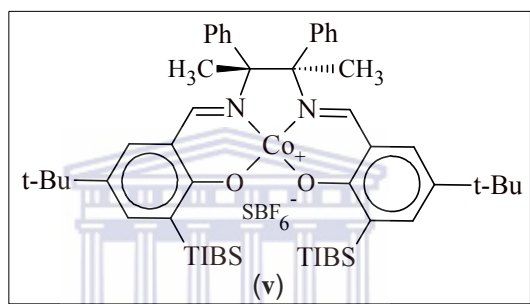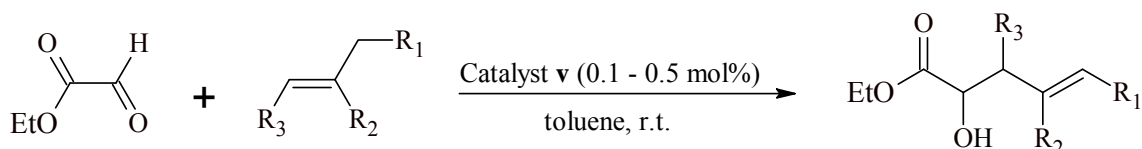
Scheme 1.4: Carbonyl-ene reaction catalysed by Co(III) salen complex (v).

The great success obtained with salen coordination systems has resulted in very little attention being given to the investigation of bidentate coordination systems containing centres of chirality within the ligand structure as catalysts for asymmetric catalysis. Nevertheless several accounts have appeared in which bidentate salicylaldimine metal complexes containing centres of chirality are present within the substituent on the imino nitrogen. For instance Iglesias et al. reported tetradentate copper complexes such as **(vi)** shown in Scheme 1.5 as well as bimetallic species such as system **(vii)** [41]. These metal complexes were evaluated in cyclopropanation of styrene using diazoacetate, however very poor enantioselectivities were obtained. The lack in enantiomeric

induction of the complexes was ascribed to the square planar coordination geometry around the metal centres as well as the lack in steric crowding around the metal centre.
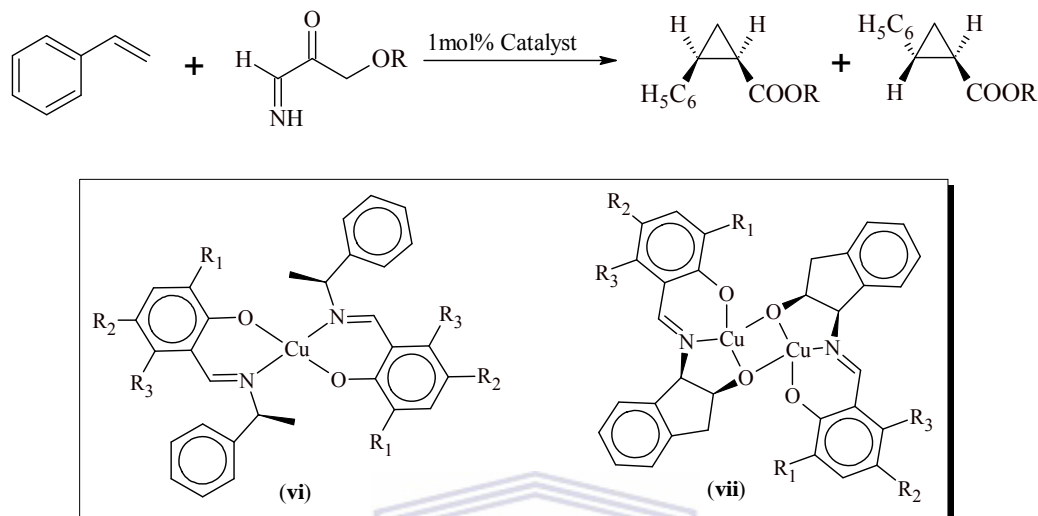
Scheme 1.5: *Investigation of catalysts derived form chiral bidentate and tridentate salicylaldimines as suitable catalysts for the cyclopropanation of styrene [41].*

1.3 HETEROGENISED SALICYLALDIMINE METAL COMPLEXES IN CATALYSIS

In recent years heterogenizing typical homogeneous catalysts has emerged as a convenient strategy to obtain recyclable catalysts. However effective implementation of these technologies industrially has been hampered by problems such as catalysts leaching, poor stability of the immobilized catalysts and mass transportation limitations due to poorly defined environments of the active sites. The later problem is particularly encountered for catalysts immobilized on linear polymers and is caused by folding of the polymeric chain. There has thus been extensive on-going research into finding suitable coordination systems and anchoring strategies to overcome the previously mentioned problems. A number of different methodologies have been developed to

21

achieve anchoring of typical homogeneous catalysts onto inorganic and organic support materials. Typical inorganic supports which have been investigated are alumina, silica, mesoporous materials such as MCM-41 and zeolites. These support media allow easier and uncomplicated separation of the immobilized catalyst from the reaction media which is typically achievable with heterogeneous catalysts. Advances in membrane technology have also increased the interest in catalysts immobilized on organic supports. The advantage in using organic supports is that the catalyst retains its homogeneous nature, however catalyst-product separation is still achieved using nanofiltration or ultrafiltration techniques [42].

1.3.1   *Catalyst immobilized on inorganic and mesoporous materials*

In several investigations immobilization of salen metal complexes has been achieved on inorganic supports such as alumina, silica and activated carbon. Recently Salavati-Niasari et al. [43] synthesised metal complexes supported on alumina based on bis(salicylaldiminato) hydrazone ligand systems. The complexes contained Cu(II), Co(II), Ni(II) and Mn(II) as metal centres (Fig 1.14) and were shown to be active for the oxidation of cyclohexene using *tert*-butyl hydroperoxide as oxidant. The activities of the immobilized complexes were found to be much higher than other alumina supported complexes. It was also shown that the catalyst could easily be separated from the reaction mixture and was found to be reusable several times for the oxidation process.

The immobilization of copper salicylaldimine complexes was also achieved by Mukherjee et al. [44]. The copper complexes were immobilized on organically modified silica. The catalytic activity of both the homogeneous complexes and immobilized systems was investigated in the oxidation of cyclohexene using oxidants

such as hydrogen peroxide and *tert*-butyl hydroperoxide. The group showed that enhanced activity and selectivity was obtained through the immobilization of the catalyst.
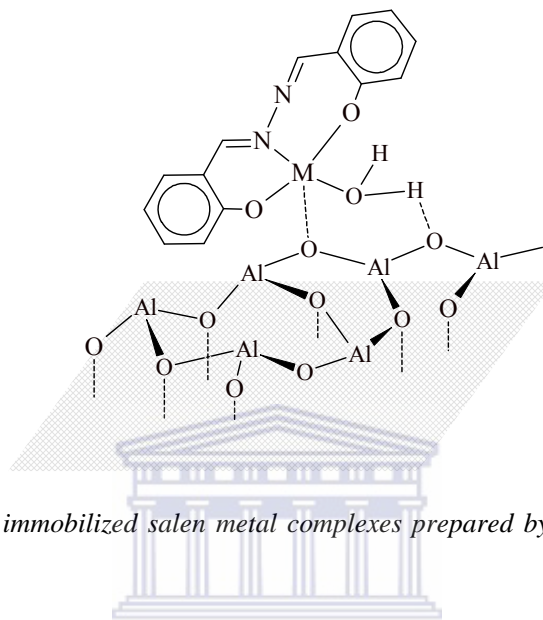
Figure 1.14*: Alumina immobilized salen metal complexes prepared by Salavati-Niasari et al. [43].*

Heterogenised chiral salen complexes have also been reported by Park et al. [45]. The group prepared organosilane functionalised MCM-41, which was used to immobilize Jacobsen type catalysts using a grafting strategy (Scheme 1.6). The immobilized complexes were investigated in the asymmetric epoxidation of styrene and *cis*-stilbene. Immobilized cobalt complexes were also prepared by Luo et al. by first functionalizing the MCM-41 with a salicylaldimine ligand system [46]. The metal complexes were then obtained by reacting metal salts with the salicylaldimine functionalised MCM-41. The catalytic activity of the heterogenised catalysts was investigated in the oxidation of styrene using hydrogen peroxide as oxidant. The catalysts were shown to have higher activities than the corresponding homogeneous systems under mild conditions and were also shown to be stable against leaching of the cobalt metal centre.
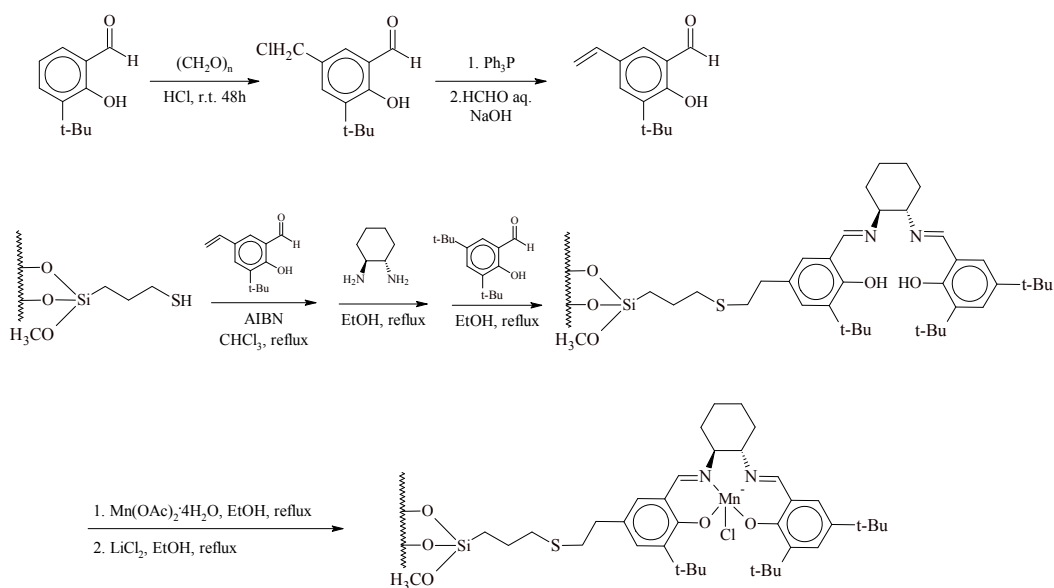
Scheme 1.6: *Grafting method utilized by Park et al. to immobilize salen complexes on MCM-41 [45].*

1.3.2   Metal complexes encapsulated in zeolites

The encapsulation of metal complexes within zeolites has recently emerged as an strategy to immobilize homogeneous catalytic systems. This method has been applied very successfully by a number of groups. One approach is to include the metal complex, which is stable under conditions of zeolite synthesis, in the synthesis mixture. The metal complex is thus trapped in the voids of the zeolite as it is synthesized. Another approach which is frequently utilized is known as the 'flexible ligand' method or the 'ship in the bottle' method. A ligand system which is able to diffuse freely into the pores of the zeolite complexes with metal ions within the pore volume. The resulting complex is too large or too rigid to diffuse out of the pores.

Copper salen complexes have been depicted in encapsulated within the pores of zeolite NaX and NaY by Ratnasamy et al. [47]. The encapsulation was achieved by synthesising the metal complexes inside the cavities of the zeolites using the 'flexible ligand' method. It was shown that a higher concentration of encapsulated complex was obtained using this method compared to strategies which involve the synthesis of the zeolite around the preformed metal complex. The catalytic activity of the encapsulated copper complex was evaluated in phenol oxidation. The degradation of hydrogen peroxide by the encapsulated complex was found to be comparable to those of enzymes.

This group has also encapsulated manganese salen complexes (Figure 1.15) in the pores of zeolite X using the zeolite synthesis method [48]. It was shown that the extent of encapsulation of the metal complexes and stability of oxidation states of the manganese metal centre is dependent on the nature of the substituent on the aromatic ring of the salen ligand. The catalytic efficiency of the encapsulated manganese complexes was evaluated in the aerobic oxidation of styrene. It was shown that deactivation of the encapsulated complex did not occur and that only slight loss in activity was observed due to the formation of polymeric material. Recyclability of the complex was also demonstrated by removal of the polymeric material with a suitable solvent.
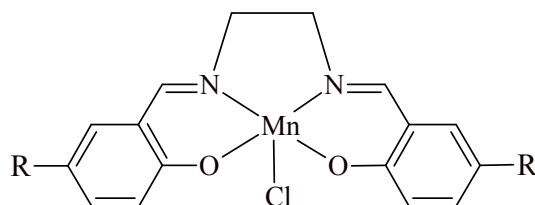
Figure 1.15: Mn(III) salen complexes encapsulated into the supercages of zeolite X by Ratnasamy et al. [48].

Recently the encapsulation of copper salen complexes (Figure 1.16) was also achieved by the group of Koner [49]. The metal complexes were immobilized inside the cage of the zeolite using the 'ship-in-a-bottle' procedure. The encapsulated catalysts were evaluated in the oxidation of phenol and 1-naphthol using H_2O_2 as oxidant. While the immobilized catalyst exhibited good activities and product selectivities, the homogeneous analogues was shown to be virtually inactive. The difference in activity was attributed to the distortion in the basal plane of the CuN_2O_2 coordination sphere which occurs when the complex is encapsulated in the zeolite matrix. The distortion in the structure of an analogues copper(II) salen complex was demonstrated using spectroscopic studies which indicated the coordination sphere of the entrapped complex undergoes significant distortion after encapsulation [50]. Investigation of the activity of the encapsulated complex and its homogeneous analogue revealed similar results for the oxidation of phenol and 1-naphthol, which showed the immobilized catalyst to have higher activity than the non-encapsulated catalyst.
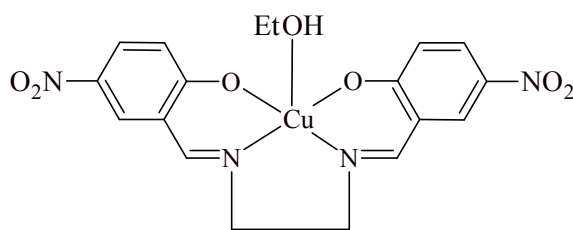
Figure 1.16: *Salen copper(II) complexes encapsulated into the pores of zeolite NaY [49].*

Another example of such a zeolite effect was reported by Mollmann et al. [51]. The group encapsulated Co-salen complexes in the pores of USY-zeolite using the 'ship in the bottle' strategy. It was found that the encapsulated catalysts showed an enantiomeric induction which was comparable to the homogeneous analogues in the trans hydrogenation of acetophenone to 1-phenylethanol. The enantioselective results

26

were ascribed to distortion in the conformation of the occluded metal complexes as a result of encapsulation.

1.3.3 Polymer anchored metal complexes

The anchoring of homogeneous catalysts on polymers has been one of the most investigated methods of immobilization. This fact is exemplified by several review articles published by Leadbeater, Bradley, Janda and Bergbreiter [52-55], which show the utilization of soluble polymer supports for designing recoverable catalysts. Immobilization of the catalyst has typically been achieved by entrapment of the catalyst in the voids of a cross-linked polymer, ion pairing utilizing suitable cation or anion functionalities incorporated on the polymer resin as well as covalent attachment to the polymer resin. Depending on the nature of the polymeric support, the supported catalyst may be soluble (when a linear polymer support is utilised) or insoluble (when a cross-linked polymer support is utilised) [56].

A new method of anchoring chiral cobalt salen complexes on polystyrene beads was achieved by Jacobsen et al. [57]. The immobilized cobalt complexes were synthesised (Scheme 1.7) by first reacting the mono-hydroxylated salen ligand with the 4-nitrophenyl carbonate derivative of the 90μm hydroxymethylpolystyrene resins. After washing to remove unbound ligand this was followed by complexation with cobalt acetate and oxidation to afford the desired cobalt complex. The immobilized complexes were evaluated in the hydrolytic kinetic resolution of terminal epoxides as batch reactions and continuous flow reactions and were shown to be highly active for the hydrolytic kinetic resolution of terminal epoxides with high enantioselectivity. It was

also demonstrated that catalyst recovery and recycling was possible with no loss of activity or enantioselectivity.
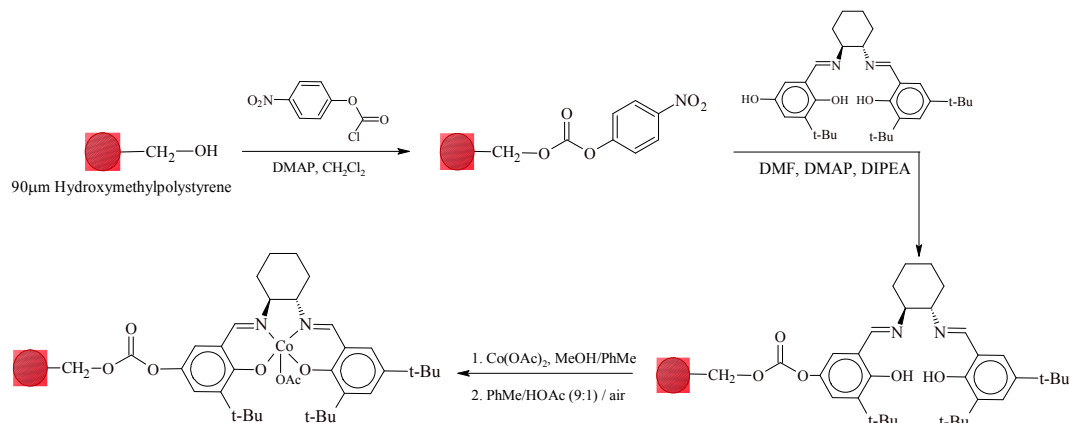
Scheme 1.7*: Covalent anchoring of chiral cobalt salen complexes on polystyrene beads [57].*

This immobilized chiral cobalt salen complex has also been shown by this group to be a suitable catalyst in the kinetic resolution of epoxides with phenols to the corresponding 1-aryloxy-2-alcohols, which are important pharmacological compounds, in high yields and enantioselectivities [58].

Recently Khan et al. synthesised polymeric vanadium salen complexes (Figure 1.17) consisting of 12 repeating salen units [59]. These polymeric catalysts were investigated in the asymmetric addition of trimethylsilyl cyanide to aldehydes at room temperature. The catalysts were shown to have very good activity with high enantiomeric excess (96%). It was also demonstrated that the catalysts could be recycled up to four times without loss in activity.
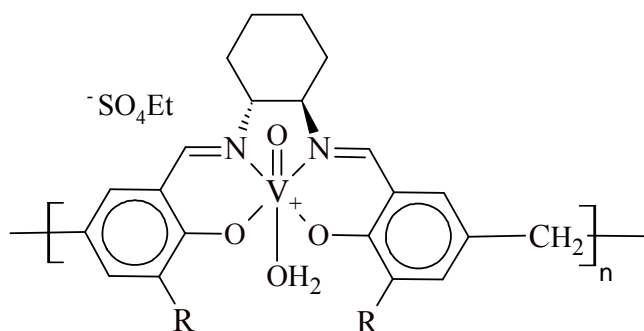
Figure 1.17*: Polymeric vanadium salen complexes developed by Khan et al. [59].*

1.3.4   Dendrimer supported catalysts

Dendrimers are three dimensional highly branched polymers which are of well defined shape, size and molecular weight. A general representation of typical dendritic architecture is shown in Figure 1.18. The unique architecture of these macromolecules has attracted interest from various groups particularly in the development of dendrimeric catalysts. The dendritic architecture provides the means of creating discrete microenvironments which allows a high degree of regio- and stereochemical control in catalytic process as demonstrated by Twyman in a recent review [60]. Due to the size of the dendrimer system, the recovery of the catalyst from the reaction stream is possible utilising precipitation or membrane filtration techniques.

The first example of catalysis using a dendrimeric supported catalyst was reported by the group of van Koten [61]. Since then the interest in dendritic supported coordination systems for catalysis has grown since these catalysts exhibit unique properties which are entirely related to structural aspects of the dendritic catalyst. For instance the three dimensional nature of the dendritic structure allows ready access to the active site thus precluding diffusion limitations generally observed for linear or cross-linked polymer supported catalysts.

C : represent dendritic core functionality

P : represent end groups on pheripery of dendrimer

Gn : represents branch subcells of denritic structure, where Gn denotes generation number.
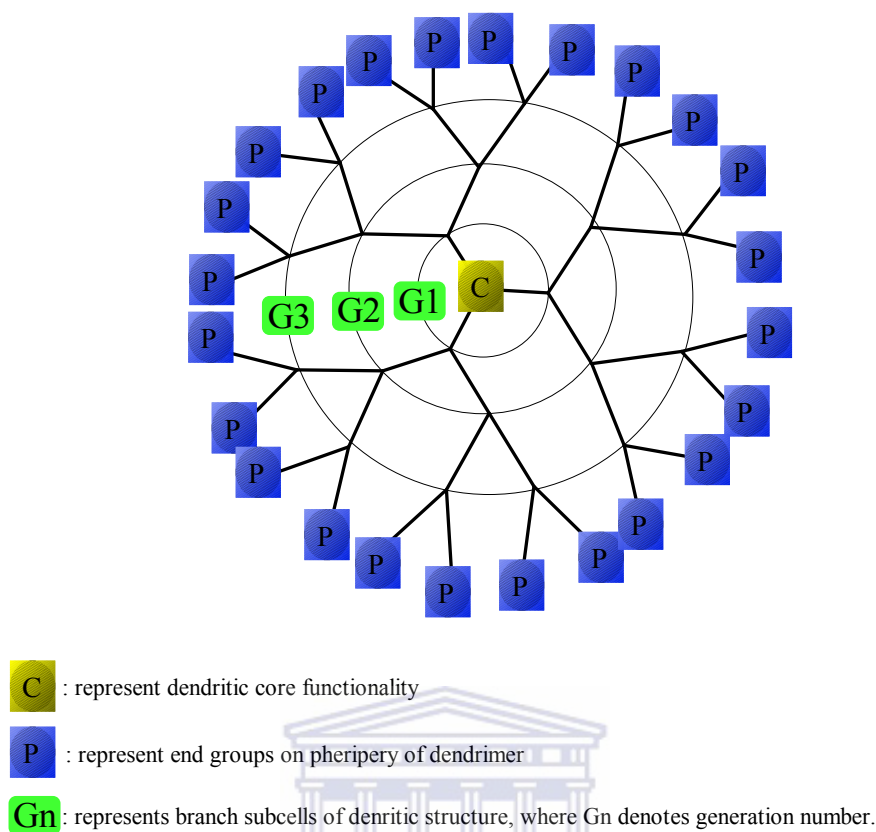
Figure 1.18: General representation of the structural features a dendrimer.

In addition a generation effect ('dendritic effect') is also observed for some catalyst where increased activity is observed in going from a low generation to a higher generation. This is generally attributed to an increase in the number of catalytic active sites. However this exponential increase in active sites may in some cases also contribute to retardation of catalysis due to undesired interactions of the active sites when in close proximity.

Another of these properties in relation to catalysis is cooperativity which is a feature observed in the catalytic processes of certain metalloenzymes. Recently the group of Jacobsen [62] reported the synthesis of chiral cobalt salen metal complexes immobilized on the periphery of polyamidoamine (PAMAM) dendrimers. These metallodendrimers
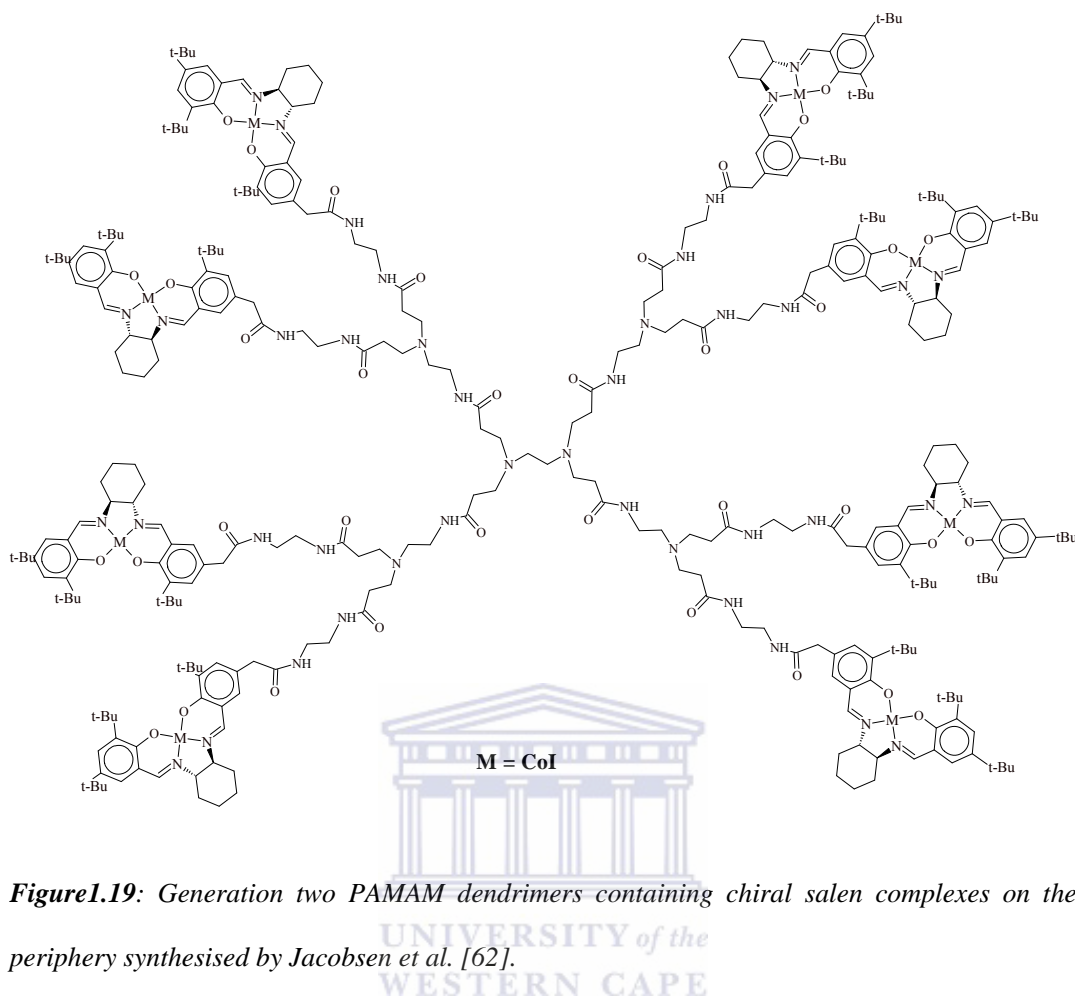
Figure1.19*: Generation two PAMAM dendrimers containing chiral salen complexes on the periphery synthesised by Jacobsen et al. [62].*

were synthesised based on the cooperative mechanism proposed for the epoxide ring opening reaction proposed for salen catalyst developed by this group. This dendrimeric catalyst was developed subsequent to the success obtained with the oligomeric catalysts (Scheme 1.6.), which were shown to have higher activity than analogous mononuclear systems. It was demonstrated that these catalysts exhibit enhanced activity in the hydrolytic kinetic resolution of terminal epoxides with activities superior to the oligomeric catalysts.

Dendritic Mn(II) complexes have also been synthesised by Yang et al. up to the sixth generation. The structure of the generation 3 dendrimer synthesised is shown in Figure

1.20 [63]. The catalytic activities of these metallodendrimers were investigated in the oxidation of cyclohexene under 1 atm, molecular oxygen. Four major products were observed under the optimised conditions shown in Scheme 1.8. Epoxide **4** (Scheme 1.8) was reported for the first time by this group for the oxidation of cyclohexene.
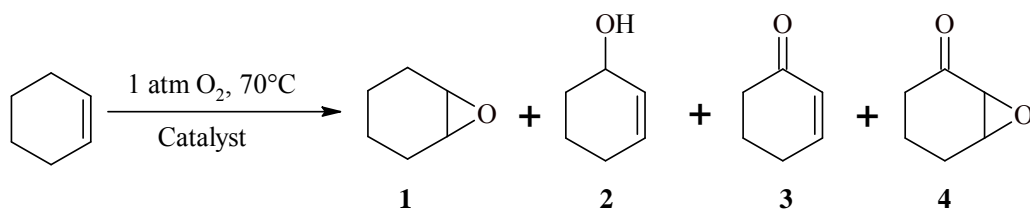
Scheme 1.8*: Oxidation of cyclohexene using Mn(II) PAMAM dendrimers (G1 – G6) synthesised by Yang et al. [63].*

In recent years a new trend in catalyst immobilization has emerged which focuses on anchoring dendrimeric coordination systems on inorganic supports. This strategy allows mechanical separation of the catalyst while exploiting the favourable attributes of the dendritic architecture. This strategy was very effectively utilised by Bu et al. to synthesise Mn(II) PAMAM metallodendrimers supported on the surface of ultrafine silica [64]. The supported dendrimer catalysts were shown to be active for the epoxidation of styrene and other cyclic olefins. A positive 'dendritic effect' was also observed with these catalysts since an increase in activity was observed with increase in generation numbers for the epoxidation of styrene.
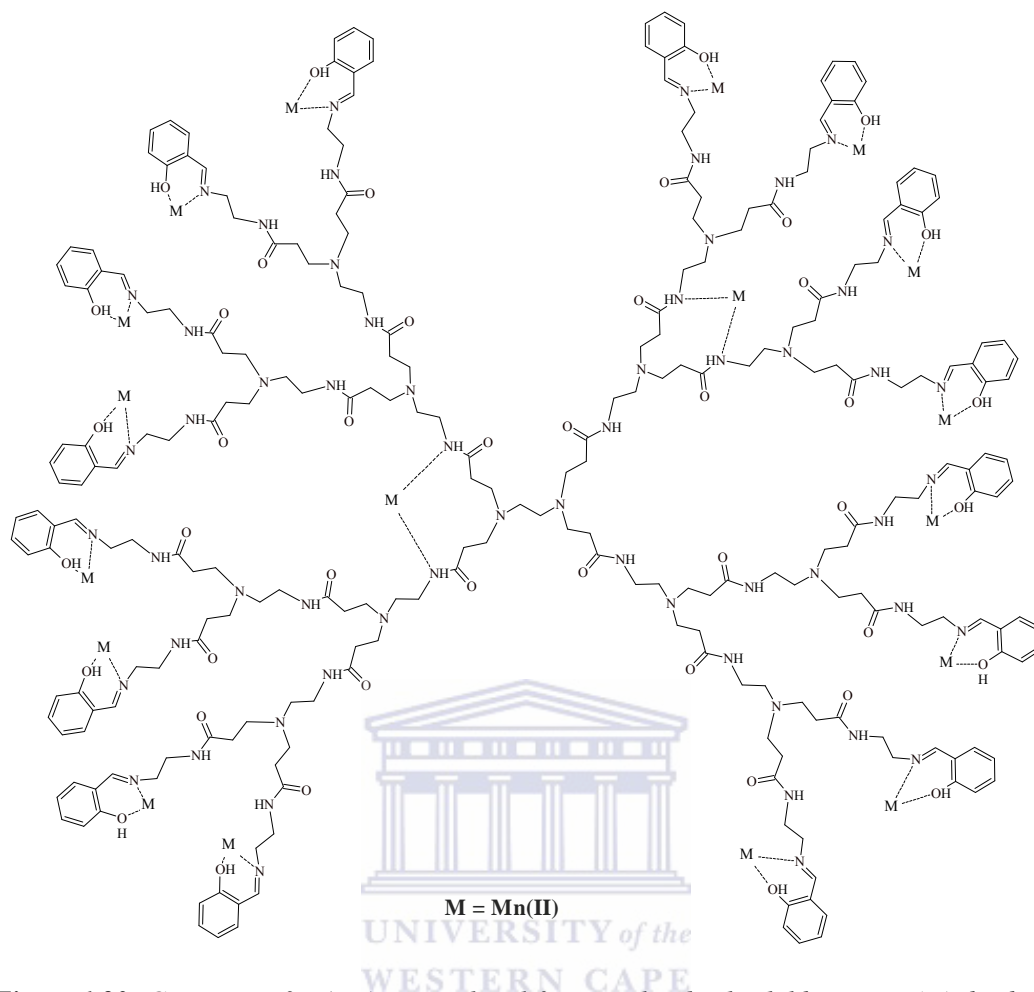
Figure 1.20: Generation 3 PAMAM peripheral functionalised salicylaldimine Mn(II) dendritic complexes synthesised by Yang et al.
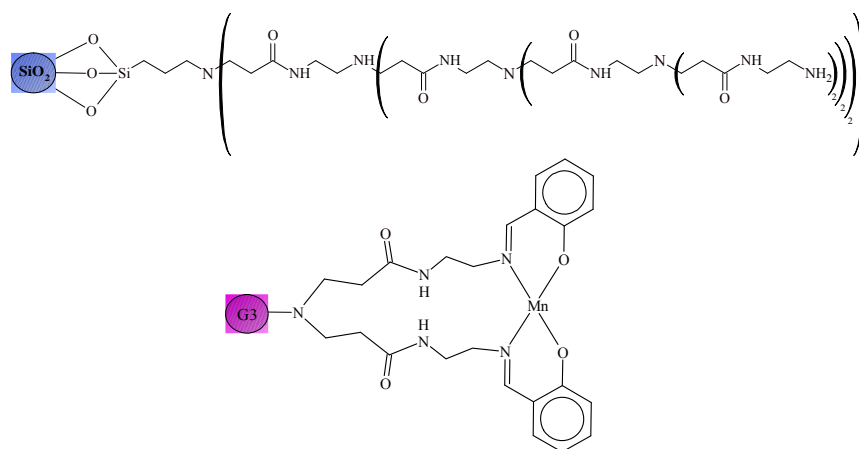
Figure 1.21: Silica immobilized G4 PAMAM dendrimer and anchored Mn(II) salen complexes synthesised by Bu et al. [64].

1.4 SCOPE AND OBJECTIVES OF THESIS

The objectives of this project have been to study the activity of metal complexes of salicylaldimines in oxidation processes with the aim of identifying suitable catalysts and optimum process conditions which potentially are suitable for *greener* organic transformation reactions. In pursuit of these aims typical homogeneous catalysts derived from *N*-(aryl)salicylaldimines as well as peripheral functionalised salicylaldimine dendrimeric complexes (heterogenised systems) were investigated as catalyst precursors for the oxidation of phenol and cyclohexene using hydrogen peroxide as oxidant. Thus previously unexplored transition metal systems are investigated for *greener* oxidation processes and the effect of dendrimer immobilization of related coordination systems are also investigated to compare the efficiency of the immobilized catalysts to homogeneous analogues.
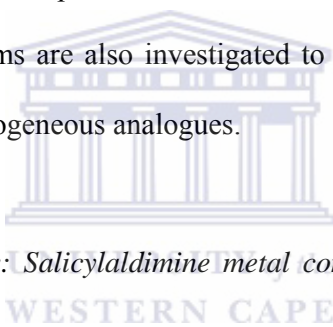
Chapter 1: Literature review: Salicylaldimine metal complexes as homogeneous and heterogenised catalysts.

This chapter provides a brief survey of literature reports focusing on the investigation of salicylaldimine metal complexes as catalyst precursors in homogeneous catalysis as well as strategies which have been utilised to immobilize transition metal complexes based on these ligands.

Chapter 2: Synthesis and characterization of N-(aryl)salicylaldimine metal complexes

This chapter deals with the synthesis and full characterization of tetra-coordinate Cu(II) and Co(II) metal complexes which were prepared by the reaction of the acetate salt of the metals with bidentate *N*-(aryl)salicylaldimines. Characterization of the complexes and ligands was with a range of physical techniques which include NMR spectroscopy,

FT-IR spectroscopy, elemental analysis, mass spectrometry as well as x-ray crystallography for several metal complexes.

Chapter 3: Synthesis and characterization of peripheral functionalised salicylaldiminato metallodendrimers

The synthesis and characterization of metallodendrimers containing copper and cobalt metal centres is described in this chapter. First and second generation metallodendrimers were prepared by functionalising the peripheral groups of commercially available poly (propyleneimine) dendrimers with salicylaldimine units.

Chapter 4: The oxidation of phenol in aqueous media using mono- and multinuclear salicylaldimine metal complexes

The oxidation of phenol using hydrogen peroxide is described in this chapter. Catalytic activity of the copper and cobalt complexes were investigated in aqueous media at different pH values. A comparative study was conducted investigating the performance of the *N*-(aryl)salicylaldimine complexes versus the metallodendrimers.

Chapter 5: The oxidation of cyclohexene with hydrogen peroxide using mono- and multi nuclear salicylaldimine metal complexes

This chapter discusses the catalytic activity of the metal complexes prepared in chapter 2 and 3 in the oxidation of cyclohexene using hydrogen peroxide as oxidant.

Chapter 6: Summary

This chapter provides a summary of the research worked described in this thesis.

1.5 REFERENCES

1 P. T. Anastas, M. M. Kirchhoff, T. C. Williamson, *Appl. Catal. A: Gen*. **2001**, *221*, 3.

2 G. Centi, S. Perathoner, *Catal. Today* **2003**, *77*, 287.

3 H. P. Dijkstra, G. P. M. van Klink, G. van Koten, *Acc. Chem. Res*. **2002**, *35*, 798.

4 C. W. Kohlpaintner, R. W. Fischer, B. Cornils, *Appl. Catal. A: Gen*. **2001**, *221*, 219.

5 B. E. Hanson, *Coord. Chem. Rev*. **1999**, *185-186*, 795.

6 W. Leitner, *Nature* **2003**, *423*, 930.

7 C. S. Consorti, G. L. P. Aydos, G. Ebeling, J. Dupont, *Org. Lett*. **2008**, *10*, 237.

8 I. T. Horvath, J. Rabai, *Science* **1994**, *266*, 72.

9 J. Yoshida, K. Itami, *Chem. Rev*. **2002**, *102*, 3693.

10 L. Frunz, R. Prins, G. D. Pirngruber, *Chem. Mater*. **2007**, *19*, 4357.

11 S. H. Lee, E. Y. Lee, D. Yoo, S. J. Hong, J. H. Lee, H. Kwak, Y. M. Lee, J. Kim, C. Kim, J. Lee, *New J. Chem*. **2007**, *31*, 1579.

12 M. Mukherjee, A. R. Ray, *J. Mol. Catal. A: Chem*. **2007**, *266*, 207.

13 V. N. Nemykin, A. E. Polshyna, S. A. Borisenkova, V. V. Strelko, *J. Mol. Catal. A: Chem*. **2007**, *264*, 103.

14 R. H. Holm, G. W. Everette Jr., A. Chakravorty, *Prog. Inorg. Chem*. **1966**, *7*, 83.

15 T. R. Youkin, E. F. Connor, J. I. Henderson, S. K. Friedrich, R. H. Grubbs, D. A. Bansleben, *Science* **2000**, *287*, 460 .

16 C. Wang, S. Friedrich, T. R. Youkin, R. T. Li, R. H. Grubbs, D. A. Bansleben, M. W. Day, *Organometallics* **1998**, *17*, 3149.

17 S. Mecking, *Angew. Chem. Int. Ed*. **2001**, *40*, 353.

18 E. F. Conner, T. R. Younkin, J. I. Henderson, S. Hwang, R. H. Grubbs, W. P. Roberts, J. J. Litzau, *J. Polym. Sci. Part A Polym. Chem*. **2002**, *40*, 2842.

19 W. –H. Sun, H. Yang, Z. Li, Y. Li, *Organometallics* **2003**, *22*, 3678.

20 C. Carlini, A. M. Raspolli-Galletti, G. Sbrana, *Polymer* **2003**, *44*, 1995.

21 D. J. Jones, V. C. Gibson, S. M. Green, P. J. Maddox, *Chem. Commun*. **2002**, 1038.

22 S. Matsui, T. Fujita, *Catal. Today* **2001**, *66*, 63.

23 M. Mitani, J. Mohri, Y. Yoshida, J. Saito, S. Ishii, K. Tsuru, S. Matsui, R. Furuyama, T. Nakano, S. Kojoh, T. Matsugi, N. Kashiwa, T. Fujita, *J. Am. Chem. Soc*. **2002**, *124*, 3327.

24 M. Lamberti, R. Gliubizzi, M. Mazzer, C. Tedesco, C. Pellecchio, *Macromolecules* **2004**, *37*, 276.

25 D. A. Pennington, S. J. Coles, M. B. Hursthouse, M. Bochmann, S. J. Lancaster, *Chem. Commun*. **2005**, 3150.

26 M. Kang, A. Sen, *Organometallics* **2005**, *24*, 3508.

27 N. S. Venkataramanan, G. Kuppuraj. S. Rajagopal, *Coord. Chem. Rev*. **2005**, *249*, 1249.

28 W. Zeng, J. Li, S. Qin, *Inorg. Chem. Commun*. **2006**, *9*, 10.

29 K Kervine, H. Korpi, M. Leskela, T Repo, *J. Mol. Catal. A: Chem*. **2003**, *203*, 9.

30 N. H. Lee, J. C. Byun, J. S. Baik, C-H. Han, S-B Han, *Bull. Korean Chem. Soc*. **2002**, *23*, 1365.

31 J. F. Larrow, E. N. Jacobsen, *Topics Organomet. Chem*. **2004**, *6*, 123.

32 T. Katsuki, *Chem. Soc. Rev*. **2004**, *33*, 437

33 P. G. Cozzi, *Chem. Soc. Rev*. **2004**, *33*, 410.

34 P. D. Knight, P. Scott, *Coord. Chem. Rev*. **2003**, *242*, 125.

35 W. Zhang, J. L. Loebach, S. R. Wilson, E. N. Jacobsen, *J. Am. Chem. Soc*. **1990**, *112*, 2801.

36 J.M. Ready, E. N. Jacobsen, *J. Am. Chem. Soc*. **2001**, *121*, 2687.

37 J. M. Ready, E. N. Jacobsen, *Angew. Chem. Int. Ed.* **2002**, *41*, 1374.

38 M.S. Sigman, E. N. Jacobsen, *J. Am. Chem. Soc.* **1998**, *120*, 5315.

39 R. Kowalczyk, L. Sidorowicz, J. Skarezewski, *Tetrahedron Asymm.* **2007**, *21*, 2581.

40 G. E. Hutson, A. H. Dave, V. H. Rawal, *Org. Lett.* **2007**, *9*, 3869.

41 A. L. Iglesias, G. Aguirre, R. Somanathan, M. Parra-Hake, *Polyhedron* **2004**, *23*, 3051.

42 J. Wöltinger, K. Drauz, A. S. Bommarius, *Appl. Catal. A: Gen.* **2001**, *221*, 171.

43 M. Salavati-Niasari, A. Amiri, *Appl. Catal. A: Gen.* **2005**, *290*, 46.

44 S. Mukherjee, S. Samanta, B. Chandra Roy, A. Bhaumik, *Appl. Catal. A: Gen.* **2006**, *301*, 79.

45 D. W. Park, S. D Choi, C. Y Lee, G. J. Kim, *Catal. Lett.* **2002**, *78*, 145.

46 Y. Luo, J. Lin, *Microporous Mesoporous Mater.* **2005**, *86*, 23.

47 C. R. Jacob, S. P. Varkey, P. Ratnasamy, *Appl. Catal. A: Gen.* **1998**, *168*, 353.

48 S. P. Varkey, C. Ratnasamy, P. Ratnasamy, *J. Mol. Catal. A: Chem* **1998**, *135*, 295.

49 B. Dutta, S. Jana, R. Bera, P. K. Saha, S. Koner, *Appl. Catal. A: Gen.* **2007**, *318*, 89.

50 P. K. Saha, B. Dutta, S. Jana, R. Bera, S. Saha, K. Okamoto, S. Koner, *Polyhedron* **2007**, *26*, 571.

51 E. Mollmann, P. Tomlinson, W. F. Holderich, *J. Mol. Catal. A: Chem.* **2003**, *206*, 253.

52 N. E. Leadbeater, M. Marco, *Chem. Rev.* **2002**, *102*, 3217.

53 C. A. McNamara, M. J. Dixon, M. Bradley, *Chem. Rev.* **2002**, *102*, 3275.

54 T. J. Dickerson, N. N. Reed, K. D. Janda, *Chem. Rev.* **2002**, *102*, 3325.

55 D. E. Bergbreiter, *Chem. Rev.* **2002**, *102*, 3345.

56 D. A. Tomalia, P. R. Dvornic, *Nature* **1994**, *372*, 617.

57 D. A. Annis, E. N. Jacobsen, *J. Am. Chem. Soc.* **1999**, *121*, 4147.

58 S. Peukert, E. N. Jacobsen, *Org. Lett.* **1999**, *1* 1245.

59 N. H. Khan, S. Agrawal, R. I. Kureshy, S. H. R. Abdi, V. Mayani, R. V. Jasra, *Tetrahedron Asymm.* **2006**, *17*, 2659.

60 L. J. Twyman, A. S. H. King, I. K. Martin, *Chem. Soc. Rev*. **2002**, *32*, 69.

61 J. W. J. Knapen, A. W. van der Made, J. C. D. Wilde, P. W. N. M. van Leeuwen, P. Wijkens, D. M. Grove, G. van Koten, *Nature* **1994**, *372*, 659.

62 R. Breinbauer, E. N. Jacobsen, *Angew. Chem. Int. Ed*. **2000**, *39*, 3604.

63 Z-W. Yang, Q-Z. Kang, H-C. Ma, C-L. Li, Z-Q. Lei, *J. Mol. Catal. A: Chem*. **2004**, *213*, 169.

64 J. Bu, Z. M. A. Judeh, C. B. Ching, S. Kawi, *Catal. Lett.* **2003**, *85*, 183.

UNIVERSITY *of the*

WESTERN CAPE

CHAPTER 2

SYNTHESIS AND CHARACTERIZATION OF *N-(ARYL)SALICYLALDIMINE* METAL COMPLEXES

CONTENT

2.1 INTRODUCTION

Coordination complexes of salicylaldimines have been known since the early 1900's and have been widely investigated in the area of inorganic chemistry [1]. These N, O-donor Schiff base ligands exhibit diverse chemical reactivity with transition metals and main group elements due to the capability of the ligand environment to accommodate a variety of metals in diverse oxidation states. A great number of salicylaldimine metal complexes have been shown to be significant as metallomesogens [2-4], biological model compounds [5-7], antimicrobial agents [8-10] and catalyst precursors as discussed in Chapter 1. Salicylaldimine metal complexes also exhibit very interesting ligand exchange reactions, which have been extensively studied by the Minkin group as described by Garnovsky and Bren in a recent review [11]. These researchers investigated the stereodynamics of a range of bidentate salicylaldimine metal complexes as well as analogues containing sulphur and selenium in place of the phenolic oxygen in the salicylaldimine framework. The ligand exchange reaction for Pd(II) and Pt(II) cationic complexes was also recently reported by Kerber et al. [12]. They demonstrated exchange of the entire ligand unit as well as exchange between the subtituents on the imino nitrogen. These exchange reactions were utilized by Kerber et al. to probe the effect of subtituents on the stability of the metal complexes.

In this chapter the synthesis of *N*-(aryl)salicylaldimine metal complexes containing Cu(II) and Co(II) metal centres is described. The ligands, as well as the metal complexes were characterized using a range of techniques which include ^{1}H-NMR and ^{13}C-NMR spectroscopy, FT-IR spectroscopy, mass spectrometry and elemental analysis. Single crystal x-ray analyses of several of the copper and cobalt complexes were also conducted.

2.2   RESULTS AND DISCUSSION

2.2.1   *Synthesis and characterization of N-(aryl)salicylaldimine ligands*

The Schiff base ligands **HL^n** were synthesised according to a well-established synthetic procedure which involved the condensation of a substituted 2-hydroxybenzaldehyde with the appropriate aromatic amine in the presence of catalytic amounts of formic acid as shown in Scheme 2.1 [13]. The ligands were obtained as pale yellow to orange yellow solids in good yields (65–93%). Structural characterization of the synthesised ligands was performed with ^{1}H and ^{13}C-NMR spectroscopy, FTIR spectroscopy and microanalysis.

HL^1 : R = H; R$_1$ = H; R$_2$ = H
HL^2 : R = H; R$_1$ = H; R$_2$ = Cl
HL^3 : R = H; R$_1$ = t-Bu; R$_2$ = t-Bu
HL^4 : R = i-Pr; R$_1$ = H; R$_2$ = H
HL^5 : R = i-Pr; R$_1$ = H; R$_2$ = Cl
HL^6 : R = i-Pr; R$_1$ = t-Bu; R$_2$ = H
HL^7 : R = i-Pr; R$_1$ = t-Bu; R$_2$ = t-Bu
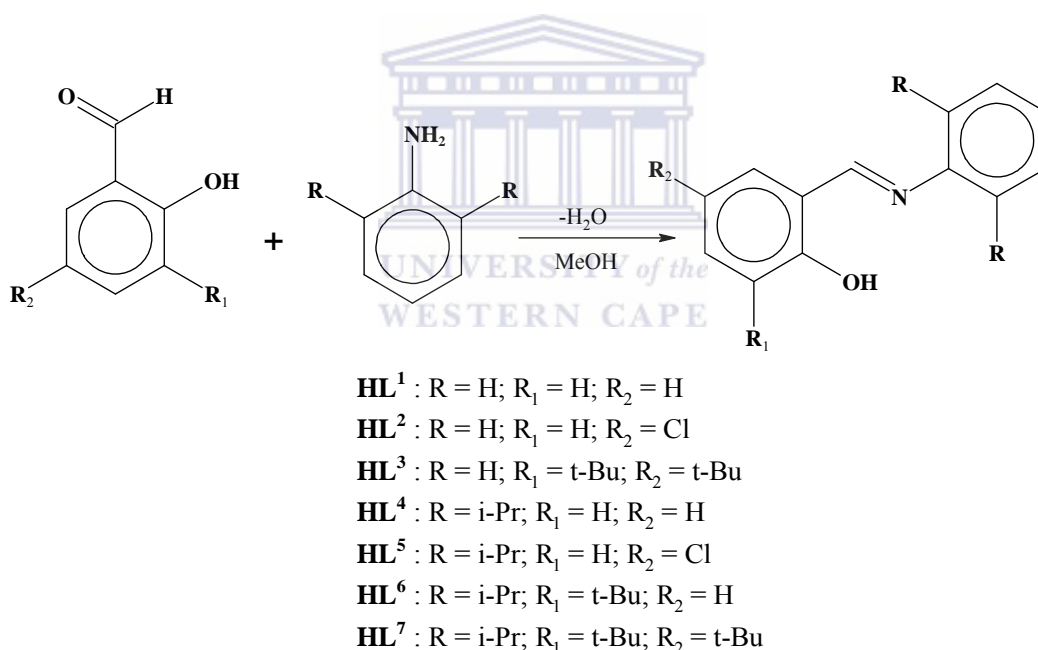
Scheme 2.1: *Synthesis of N-(aryl)salicylaldimine ligands **HL^n**.*

2.2.1.1 ^{1}*H-NMR studies of salicylaldimine ligands (**HL^n**)*

The ^{1}H-NMR spectral data for the ligands together with the relevant assignments are provided in Table 2.1. The data obtained supports the structures depicted in Scheme 2.1 and are in agreement with proton NMR data typically observed for salicylaldimines [14,

15] The resonance for the H̲C=N proton is observed as a sharp singlet in the region δ8.31 – 8.57 ppm in the spectra for all the ligands, which confirms condensation of the amine with the aldehyde. The chemical shifts due to the aromatic ring protons of both the phenolic moiety and the phenyl ring on the imino nitrogen are observed as multiplets in the region δ6.9 – 7.9 ppm for all the ligands. The spectra of ligands containing two isopropyl substituents show a doublet due to the CH̲₃ protons of the methyls and a mutilpet due to the CH̲ proton in the regions δ1.24 – 1.26 ppm and δ3.02 – 3.07 ppm respectively. The protons of the *tert*-butyl groups are observed as two sharp singlets in the ranges δ1.29 – 1.42 ppm and δ1.45 – 1.58 ppm indicating that the *tert*-butyl groups on the phenolic ring are magnetically non-equivalent. The spectra of some of the ligands (**HL^1** – **HL^3**) also show a singlet upfield in the region δ13.2 – 13.69 ppm which is due to the exchangeable hydroxyl proton of the phenolic moiety.
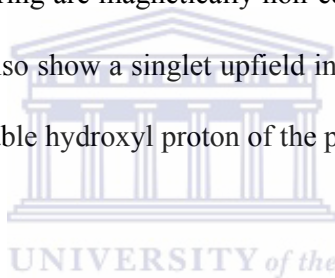
2.2.1.2   *{^{1}H}^{13}C-NMR studies of N-(aryl)salicylaldimine ligands (**HL^n**)*

The ^{13}C-NMR data obtained and the corresponding assignments are listed in Table 2.2 for the salicylaldimine ligands. The signal for the carbon of the imine functionality is observed in the region δ162–167 ppm in the ^{13}C-NMR spectra. Aromatic carbons are observed in the region δ118–148 ppm and the signal for the carbon attached to the OH group appears in the region δ158–161 ppm. Due to the magnetic non-equivalence of the *tert*-butyl groups the carbon signals of these substituents are observed as 4 signals in the range δ29.46–35.20 ppm. The isopropyl groups are observed as two signals at δ28 ppm and δ23 ppm for the CH̲(CH₃)₂ and CH(CH̲₃)₂ respectively.

2.2.1.3   Infrared spectroscopy and elemental analysis for ligands HL^n

The elemental analysis data obtained for the ligands were in agreement with the proposed formulations depicted in Scheme 2.1. (Table 2.3). Further characterization of the ligands with infrared spectroscopy revealed a broad band in the range 2800 – 3000 cm^{-1} in the spectra of the ligands which is due to the O-H stretching vibration. Infrared spectroscopic studies conducted for similar compounds by Freedman et al. showed the vibrational mode for the phenolic OH to extend over the range 3300 – 2300 cm^{-1} due to strong intramolecular hydrogen bonding of O-H to C=N. Although an exact frequency for the O-H vibration could not be assigned, studies conducted in chloroform or carbon tetrachloride showed a strong band centered at 2800 cm^{-1} in the spectra of the investigated compounds which was assigned to the O-H stretching vibration [16]. The v(C=N) band for the ligands is observed in the region 1613 – 1625 cm^{-1} confirming the presence of the imine functionality. The assignment of this band is based on literature values obtained for *N*-aryl imines in the region 2000 – 1500 cm^{-1} as reported by Ledbetter [17]. The phenolic v(C-O) stretching vibration is observed in the region 1269 – 1279 cm^{-1}. The absence of the C=O and N-H vibrational modes in the infrared spectra of the ligands confirms the dominance of the phenol-imine tautomeric form of the ligands (Scheme 2.2).

keto-amine   phenol-imine
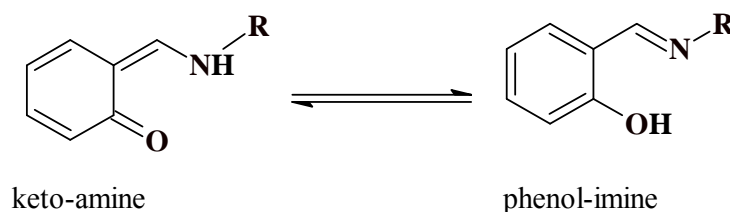
Scheme 2.2: *Keto-enol tautomeric forms of salicylaldimines*

Table 2.1: ^{1}H-NMR[a] chemical shifts δ (ppm) for *N*-(aryl)salicylaldimine ligands (**HL[n]**).

Ligand	O$\underline{\text{H}}$	$\underline{\text{H}}$C=N	Ar-$\underline{\text{H}}$	[b]C(C$\underline{\text{H}}_3$)$_3$	[c]C(C$\underline{\text{H}}_3$)$_3$	C$\underline{\text{H}}$(CH$_3$)$_2$	CH(C$\underline{\text{H}}_3$)$_2$
HL^1	13.2 (br s,1H)	8.57 (s, 1H)	6.84 – 7.02 (m, 2H, *J* = 7.4 Hz); 7.20 – 7.42 (m, 7H, *J* = 7.0 Hz)	-	-	-	-
HL^2	13.26 (br s,1H)	8.51 (s, 1H)	6.92 (m, 1H, *J* = 8.4 Hz); 7.2 – 7.4 (m, 7H, *J* = 7.6 Hz)	-	-	-	-
HL^3	13.69 (s, 1H)	8.60 (s, 1H)	6.9 – 7.2 (m, 4H, *J* = 2.2 Hz); 7.4 (m, 3H, *J* = 2.2 Hz)	1.45 (s, 9H)	1.29 (s, 9H)	-	-
HL^4	-	8.37 (s, 1H)	7.04 (t, 1H, *J* = 7.7 Hz); 7.17 (d, 1H, *J* = 8.4 Hz); 7.41 – 7.54 (m, 2H, *J* = 6.8 Hz)		-	3.07 (m, 2H, *J* = 6.8 Hz)	1.25 (d, 12H, *J* = 6.8 Hz)
HL^5	-	8.31 (s,1H)	7.09 (d, 1H, *J* = 9.4 Hz); 7.25 (s, 3H); 7.39 – 7.44 (m, 2H, *J* = 7.8 Hz)	-	-	3.02 (m, 2H, *J* = 6.8 Hz)	1.24 (d, 12H, *J* = 6.8 Hz)
HL^6	-	8.37 (s, 1H)	6.89 (t, 1H, *J* = 6.8 Hz); 7.26 (s, 3H); 7.6 (dd, 2H, *J* = 7.8 Hz)	1.57 (s, 9H)	-	3.07 (m, 2H, *J* = 6.8 Hz)	1.26 (d, 12H, *J* = 6.8 Hz)
HL^7	-	8.38 (s, 1H)	7.24 (m, 4H, *J* = 2.6 Hz); 7.59 (d, 1H, *J* = 2.6 Hz)	1.58 (s 9H)	1.42 (s 9H)	3.11 (m, 2H, *J* = 6.6 Hz)	1.25 (d, 12H, , *J* = 7.0 Hz)

[a] Spectra obtained in CDCl$_3$; [b] [t]Bu ortho to phenolic OH; [c] [t]Bu para to phenolic OH; s, singlet; d, doublet; t, triplet; dd, doublet of doublets; m, multiplet

Table 2.2: {^{1}H}^{13}C-NMR[a] chemical shifts δ (ppm) for *N*-(aryl)salicylaldimine ligands (**HL^n**).

Ligand	H**C**=N	Ar-**C**	**C**(CH₃)	C(**C**H)₃	**C**H(CH₃)₂	CH(**C**H₃)₂
HL¹	162.6	161.0, 148.4, 133.1, 132.3, 129.3, 126.8, 121.1, 118.98, 118.0, 117.2	-	-	-	-
HL²	161.26	159.72, 148.01, 132.89, 131.20, 129.48, 127.3, 123.66, 119.97, 118.84	-	-	-	-
HL³	163.81	158.28, 148.79, 140.57, 137.02, 129.32, 127.99, 126.8, 126.50, 121.16, 118.34	35.13, 34.19	31.49, 29.46	-	-
HL⁴	166.57	161.23, 146.19, 138.66, 133.19, 132.17, 125.43, 123.23, 118.98, 118.68, 117.32,	-	-	28.11	23.48
HL⁵	165.48	159.82, 145.77, 138.59, 133.05, 131.23, 125.77, 123.73, 123.35, 119.40, 118.96	-	-	28.19	23.51
HL⁶	167.28	160.72, 146.35, 138.91, 137.86, 130.58, 130.4, 125.36, 123.25, 118.58, 118.21	34.99	29.46	28.14	23.60
HL⁷	167.53	158.46, 146.43, 140.48, 138.88, 137.18, 128.10, 126.65, 125.23, 123.17, 117.77	35.2, 34.21	31.49, 29.52	28.06	23.62

[a] Spectra obtained in CDCl₃

Table 2.3: Elemental analysis and IR data for mono-functional ligands $\mathbf{HL^1 - HL^7}$

Ligand	M.p. (°C)	Formula	Anal Found (Calcd.)			IR (cm^{-1})^a	
			C	H	N	ν(C=N)	ν(C-O)
$\mathbf{HL^1}$	49 - 50	$C_{13}H_{11}NO$	78.79 (79.16)	5.58 (5.62)	7.74 (7.10)	1617	1273
$\mathbf{HL^2}$	107 - 108	$C_{13}H_{10}ClNO$	67.32 (67.40)	4.26 (4.35)	5.60 (6.05)	1614	1276
$\mathbf{HL^3}$	108 - 110	$C_{21}H_{27}NO$	81.50 (81.51)	8.69 (7.89)	4.15 (4.53)	1613	1272
$\mathbf{HL^4}$	55 - 57	$C_{19}H_{23}NO$	81.24 (81.10)	8.70 (8.24)	5.22 (4.98)	1625	1279
$\mathbf{HL^5}$	114- 115	$C_{19}H_{22}ClNO$	72.19 (72.25)	6.98 (7.02)	4.02 (4.48)	1625	1273
$\mathbf{HL^6}$	66 - 68	$C_{23}H_{31}NO$	81.43 (81.85)	9.24 (9.26)	3.95 (4.15)	1618	1269
$\mathbf{HL^7}$	114- 115	$C_{27}H_{39}NO$	82.52 (82.39)	10.13 (9.99)	3.92 (3.56)	1620	1270

^{a} Recorded as nujol mulls between NaCl plates

2.2.2 Synthesis and characterization of bis-salicylaldimine Cu(II) and Co(II) complexes

The mononuclear tetra-coordinate copper(II) complexes **1** – **7** were quite readily obtained via a 2:1 mole equivalent reaction of the appropriate ligand with copper acetate monohydrate. The reaction of **HL^7** in a 1:1 mole ratio with copper acetate afforded the bimetallic complex **8**. Similar bimetallic species were not obtained with the other ligand systems. The formation of bimetallic species has previously been reported in cases where bi and tridentate salicylaldimine ligands were reacted with metal halides, nitrates and perchlorates [18]. Alkoxy bridged dimers containing iron [19] and zinc [20] have also been reported recently.

1 : R = H; R$_1$ = H; R$_2$ = H
2 : R = H; R$_1$ = H; R$_2$ = Cl
3 : R = H; R$_1$ = t-Bu; R$_2$ = t-Bu
4 : R = i-Pr; R$_1$ = H; R$_2$ = H
5 : R = i-Pr; R$_1$ = H; R$_2$ = Cl
6 : R = i-Pr; R$_1$ = t-Bu; R$_2$ = H
7 : R = i-Pr; R$_1$ = t-Bu; R$_2$ = t-Bu
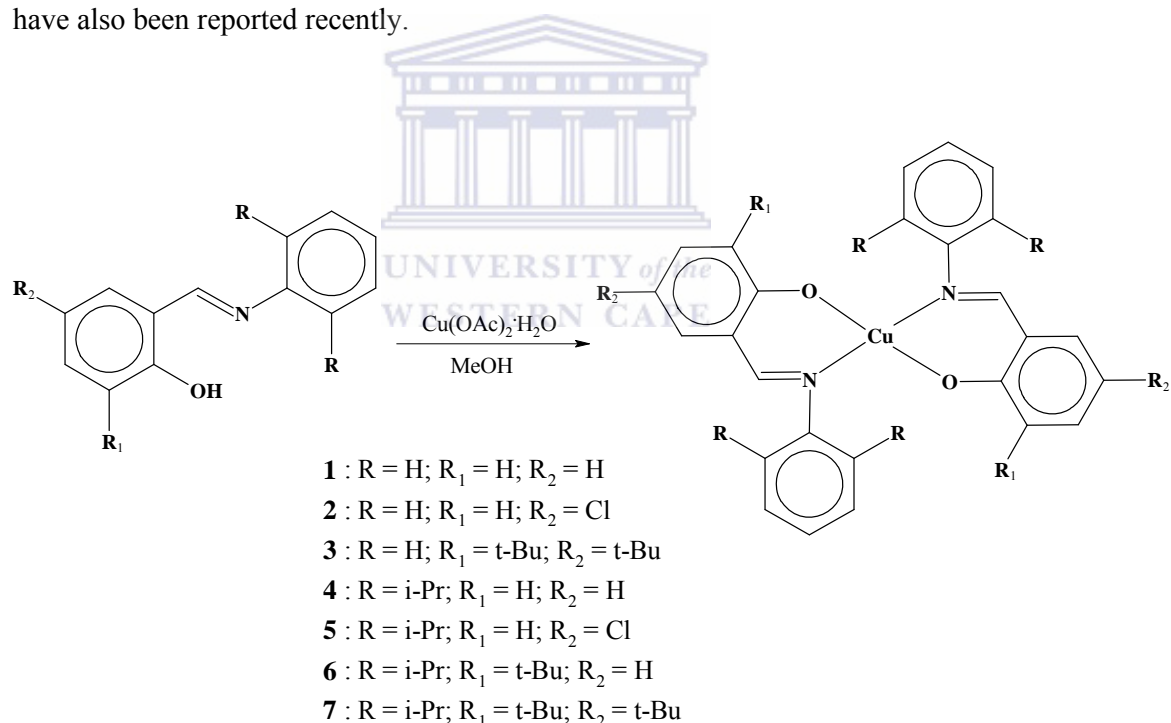
Scheme 2.3: *Synthetic procedure for the synthesis of copper(II) salicylaldiminato complexes **1**-**7**.*
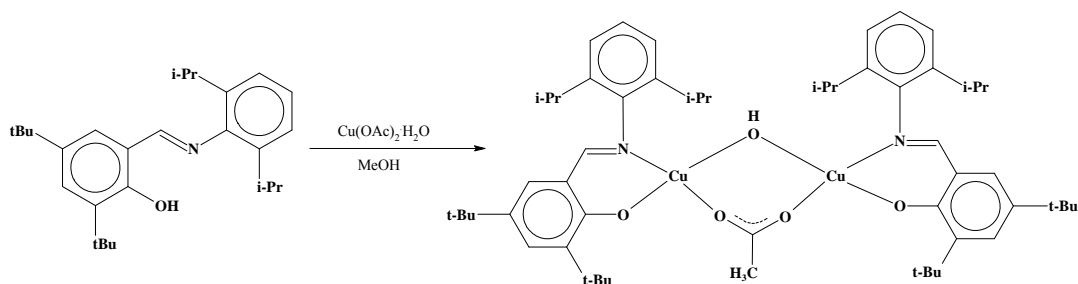
Scheme 2.4: *Synthesis of bimetallic copper complex 8.*

The cobalt(II) analogues (**9** - **15**) were obtained by reacting the salicylaldimine ligands in a 2:1 mole ratio with cobalt acetate tetrahydrate in the presence of sodium hydroxide. Coordination of the ligand to the metal centre was only observed when a base was used to deprotonate the salicylaldimine ligands. No reaction was observed in the absence of the base. Instead a mixture of the unreacted ligand and metal acetate was isolated after the reflux period. The cobalt complexes were observed to precipitate from solution during the reaction as orange-brown solids, which were purified by recrystallization by slow diffusion of ethanol into concentrated dichloromethane solutions of the complexes at low temperature.

9 : R = H; R_1 = H; R_2 = H
10 : R = H; R_1 = H; R_2 = Cl
11 : R = H; R_1 = t-Bu; R_2 = t-Bu
12 : R = i-Pr; R_1 = H; R_2 = H
13 : R = i-Pr; R_1 = H; R_2 = Cl
14 : R = i-Pr; R_1 = t-Bu; R_2 = H
15 : R = i-Pr; R_1 = t-Bu; R_2 = t-Bu
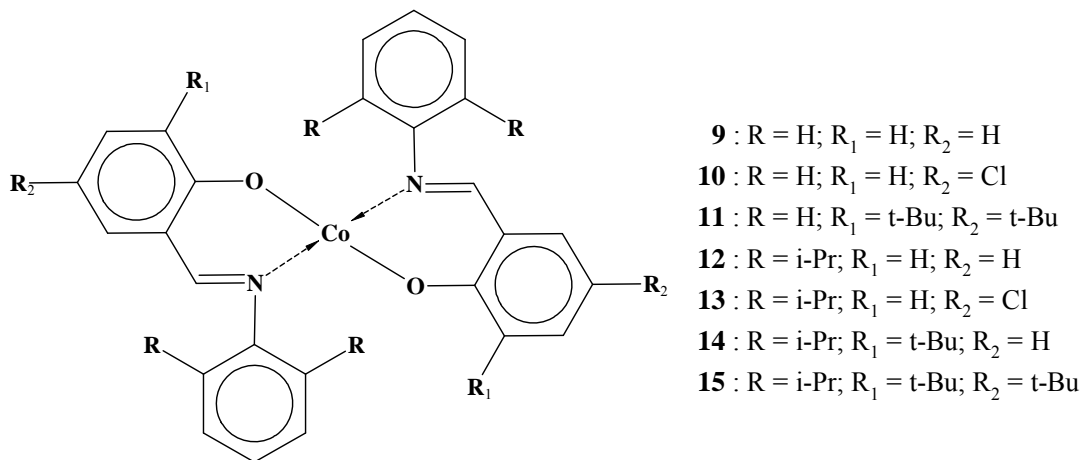
Figure 2.1: *General structures of N-(aryl)salicylaldimine Co(II) complexes.*

2.2.2.1   Infrared spectroscopy and mass spectrometry studies

Structural characterization data for the copper(II) complexes (**1 – 8**) and cobalt complexes (**9 – 15**) are provided in Table 2.4 and Table 2.5 respectively. Elemental analysis data obtained for the metal complexes confirmed the 2:1 ligand to metal ratio expected for the mononuclear complexes proposed in Scheme 2.3 and the 1:1 ligand to metal ratio for bimetallic complex **8** shown in Scheme 2.4. According to the elemental analysis data several of the copper and cobalt complexes occur as hydrated species. All the complexes exhibit good solubility in common organic solvents such as dichloromethane, THF and acetone. The copper complexes were observed to be very stable in solution and in the solid state at room temperature. The cobalt analogues were also found to be very stable in the solid state at room temperature, however in solution a gradual colour change to dark brown is observed with formation of a dark brown precipitate in some cases. This phenomenon is attributed to slow oxidation of the metal complex in air. The oxidation of salicylaldimine cobalt complexes in air over several days is known to occur and has been shown to be dependant on the nature of the solvent, steric factors, temperature and the ligand-field strength [21, 22].   In the presence of hydrogen peroxide this oxidation is observed to be much more rapid.

Comparison of the IR spectra of the metal complexes with the spectra of the ligands indicated that coordination occurs via the azomethine nitrogen and the deprotonated phenolic oxygen as expected. The observed IR data is in agreement with typical vibrational modes observed for ν(C=N) and ν(C-O) for tetra-coordinate salicylaldimine metal complexes. The stretching mode of ν(C=N) showed a negative shift of ~4 – 25 cm^{-1} whereas the ν(C-O) stretching vibration showed a positive shift from ~1270 cm^{-1} to ~1320 cm^{-1}. The absence of the broad OH band in the IR spectra of the metal

complexes provided additional confirmation of the formation of the MN_2O_2 coordination sphere. IR data for the copper(II) and cobalt(II) complexes are provided in Tables 2.4 and 2.5 respectively.

Mass spectra of the mononuclear metal complexes were obtained using electron impact ionization. Data obtained for the molecular ions observed for the complexes are shown in Table 2.4 and Table 2.5 respectively. The parent ions for the complexes were observed as either M^+ or $[M+H]^+$. In the case of cobalt complex **10**, the parent ion is not observed, however a fragment due to $[M-H]^+$ is observed. The series of copper complexes **1 – 7** showed fairly similar fragmentation patterns as did the series of cobalt complexes **9 – 15**. However the fragmentation pattern observed for the copper coordination systems differed to a certain degree from the cobalt analogues. A typical fragmentation pattern for the copper systems consisted of initial loss of the metal thus producing free ligands. Subsequent fragments observed in the mass spectra were due to fragmentation of the free ligands. In the mass spectra of the cobalt complexes fragments due to the free ligand were also observed as well as adducts due to subsequent fragmentation of this species. However fragmentation species which still contained the metal were also observed in the spectra of the cobalt complexes, which is not the case for the copper complexes.

Table 2.4: Characterization data for copper(II) salicylaldiminato complexes **1 – 8**.

Complex	Formula	M⁺ (calcd) m/z	Anal Found (Calcd.)			IR spectra (cm⁻¹)[a]	
			C	H	N	ν(C=N)	ν(C-O)
1	$C_{26}H_{20}CuN_2O_2 \cdot \frac{1}{2}H_2O$	455 (455.99)	67.85(67.17)	4.17(4.42)	6.01(6.14)	1606	1327
2	$C_{26}H_{18}Cl_2CuN_2O_2 \cdot \frac{1}{2}H_2O$	[b]525 (525.89)	58.41(58.49)	3.23(3.46)	5.54(5.34)	1606	1322
3	$C_{42}H_{52}CuN_2O_2$	680 (680.42)	74.57(74.14)	7.73(7.70)	4.13(4.12)	1609	1317
4	$C_{38}H_{44}CuN_2O_2$	624 (624.31)	72.90(73.11)	7.11(7.10)	4.45(4.49)	1602	1323
5	$C_{38}H_{42}Cl_2CuN_2O_2$	[b]694 (694.20)	65.46(65.84)	6.12(6.11)	3.77(4.04)	1610	1322
6	$C_{46}H_{60}CuN_2O_2$	736 (736.53)	74.81(75.01)	8.17(8.21)	3.78(3.80)	1602	1318
7	$C_{54}H_{76}CuN_2O_2 \cdot 2H_2O$	848 (848.74)	73.62(73.32)	8.73(9.06)	2.53(2.97)	1610	1324
8	$C_{56}H_{80}Cu_2N_2O_5\ H_2O$	n.d.	66.50(66.84)	8.13(8.21)	2.75(2.78)	1614	1325

[a] Recorded as nujol mulls between NaCl plates

[b] m/z for [M+H]⁺

[c] not determined

Table 2.5: Characterization data for cobalt(II) salicylalidminato complexes **9 – 15**.

Complex	Formula	[M+H]$^+$ (calcd.) m/z	Anal Found (calcd.)			IR spectra (cm^{-1})^a	
			C	H	N	ν(C=N)	ν(C-O)
9	C$_{26}$H$_{20}$CoN$_2$O$_2$¼H$_2$O	^{b}451 (451.38)	68.59 (68.50)	4.44 (4.79)	5.77 (6.14)	1604	1318
10	C$_{26}$H$_{18}$Cl$_2$CoN$_2$O$_2$	^{c}519 (519.27)	59.38 (60.02)	3.49 (3.56)	4.10 (5.38)	1610	1312
11	C$_{42}$H$_{52}$CoN$_2$O$_2$	676 (676.81)	74. 58 (74.64)	7.88(7.76)	4.15 (4.19)	1611	1323
12	C$_{38}$H$_{44}$CoN$_2$O$_2$·½H$_2$O	620 (620.70)	72.60 (72.59)	7.48 (7.21)	4.43 (4.46)	1604	1314
13	C$_{38}$H$_{42}$Cl$_2$CoN$_2$O$_2$ 2H$_2$O	689 (689.59)	63.20 (62.99)	5.91 (6.40)	3.33 (3.87)	1602	1314
14	C$_{46}$H$_{60}$CoN$_2$O$_2$	732 (732.91)	75.09 (75.49)	8.28 (8.26)	3.39 (3.83)	1600	1318
15	C$_{54}$H$_{76}$CoN$_2$O$_2$·¼H$_2$O	^{b}844 (844.13)	76.23 (76.43)	9.12 (8.99)	2.92 (3.29)	1610	1323

^{a} Recorded as nujol mulls between NaCl plates

^{b} Represents m/z for M$^+$

^{c} Represents m/z for the fragment [M-H]$^+$

2.2.2.2   X-Ray crystallography of Cu(II) and Co(II) salicylaldiminato complexes

Suitable crystals for x-ray analysis were obtained by slow diffusion of ethanol into concentrated dichloromethane solutions of the metal complexes. The crystal structural data and crystal structure refinement parameters for the copper and cobalt complexes are provided in Table 2.12 and Table 2.13 respectively. Recently Parkin et al. [23] developed a cluster analysis method which was utilised as a means to classify the coordinate geometries observed for a number of bis-salicylaldimine metal complexes found in the Cambridge Structural Database. The three most abundant geometrical arrangements were found to be square planar *cis*, square planar *trans* and tetrahedral depending on the nature of the metal centre as well as steric constraints imposed by substituents on the ligand backbone. Further classifications were also made which depended on the M-O and M-N bond distances as well as the conformation adopted by the ligands [23]. The analysis showed that the geometrical arrangement of the ligands depended on the nature of the metal centre. It was observed that copper complexes prefer a square planar geometry whereas cobalt systems adopt a tetrahedral arrangement.

Description of Cu(L^1)$_2$ (complex 2)

The ORTEP drawing depicting the molecular structure of **2** is shown in Figure 2.2 with selected bond distances and angles for the coordination sphere CuN$_2$O$_2$ provided in Table 2.6. The molecular structure of **2** shows two ligands coordinated to one copper atom in a bidentate fashion. The arrangement of the N$_2$O$_2$ donors for **2** is *cis* despite the bulky phenyl ring on the imino nitrogens. A similar geometrical arrangement of the ligands was observed by Kasumov et al. for the complex bis(*N*-3,5-(t-Bu)$_2$-phenylsalicylaldiminato)copper(II) [24]. The ligands contained di-substituted *tert*-butyl

groups on the aromatic rings attached to the imino nitrogens of the ligands. In **2** Cu(1) is situated on a cente of symmetry on a two fold axis. The phenyl rings attached to N(1) and N(1)[i] are almost co-planar (dihedral angle 6.3(1)°) with the distance between the ring centroids being 3.62 Å. This may be an indication of intermolecular π···π interactions. The geometrical environment of the copper centre in **2** is distorted square planar with the bond angles O(1)-Cu(1)-N(1), O(1)-Cu(1)-N(1)[i], O(1)-Cu(1)-O(1)[i] and N(1)-Cu(1)-N(1)[I] observed to be 93.56(6)°, 151.86(6)°, 88.07(8)° and 97.93(8)° respectively. These values are in agreement with bond angles observed for the bis(N-3,5,^{t}Bu$_2$-phenylsalicylaldiminato) copper(II) complex synthesised by Kasumov et al. [24]. The bond angle O(1)-Cu(1)-N(1)[i] for **2** (151.86(6)°) is significantly smaller than values reported by Rothaus et al. and Khandar et al. (175.6° and 171.8° respectivly) for copper(II) salen complexes which typically adopt a square planar configuration, which indicates that the distortion from square planarity is much greater for complex **2** [25, 26].
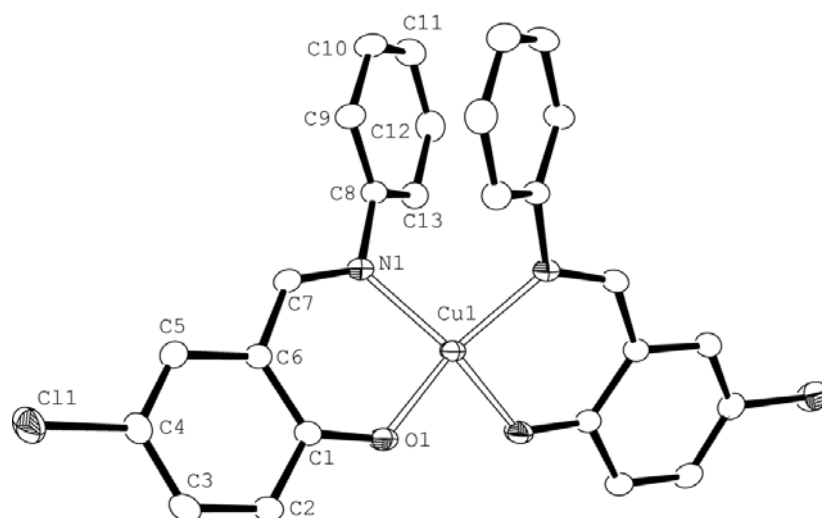
Figure 2.2: *The molecular structure of **2** showing the crystallographic numbering. Cu(1) is situated on a two-fold axis.*

Table 2.6: Selected bond distances (Å) and angles (°) for the core of **2**.

Cu(1)–N(1)	1.985(1)	O(1)–Cu(1)–N(1)	93.56(6)
Cu(1)–O(1)	1.901(1)	O(1)–Cu(1)–N(1)[i]	151.86(6)
		O(1)–Cu(1)–O(1)[i]	88.07(8)
		N(1)–Cu(1)–N(1)[i]	97.93(8)

Symmetry code: (i): -*x*, *y*, 1.5 - z.

The Cu(1)-N(1) and Cu(1)-O(1) bond distances for **2** are observed to be 1.985(1) Å and 1.901(1) Å respectively and are in agreement with values obtained for other tetradentate coordinate copper systems [26, 27].

Description of Cu(L⁴)₂ (complex 4)

The molecular stuctrure for **4** is shown in Figure 2.3, with selected bond distances and angles around the metal centre listed in Table 2.7. As for complex **2** the molecular structure of **4** shows bidentate chelation of two salicylaldimine ligands to one copper atom. However the the N_2O_2 donors are in a *trans* arrangement around Cu(1). The bond angles O(1)–Cu(1)–N(1) and O(1)–Cu(1)–N(1)[I] are 91.39(9)° and 88.61(9)° respectively and are comparable to values for analogous angles in similar bis(salicylaldiminato)copper(II) complexes synthesised by Carlini et al. [27] which also shows a *trans* arrangement of two salicylaldimine ligands around the copper centre.
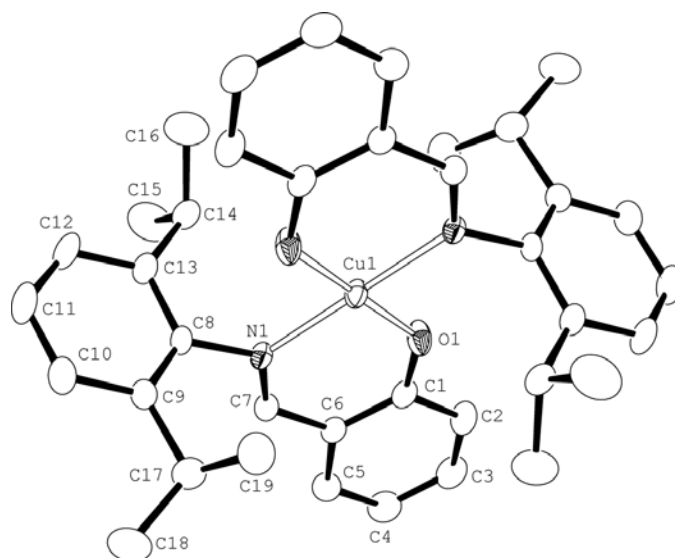
Figure 2.3: *The molecular structure of* ***4*** *showing the crystallographic numbering. Cu(1) is situated on a centre of symmetry.*

The geometry around the copper atom for **4** can thus also be described as distorted square planar. In complex **4**, Cu(1) is situated on a centre of symmetry so that N(1)–Cu(1)–N(1)[i] and O(1)–Cu(1)–O(1)[i] are both exactly 180°, which provides further evidence indicating a square planar geometrical arrangement. The bond distances Cu(1)–N(1) and Cu(1)–O(1) are 1.999(2) Å and 1.869(2) Å respectively. These values are comparable to values observed for **2** (1.985(1) Å and 1.901(1) Å) and the copper complex synthesised by Carlini et al. (Cu-O, 1,890 Å and Cu-N, 1.976 Å) [27].

Table 2.7: Selected bond distances (Å) and angles (°) for the core of **4**.

Cu(1)–N(1)	1.999(2)	O(1)–Cu(1)–N(1)	91.39(9)
Cu(1)–O(1)	1.869(2)	O(1)–Cu(1)–N(1)[i]	88.61(9)

Symmetry code: (i): -*x*, -*y*, 1 - z.

Description of Cu$_2$(L^7)$_2$ (complex 8)

X-ray analysis of complex **8** (Figure 2.4) revealed coordination of one ligand per copper centre with an acetoxy and a hydroxy group bridging between the two copper centres. As for complexes **2** and **4** the geometry around each metal centre is also observed to be distorted square planar since the observed bond angles 93.6(1), 91.9(1), 93.1(1), 88.1(1) due to N(1)–Cu(1)–O(1), N(1)–Cu(1)–O(3), N(2)–Cu(2)–O(2) and N(2)–Cu(2)–O(4) respectively, deviate slightly from 90°, the ideal angle expected for square planarity. The bond angles N(1)–Cu(1)–O(5) (166.5(1)°) and N(2)–Cu(2)–O(5) (166.8(1)°) are bigger than analogous angles for **2**. This indicated that the distortion around Cu(1) and Cu(2) is not as great as observed for **2** even though the ligands are coordinated in the same orientation. The bond distances observed for Cu-N and Cu-O for both metal centers in complex **8** are similar to the bond lengths observed for **2** and **4** and are in agreement with values in the literature. The bond distances for Cu(1)–O(3) (1.960(3)Å) and Cu(2)–O(4) (1.956(4) Å) of the bridging acetoxy group are fairly similar [28].
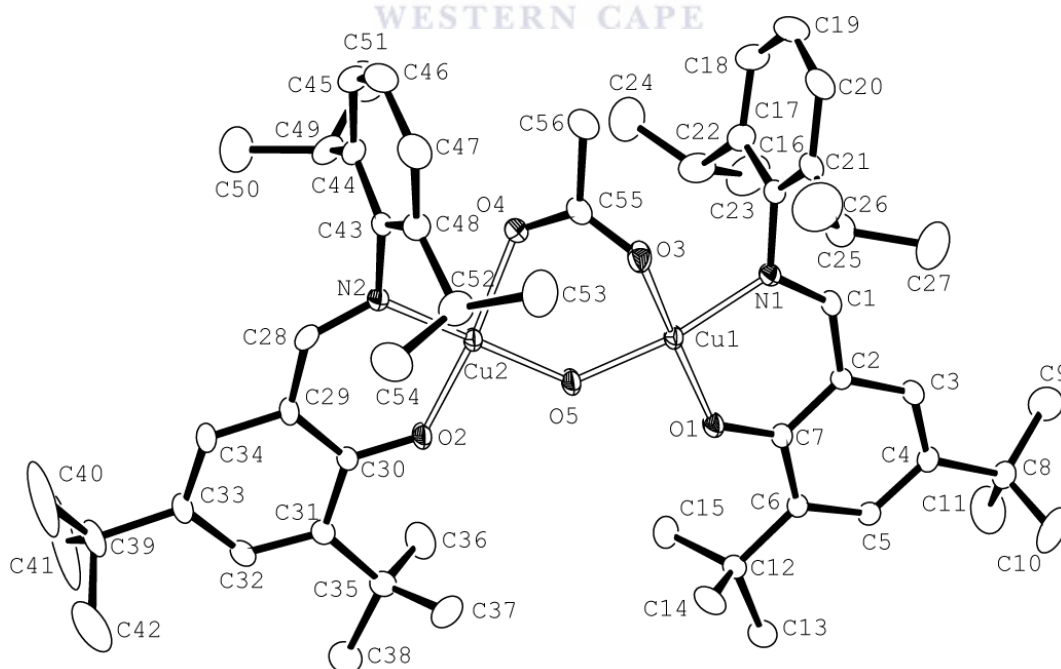
Figure 2.4: *The molecular structure of 8 showing the crystallographic numbering.*

Table 2.8: Selected bond distances (Å) and angles (°) for the core of **8**.

Cu(1)–N(1)	1.951(3)	Cu(2)–N(2)	1.952(3)
Cu(1)–O(1)	1.884(3)	Cu(2)–O(2)	1.881(3)
Cu(1)–O(3)	1.960(3)	Cu(2)–O(4)	1.956(4)
Cu(1)–O(5)	1.880(3)	Cu(2)–O(5)	1.880(3)
N(1)–Cu(1)–O(1)	93.6(1)	N(2)–Cu(2)–O(2)	93.1(1)
N(1)–Cu(1)–O(3)	91.9(1)	N(2)–Cu(2)–O(4)	88.1(1)
N(1)–Cu(1)–O(5)	166.5(1)	N(2)–Cu(2)–O(5)	166.8(1)
O(1)–Cu(1)–O(3)	166.4(1)	O(2)–Cu(2)–O(4)	165.8(1)
O(1)–Cu(1)–O(5)	89.6(1)	O(2)–Cu(2)–O(5)	90.1(1)
O(3)–Cu(1)–O(5)	91.9(1)	O(4)–Cu(2)–O(5)	92.0(1)

*Description of Co(L^1)$_2$ (complex **9**.)*

The ORTEP drawing of the molecular structure of **9** (Figure 2.5) depicts a tetra-coordinate coordination system with two *N*-(phenyl) salicylaldimine ligands coordinated to the cobalt metal centre. Bond distances and bond lengths around the cobalt metal centre are provided in Table 2.9. The geometry around Co(1) is distorted tetrahedral, which is the typical geometrical arrangement observed for *N*-(aryl)salicylaldimine cobalt systems [29]. The bond angles N(1)-Co(1)-N(2), N(1)-Co(1)-O(2), N(2)-Co(1)-O(1) and O(1)-Co(1)-O(2) are in the range 110-119° and are significantly bigger than the ideal 109° angle expected for tetrahedral geometry. The bond distances of Co-N (2.007Å and 2.009Å) are observed to be longer than the Co-O bond distances (1.913 Å and 1.900 Å). These values are consistent with data obtained for a bis-salicylaldimine cobalt complex reported by Wang et al. [30].
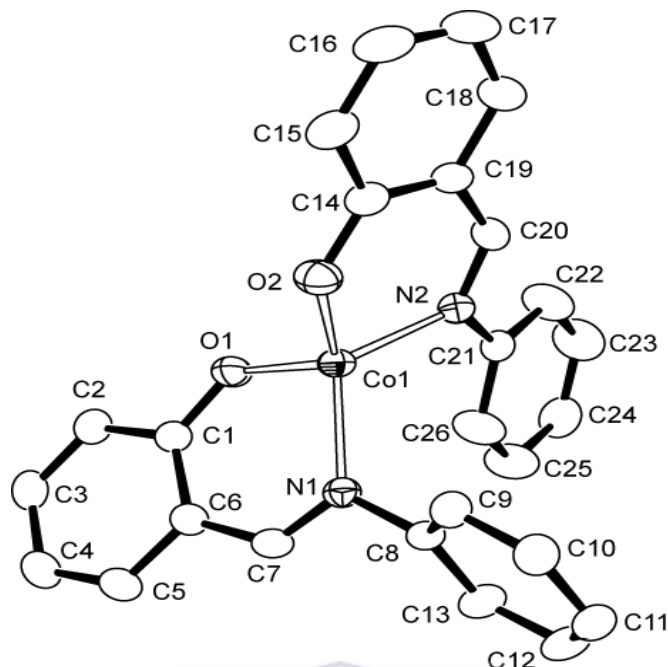
Figure 2.5: The molecular structure of 9 showing the crystallographic numbering.

Table 2.9: Selected bond distances and angles for the core of **9**.

Co(1)–N(1)	2.007(2)	N(1)–Co(1)–N(2)	118.49(9)
Co(1)–N(2)	2.009(2)	N(1)–Co(1)–O(1)	95.72(9)
Co(1)–O(1)	1.913(2)	N(1)–Co(1)–O(2)	119.89(9)
Co(1)–O(2)	1.900(2)	N(2)–Co(1)–O(1)	110.91(9)
		N(2)–Co(1)–O(2)	96.77(9)
		O(1)–Co(1)–O(2)	116.14(9)

*Description of Co(L^4)$_2$ (complex **12**)*

The molecular structure of **12** (Figure 2.6) also shows bidentate chelation of two salicylaldimine ligands to one cobalt centre. As for **9** the coordination around the metal is observed to be distorted tetrahedral. However the distortion around Co(1) is observed

to be much greater. This is evident form the bond angle N(1)-Co(1)-N(2) which is found to be 128.53°. The greater distortion is attributed to the isopropyl substituents on the phenyl ring on the imino nitrogen which creates a highly steric demanding environment especially since the orientation of the ligands brings the phenyl group on the imino nitrogens closer in proximity. The bond angles N(1)-Co(1)-O(2), N(2)-Co(1)-O(1) and O(1)-Co(1)-O(2) are in the same range as the bond angles observed for **9**. The bond distances for Co-N (2.007 and 2.014) and Co-O (1.909 and 1.911) are also observed to be similar to the values obtained for **9** despite the greater distortion in the geometrical arrangement of the coordination sphere.
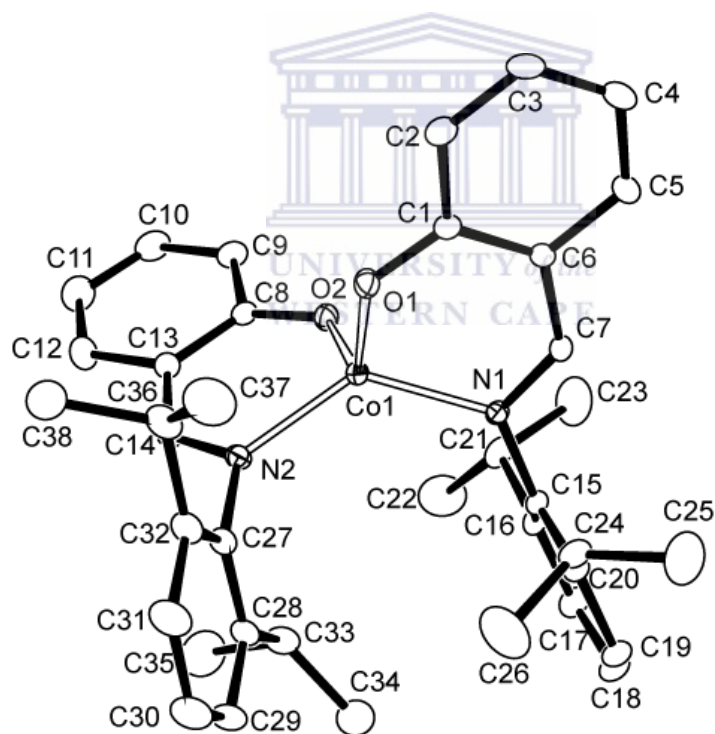
Figure 2.6: *The molecular structure of **12** showing the crystallographic numbering.*

Table 2.10: Selected bond distances (Å) and angles (°) for the core of **12**

Co(1)–N(1)	2.007(2)	N(1)–Co(1)–N(2)	128.53(6)
Co(1)–N(2)	2.014(2)	N(1)–Co(1)–O(1)	94.12(6)
Co(1)–O(1)	1.909(2)	N(1)–Co(1)–O(2)	112.38(6)
Co(1)–O(2)	1.911(1)	N(2)–Co(1)–O(1)	113.61(7)
		N(2)–Co(1)–O(2)	94.38(6)
		O(1)–Co(1)–O(2)	115.27(7)

*Description of Co(L^6)$_2$ (complex **14**)*

The molecular structure of **14** (Figure 2.7), shows a mononuclear coordination system with a coordination sphere consisting of CoN$_2$O$_2$. However unlike **9** and **12** the ligands are observed to adopt an arrangement closer to the ideal tetrahedral geometry since the bond angle due to O(1)-Co(1)-O(2) is observed to be 109.51°. However some distortion in the geometry of the coordination sphere is still evident, since the bond angles of N(1)-Co(1)-N(2), N(1)-Co(1)-O(1) and N(2)-Co(1)-O(1), which have values of 122.83, 120.54 and 117.51 respectively are significantly greater than the ideal angle. This distortion is most likely due to the steric constrains imposed by the ligands which contain two isopropyl subtituents on the phenyl ring of the imine and a *tert*-butyl subtituent on the phenolic ring. The bond distances for Co-N and Co-O are found to be in the same range as values observed for **9** and **12** even though the coordination geometry is less distorted.
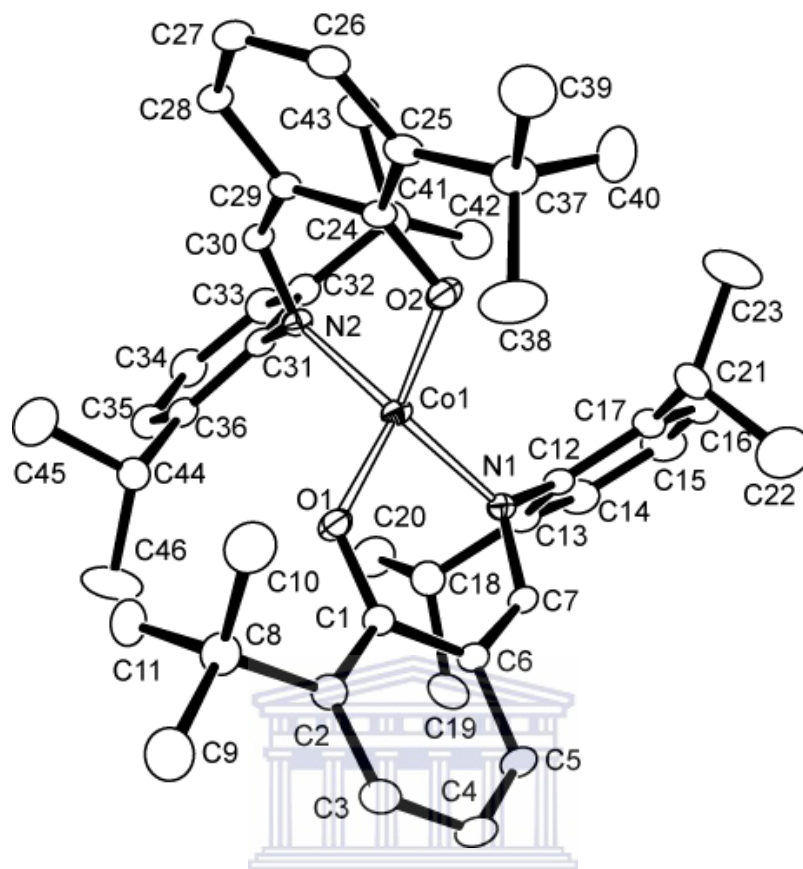
Figure 2.7*: The molecular structure of **14** showing the crystallographic numbering.*

Table 2.11: Selected bond distances (Å) and angles (°) for the core of **14**.

Co(1)–N(1)	2.001(2)	N(1)–Co(1)–N(2)	122.83(6)
Co(1)–N(2)	2.014(2)	N(1)–Co(1)–O(1)	94.47(7)
Co(1)–O(1)	1.908(2)	N(1)–Co(1)–O(2)	120.54(7)
Co(1)–O(2)	1.912(2)	N(2)–Co(1)–O(1)	117.51(7)
		N(2)–Co(1)–O(2)	93.19(7)
		O(1)–Co(1)–O(2)	109.51(8)

2.3   CONCLUSIONS

A range of tetra-coordinate complexes of *N*-(aryl)salicylaldimines containing copper and cobalt metal centres were successfully obtained by the reaction of the various ligands with the acetate salt of the metals using a ligand to metal ratio of 2:1. Slightly different procedures were utilised to synthesise the metal complexes since it was observed that the ligands did not coordinate cobalt as readily as copper. The reaction of ligand **HL**^{7} with copper acetate in a 1:1 ratio produced a bimetallic coordination system. An analogous complex was not obtained with cobalt and this may be due to the different synthetic methods used to synthesise the cobalt systems.   Characterization of the complexes with FT-IR spectroscopy, elemental analysis and mass spectrometry confirmed the formation of the expected coordination systems. X-ray crystal structural data was also obtained for copper complexes **2**, **4** and **8** as well as for cobalt complexes **9**, **12** and **14**. The molecular structures of the copper complexes showed the geometry around the metal centres to be distorted square planar. The distortion from square planarity for both the copper centres in **8** was observed to be intermediate between **2** and **4**.   Coordination of the ligand in **2** was observed to be *cis* whereas a *trans* arrangement was adopted by the ligands in **4**. The greater distortion is ascribed to steric interactions of the phenyl rings on the imino nitrogens in **2** which are observed to be almost co-planar. The trans arrangement of the ligands around the copper centre of **4** reduces steric interactions of the much bulkier ligands resulting in the 180° bond angles observed for N(1)–Cu(1)–N(1)$^{\text{I}}$ and O(1)–Cu(1)–O(1)$^{\text{i}}$. The coordination geometry of the ligand in **9**, **12** and **14** are described as distorted tetrahedral. This observation is consistent with molecular structures of bis-*N*-(aryl) salicylaldiminato cobalt(II) complexes found in literature. In both **9** and **12** the distortion of the CoN_2O_2 sphere was observed to be greater in comparison to **14**.

2.4 EXPERIMENTAL

2.4.1 Materials and Instrumentation

All chemicals were of reagent grade and were used without further purification. All solvents were dried over the appropriate drying agent and distilled prior to use. Reactions and other manipulations were carried out using a dual vacuum/nitrogen line and standard Schlenk techniques unless stated otherwise. ^{1}H NMR (200 MHz) and ^{13}C NMR (50.3 MHz) spectra were recorded on a Varian XR200 spectrometer, using tetramethylsilane as an internal standard. Infrared spectra were recorded on a Perkin Elmer Paragon 1000PC FT-IR spectrophotometer as nujol mulls using NaCl windows. Elemental analysis was performed by the University of Cape Town Microanalytical Laboratory. GC-MS analysis was performed using a Finnigan Matt GCQ Gas Chromatograph equipped with an electron impact ionization source at 70 eV.
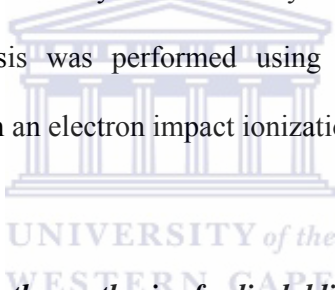
2.4.2 General procedure for the synthesis of salicylaldimine ligands HL^n

The salicylaldimine ligands were synthesized via Schiff base condensation using the appropriate 2-hydroxybenzaldehyde and aromatic amine. The synthetic procedure is described using the synthesis of **HL^1** as an example. To a Schlenk tube containing salicylaldehyde (12 mmol) and formic acid (0.5 ml) in methanol (15 mL) was added aniline (16 mmol). The resulting orange-brown reaction mixture was stirred at room temperature for approximately 15 hours. During this time a yellow solid precipitated from solution which was isolated by vacuum filtration, washed with cold methanol and dried under vacuum. The salicylaldimine ligands were obtained as light yellow to orange yellow solids in yields of 65 – 93%.

2.4.3 General procedure for the synthesis of copper complexes 1 – 8

Copper acetate monohydrate (0.5 mmol) and the appropriate Schiff base ligand (1 mmol) were placed in a round bottom flask, followed by methanol (20 mL). The resulting reaction mixture was stirred under reflux for 4 hours under a nitrogen atmosphere. During this time a solid precipitates from solution. The reaction mixture was cooled to 0°C for approximately 15 minutes and the solid isolated by vacuum filtration. Complex **8** was prepared using a 1:1 mol ratio of ligand **HL**[7] to copper acetate. Complexes were recrystallized by slow diffusion of ethanol into a concentrated dichloromethane solution of the complexes at low temperature. All complexes were obtained as dark green crystals.

2.4.4 General procedure for the synthesis of cobalt complexes 9 – 15

Cobalt acetate tetrahydrate (0.5 mmol), sodium hydroxide (1 mmol) and the appropriate Schiff base ligand (1 mmol) were refluxed in methanol (20 mL) for 4 hours under a nitrogen atmosphere. During this time a solid precipitated from solution. The reaction mixture was cooled to 0°C for approximately 15 minutes and the solid isolated by vacuum filtration. The complexes were isolated as orange to orange-brown solids. The complexes were recrystallized by slow diffusion of ethanol into a concentrated dichloromethane solution of the complexes.

2.4.5 X-ray Crystallography

Crystals of metal complexes were mounted on glass capillaries and transferred to a Rigaku R-AXIS IIc diffractometer. Diffracted intensities were measured at ambient temperature, using graphite-monochromated Mo-Kα radiation (λ = 0.71073 Å) from a

RU-H3R rotating anode operated at 50 kV and 90 mA. Ninety oscillation photographs with a rotation angle of 2° were collected and processed using the CrystalClear software package. Empirical corrections were applied for the effects of absorption using the REQAB program under CrystalClear. The structures were solved by direct methods [31] and refined using full-matrix least-squares calculations on F^2 (SHELXL-97) [32] on all reflections, both programs operating under the WinGX program package [33]. Anisotropic thermal displacement parameters were refined for all non-hydrogen atoms; the hydrogen atoms were included as a riding contribution except for those of the amine groups which were located from difference maps and refined with fixed isotropic thermal parameters. Structural illustrations have been drawn with ORTEP-3 for Windows [34] under WinGX [33]. Supplementary crystallographic data of complexes discussed in this chapter have been deposited at The Cambridge Crystallographic Data Centre [35].
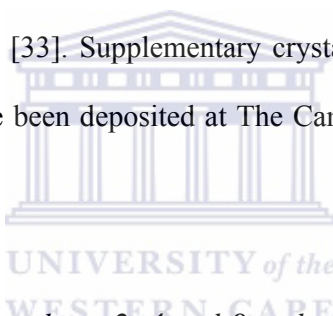
*Description of crystals for complexes **2**, **4** and **8** and refinement parameters for data collection.*

Complex **2**: Dark-green crystal fragment with approximate dimensions 0.25 x 0.25 x 0.40 mm. Refinement of 151 parameters based on all 2235 reflections yielded R_1 = 0.032 and wR_2 = 0.090 for $I > 2\sigma(I)$ (2129 reflections) and R_1 = 0.034 and wR_2 = 0.091 for all reflections; maximum and minimum residual electron density: 0.27; -0.35 e Å^{-3}.

Complex **4**: Needle-shaped brownish-green crystal with approximate dimensions 0.15 x 0.15 x 0.3 mm. Refinement of 206 parameters based on all 3230 reflections yielded R_1 = 0.055 and wR_2 = 0.114 for $I > 2\sigma(I)$ (2307 reflections) and R_1 = 0.069 and wR_2 =

0.119 for all reflections; maximum and minimum residual electron density: 0.45; -0.86 e Å^{-3}.

Complex **8**: Needle-shaped greyish-green crystal with approximate dimensions 0.15 x 0.15 x 0.40 mm. The hydroxyl hydrogen on O(5) was located from a difference map and refined with a fixed isotropic thermal parameter = 0.05 Å^3. Refinement of 589 parameters based on all 9953 reflections yielded R_1 = 0.064 and wR_2 = 0.147 for $I >$ 2σ(I) (7185 reflections) and R_1 = 0.106 and wR_2 = 0.167 for all reflections; maximum and minimum residual electron density: 1.33; -0.40 e Å^{-3}.

*Description of crystals for complexes **9**, **12** and **14** and refinement parameters for data collection.*

Complex **9**: Red prismatic crystal with approximate dimensions 0.20 x 0.20 x 0.20 mm. Refinement of 281 parameters based on all 3626 reflections yielded R_1 = 0.055 and wR_2 = 0.111 for $I > 2σ(I)$ (3464 reflections) and R_1 = 0.058 and wR_2 = 0.113 for all reflections; maximum and minimum residual electron density: 0.21; -0.23 e Å^{-3}.

Complex **12**: Brownish-red irregular-shaped crystal fragment with approximate dimensions 0.20 x 0.20 x 0.20 mm. Refinement of 397 parameters based on all 6858 reflections yielded R_1 = 0.042 and wR_2 = 0.100 for $I > 2σ(I)$ (5185 reflections) and R_1 = 0.055 and wR_2 = 0.104 for all reflections; maximum and minimum residual electron density: 0.33; -0.36 e Å^{-3}.

Complex **14**: Red rhombic crystal with approximate dimensions 0.35 x 0.20 x 0.20 mm. Refinement of 475 parameters based on all 7702 reflections yielded R_1 = 0.051

and $wR_2 = 0.131$ for $I > 2\sigma(I)$ (6208 reflections) and $R_1 = 0.061$ and $wR_2 = 0.135$ for all

reflections; maximum and minimum residual electron density: 0.41; -0.44 e Å^{-3}.

Table 2.12: Crystallographic data for **2**, **4** and **8**

Compound	2	4	8
Empirical formula	$C_{26}H_{18}Cl_2CuN_2O_2$	$C_{38}H_{44}CuN_2O_2$	$C_{56}H_{80}Cu_2N_2O_5$
Mr	524.9	624.3	988.3
Crystal system	monoclinic	triclinic	monoclinic
Space group	*C2/c*	$P\bar{1}$	$P2_1/c$
a (Å)	23.634(7)	8.0725(16)	14.944(2)
b (Å)	9.337(2)	10.2332(9)	24.968(3)
c (Å)	15.087(5)	11.7022(3)	14.736(2)
α (°)	90	60.62(2)	90
β (°)	137.343(7)	76.39(3)	94.539(4)
γ (°)	90	81.64(4)	90
V (Å3)	2256(1)	818.2(1)	5481(1)
Z	4	1	4
*D*calc (g cm-3)	1.54	1.27	1.20
μ(MoKα) (cm^{-1})	12.32	7.0	8.21
Temperature (°C)	20(2)	20(2)	20(2)
2θ range (°)	$7.6 < 2\theta < 54.0$	$4.0 < 2\theta < 54.0$	$3.6 < 2\theta < 52.0$
Absorption correction	Empirical	Empirical	Empirical
Data/restraints/par.	2235 / 0 / 151	3230 / 0 / 206	9953 / 0 / 589
R_1 ($I > 2\sigma(I)$)	0.032	0.055	0.064
wR_2 (all reflections)	0.0909	0.119	0.167
Max/min residual electrondensity (e Å-3)	0.27; -0.35	0.45; -0.86	1.33; -0.40

Table 2.13: Crystallographic data for **9**, **12** and **14**

Compound	9	12	14
Empirical formula	$C_{26}H_{20}CoN_2O_2$	$C_{38}H_{44}CoN_2O_2$	$C_{46}H_{60}CoN_2O_2$
Mr	451.4	619.7	731.9
Crystal system	orthorhombic	triclinic	triclinic
Space group	*Pbca*	$P\bar{1}$	$P\bar{1}$
a (Å)	9.798(1)	9.732(2)	10.996(3)
b (Å)	17.960(2)	10.653(2)	12.416(2)
c (Å)	24.829(3)	18.056(4)	16.382(3)
α (°)	90	93.937(7)	90.708(6)
β (°)	90	100.140(7)	102.865(9)
γ (°)	90	108.444(4)	98.330(8)
V (Å^3)	4369.0(9)	1732.4(7)	2155.0(8)
Z	8	2	2
$F(000)$	1864	658	786
Dcalc (g cm-3)	1.37	1.19	1.13
μ(MoKα) (cm^{-1})	8.10	5.29	4.34
Temperature (°C)	20(2)	20(2)	20(2)
2θ range (°)	$3.3 < 2\theta < 50.0$	$5.7 < 2\theta < 54.0$	$3.3 < 2\theta < 52.0$
Absorption correction	Empirical	Empirical	Empirical
Data/restraints/par.	3626 / 0 / 281	6858 / 0 / 397	7702 / 0 / 475
R_1 ($I > 2\sigma(I)$)	0.055	0.042	0.051
wR_2 (all reflections)	0.113	0.104	0.135
Max;min residual electron density (e Å^{-3})	0.21; -0.23	0.33; -0.36	0.41; -0.44

$R_1 = \Sigma \mid \mid F_o \mid - \mid F_c \mid \mid / \Sigma \mid F_o \mid$; $wR_2 = \{\Sigma[w(F_o^2 - F_c^2)^2 / \Sigma[w(F_o^2)^2)]\}^{1/2}$

2.5 REFERENCES

1. R. H. Holm, G. W. Everette, Jr., A. Chakravorty, *Prog. Inorg. Chem*. **1966**, *7*, 83.

2. K. Binnemans, D. W. Bruce, S. R. Collinson, R. van Deun, Y. G. Galymanetdinov, F. Martin, *Phil. Trans. R. Soc. Lond. A* **1999**, *357*, 3063.

3. N. Hoshino, *Coord. Chem. Rev*. **1998**, *174*, 77.

4. R. W. Date, E. Fernandez-Iglesias, K. E. Rowe, J. M. Elliott, D. W. Bruce, *Dalton Trans*. **2003**, 1914.

5. T.C.O. MacLeod, V.P. Barros, A.L. Faria, M.A. Schiavon, I.V.P. Yoshida, M.E.C. Queiroz , M.D. Assis, *J. Mol. Catal. A: Chem*. **2007** *273*, 259.

6. A. M. Da Costa Ferreira, M. L. Pires Dos Santos, E. M. Pereira, M. Oliveira Damasceno, W. A. Alves, *An. Acad. Bras. Ciênc*. **2000**, *72*, 51.

7. E.G. Jäger, J. Knaudt, M. Rudolph, M. Rost, *Chemische Berichte* **1996**, *129*, 1041.

8. Z. H. Chohan, A. Raup, S. Noreen, A. Scozzafava, C. T. Supuran, *J. Enz. Inhib. Med. Chem.* **2002**, *17*, 101.

9. P. P. Dholakiya, M. N. Patel, *Synth. React. Inorg. Met. Org. Chem*. **2002**, *32*, 753.

10. J. Ziegler, T. Schuerle, L. Pasierb, C. Kelly, A. Elamin, K. A. Cole, D. W. Wright, *Inorg. Chem*. **2002**, *39*, 3731.

11. A. D. Garnovsky, V. A. Bren, *ARKIVOC* **2005**, *7*, 1.

12. W. D. Kerber, D. L. Nelsen, P. S. White, M. R. Gagné, *Dalton Trans*. **2005**, 1948.

13. C. Wang, S. Friedrich, T. R. Youkin, R. T. Li, R. H. Grubbs, D. A. Bansleben, M. W. Day, *Organometallics* **1998**, *17*, 3149.

14. V. T. Kasumov, F. Koksal, *Spectrochimica Acta Part A* **2002**, *58*, 2199.

15. V. T. Kasumov, A. A. Medjidov, N. Yayli, Y. Zeren, *Spectrochimica Acta Part A* **2004**, *60*, 3037.

16. H. H. Freedman, *J. Am. Chem. Soc*. **1961**, *83*, 2900.

17. J. W. Ledbetter, *J. Phys. Chem.* **1977**, *81*, 54.

18. R.B. Coles, C.M. Harris, E. Sinn, *Inorg. Chem*. **1969**, *8*, 2607.

19. H. Chen, H-H. Wei, G-H. Lee, Y. Hung, *Polyhedron* **2001**, *20***,** 515.

20. E. Schön, D.A. Plattner, P. Chen, *Inorg. Chem*. **2004**, *43*, 3164.

21. K. Kurzak, I. Biernacka, B. Zurowska, *J. Solution. Chem.* **1999**, *28*, 133.

22. I. Biernacka, A. Bartecki, K, Kurzak, *Polyhedron* **2003**, *22*, 997

23. A. Parkin, G. Barr, A. Collins, W. Dong, C. J. Gilmore, P. A. Tasker, C. C. Wilson, *Acta Cryst.* **2007**, *B63*, 612.

24. V. T. Kasumov, A. Bulut, F. Köksal, M. Aslanoglu, I. Ucar, C. Kazak, *Polyhedron* **2006**, *25*, 1133.

25. O. Rotthaus, O. Jarjayes., F. Thomas, C. Philouze, E. Saint-Aman, J. Pierre, *Dalton Trans.*, **2007**, 889.

26. A. A. Khandar, K. Nejati, *Polyhedron* **2000**, *19*, 607.

27. C. Carlini, S. Giaiacopi, F. Marchetti, C. Pinzino, A. M. Galletti, G. Sbrana, *Organometallics* **2006**, *25*, 3659.

28. G. Xu, S. Yan, D. Liao, Z. Jiang, P. Cheng, *Acta Cryst*. **2005**, *E61*, m933.

29. S. Yamada, K. Yamanouchi, *Bull. Chem. Soc. Jpn*. **1982**, *55*, 453.

30. Q. Wang, X-Y. Qiu, *Acta Cryst*. **2006**, *E62*, m3000.

31. A. Altomare, G. Cascarano, C. Giacovazzo, A. Guagliardi, *J. Appl. Crystallogr*. **1993**, *26*, 343.

32. SHELX97 (Release 97-2). G. M. Sheldrick, Institut für Anorganische Chemie der Universität, Tammanstrasse 4, D-3400 Göttingen, Germany, (1998).

33. L. J. Farrugia, *J. Appl. Crystallogr*. **1999**, *32*, 837.

34. L. J. Farrugia, *J. Appl. Crystallogr*. **1997**, *30*, 565.

35. CCDC 622393 – 622395 and CCDC 657287 – 657289 contains the supplementary

crystallographic data for the copper and cobalt complexes discussed in this chapter.

These data can be obtained free of charge from The Cambridge Crystallographic

Data Centre *via* www.ccdc.cam.ac.uk/data_request/cif.

CHAPTER 3

SYNTHESIS AND CHARACTERIZATION OF SALICYLALDIMINE FUNCTIONALISED DENDRITIC LIGANDS AND METALLODENDRIMERS

CONTENT

3.1   INTRODUCTION

Anchoring transition metal complexes on polymer supports has been one of the most investigated methods of catalyst immobilization. This typically involves anchoring transition metal catalysts on a linear polymeric chain thus allowing the catalyst to retain its homogeneous nature. Alternatively the catalyst can be included into the voids of a cross-linked polymer producing an insoluble catalyst. The efficiency of the catalytic process for both types of immobilized polymeric catalysts is usually governed by accessibility of the reactants to the catalytic active site. In the case of cross-linked polymeric catalysts, catalysis occurs within the voids of the polymer matrix and thus mass transport limitations affect efficiency. However in the case of linear polymeric catalysts accessibility to the active sites depends on conformation of the polymeric chain which in turn depends on the solvent medium as well as the temperature of the catalytic process [1].
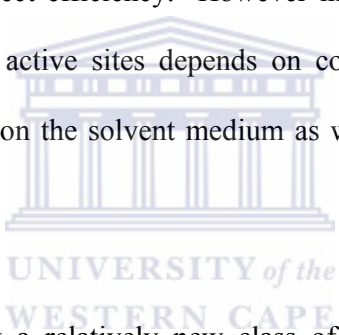
Dendritic polymers represent a relatively new class of macromolecular architecture which can be divided into four subclasses based on the relative degree of control within the structures of these molecules. These subclasses are hyperbranched polymers, dendrigraft polymers, dendrons and dendrimers. Structural representation of these macromolecular systems is provided in Figure 3.1 [2]. Hyperbranched polymers represent the class of dendritic polymers which have the least degree of control in terms of the polymeric architecture. This class of dendritic polymers were first hypothesized by Flory and are generally prepared by a one pot synthesis using AB_2-type monomers [3]. They are known for the statistical nature of their structures and have broad polydispersities. Dendrigraft polymers are a much more recent contributions to the dendritic polymer subset which were independently developed by Tomalia et al. and

Gauthier et al. [4, 5]. They are constructed from oligomers or polymers and as a result the structures of these polymers are much more ordered compared to hyperbranched polymers. The structures of dendrigrafts are typically very big and ultrahigh molecular weight polymers are obtainable. Dendrons and dendrimers represent the subsets of dendritic polymers which have a high degree of control in their molecular architecture. Both of these polymers are characterized by their three dimensional highly branched structure, which are of well-defined size. In addition these molecules have narrow polydispersities. They are constructed in a step wise manner using either a divergent or a convergent approach [6, 7].

Hyperbranched polymer   Dendrigraft polymer   Dendron   Dendrimer
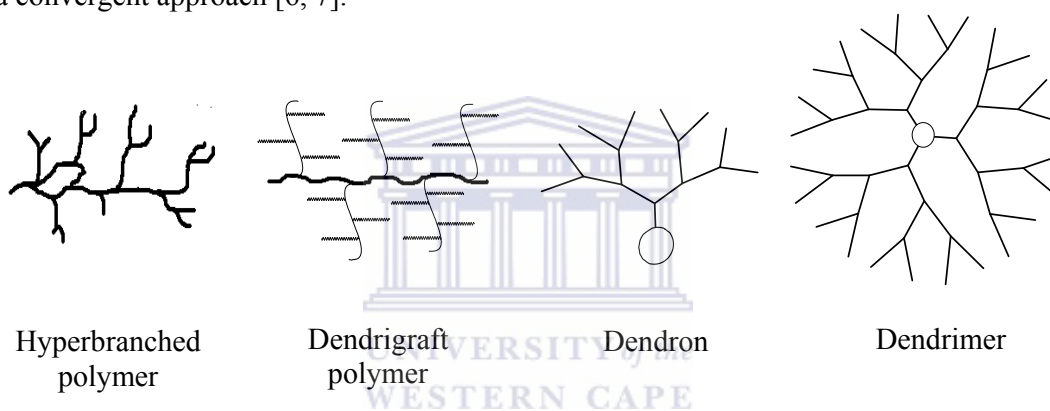
Figure 3.1: *Structural representation of the different subclasses of dendritic architectures [2].*

Dendrimers can structurally be divided into three main segments, viz. the core, repeating branch cells (generations) and peripheral groups (Figure 3.2). Each segment contributes to the structural characteristics of the dendrimeric architecture as well as to the physical and chemical properties of the dendrimers. For instance high generation dendrimers may form rigid spheroid, ellipsoid or cylindrical structures depending on the geometrical shape of the core. This was very eloquently demonstrated by Hecht and Fréchet in a review in which they discussed the wide array of core functionalities utilized to obtain either cylindrical or spheroid dendritic architectures [8].

C : represent dendritic core functionality

P : represent end groups on pheripery of dendrimer

Gn : represents branch subcells of denritic structure, where Gn denotes generation number.
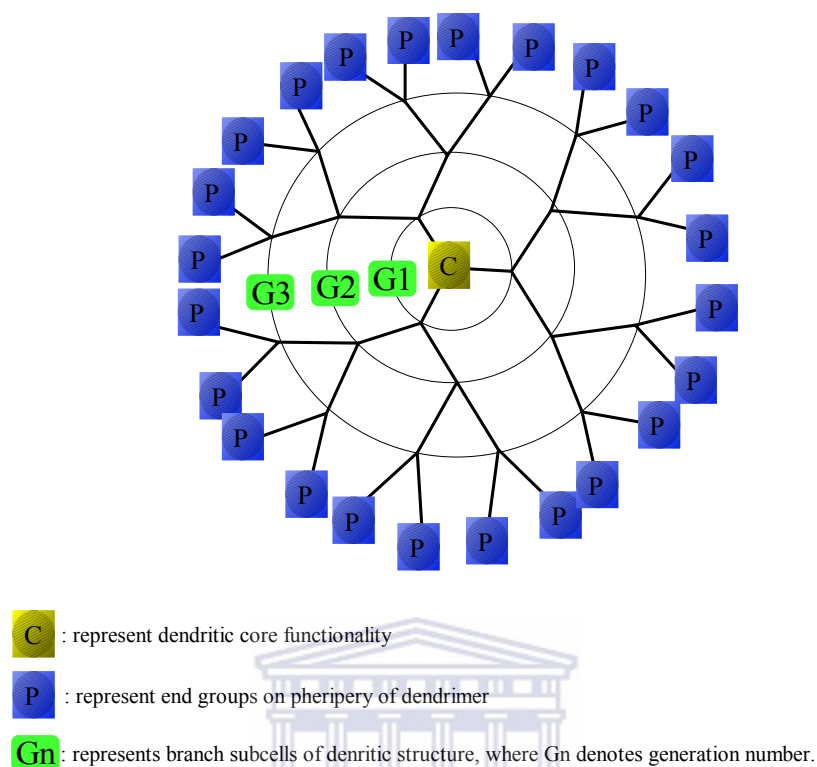
Figure 3.2: General structural representation of a dendritic structure.

In Chapter 1 various strategies were discussed in which homogenous catalytic systems have been heterogenised in an attempt to bridge the gap between traditional homogeneous and heterogeneous catalysts. Finding a means of integrating the advantages of both these catalytic technologies ultimately allows for the development of *greener* commercial processes which are environmentally and economically sustainable. An attractive approach to reaching this goal has been to incorporate metal centres into the dendritic framework. The inclusion of metal centres within the dendritic architecture can be achieved in various ways (Fig. 3.3) producing a wide variety of metallodendritic archetypes which have been shown to be useful in a wide variety of catalytic processes. The synthesis of metallodendrimers is typically achieved using the same methodologies developed for their non-metallated counterparts. The inclusion of

metal centres within the dendritic architecture has been reviewed by several authors [9, 10].

(a) **(b)** **(c)**

(d) **(e)** **(f)**
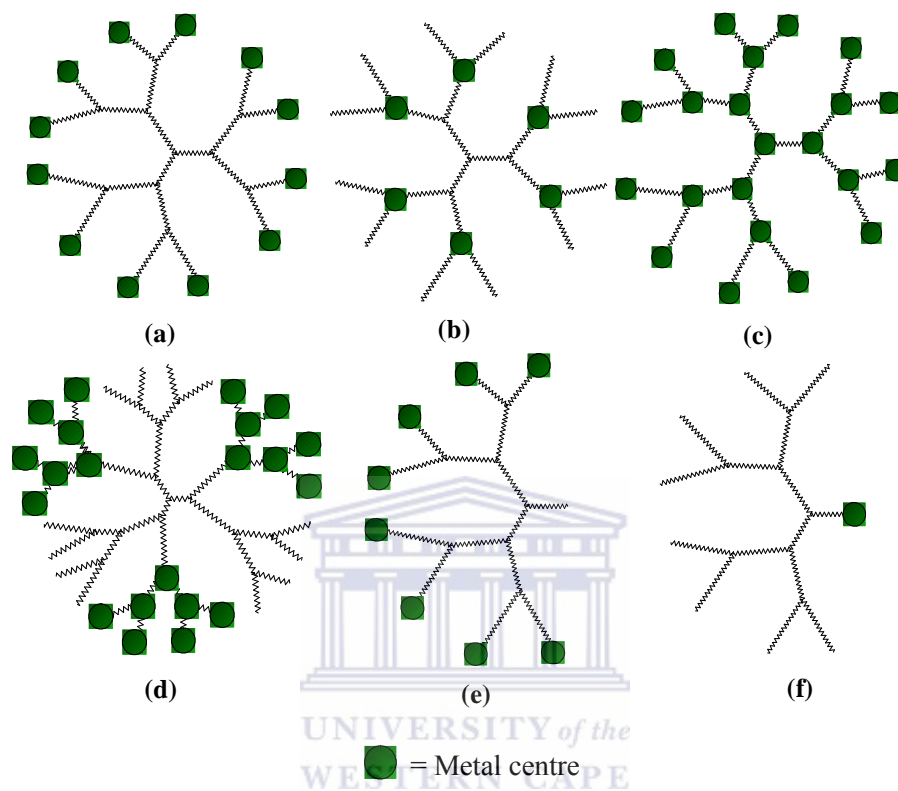
= Metal centre

Figure 3.3: Various metallodendritic archetypes which show inclusion of metal centres within the structure of the dendrimers.

The value of these macromolecules is in their unique architecture which allows the synthesis of catalysts with well defined micro-environments. Utilizing dentritic scaffolds to develop new catalysts not only provides a means of obtaining reusable catalyst systems but also potentially allows the development of catalysts with much higher activities than typical homogeneous catalysts. These metallodendrimers contain multiple metal centers which are incorporated into the dendrimer framework and site isolation of these catalytic sites prevents deactivation pathways possible with typical

homogeneous catalytic systems. Although dendritic catalysts do not nearly have the same amount of available active sites compared to conventional heterogeneous catalyst, the fact that the molecular structure of the active sites are known allows tailoring of the catalysts for process optimization. This is not possible for typical heterogeneous catalyst since very little information about the active site is known. Another attribute which makes dendrimers desirable candidates is the observation often of a positive dendritic effect where an increase in catalytic activity is observed in going from a low generation to a higher generation. This positive dentritic effect is often attributed to an increase in the number of active sites available on going from a lower generation to a higher generation. Several accounts of cooperative effects have also been reported for catalytic processes mediated by dendrimeric catalysts [11]. Usually cooperativity is observed for enzymes to assist with catalysis, via substrate binding and substrate recognition.

Immobilization of transition metal complexes on soluble supports has meant that the homogeneous nature of the catalytic process is maintained. However the catalyst can still be recovered using suitable membranes. Several accounts of the application of dendrimeric catalysts in continuous catalytic processes have appeared [12]. Research conducted to affect separation of enlarged homogeneous catalysts from reaction mixtures and also to develop potential continuous catalytic processes has been the driving force in the area of membrane filtration systems which are suitable for catalyst-product separation of enlarged homogeneous catalysts. Thus filtration strategies have been developed to achieve separation of a wide variety of enlarged catalysts which is based on the molecular size of the species to be retained. In recent years there have been significant advances in polymeric membranes and their application in reactors for continuous process has been discussed by Vankelecom in a review [13].

The suitability of a particular enlarged homogeneous catalyst for continuous catalysis is generally determined by the retention of the catalyst in a continuous reactor with a suitable membrane [14]. It has widely been established that a retention of 99.9% is required for a catalysts to be deemed suitable for continuous catalysis. This requirement has been determined by several researchers who have shown that retention which is marginally lower than the above mentioned value results in losses which are unacceptable by industrial standards [14]. Thus the retention factor of the enlarged soluble catalysts is an important criterion for these catalysts to be viable from an industrial point of view.

In this chapter the synthesis and characterization of peripheral functionalised salicylaldimine poly(propyleneimine) dendrimers and metallodendrimers of these ligands systems are discussed. The multi-functional salicylaldimine ligands were obtained by modifying the peripheral groups of the poly(propyleneimine) dendrimer (DAB-$(NH_2)_n$) which is commercially available. Copper(II) and cobalt(II) complexes of the functionalised dendritic ligands were obtained by reacting the ligands with appropriate acetate salts of the respective metals. The functionalised dendritic ligands and metallodendrimers were characterised using NMR spectroscopy, elemental analysis, FT-IR spectroscopy, UV-Vis spectroscopy, ESI mass spectrometry and thermogravimetric analysis (TGA).

3.2   RESULTS AND DISCUSSION

3.2.1   *Synthesis of salicylaldimine peripheral functionalised DAB dendrimers.*

First and second generation poly(propyleneimine) dendrimers containing the salicylaldimine functionality on the periphery were obtained by reacting the appropriate

2-hydroxybenzaldehyde with commercial samples of the G1-DAB-$(NH_2)_4$ and G2-DAB-$(NH_2)_8$ dendrimers using a dendrimer to aldehyde ratio of 1:4 (for **DL^1** and **DL^2**) and 1:8 (for **DL^3** and **DL^4**) respectively. The synthetic strategy utilised is based on the synthesis of pyraldimine functionalised poly(propyleneimine) dendrimers synthesized by Mapolie et al. [15, 16]. A schematic representation of the synthesis of functionalised first generation dendritic ligands is shown in Scheme 3.1. A similar procedure was utilised to obtain the second generation (Fig. 3.4) systems. Both the first and second generation crude functionalised dendrimers were obtained as yellow oils, however after extensive purifications steps, which consisted of extraction of dichloromethane solutions of the crude ligands with water, the ligands **DL^1**, **DL^2** and **DL^4** were obtained as yellow powders. Ligand **DL^3** was only obtained as a yellow oil despite several purification attempts. All the dendritic ligands are very soluble in organic solvents such as dichloromethane, tetrahydrofuran, acetone and diethyl ether and are air stable.
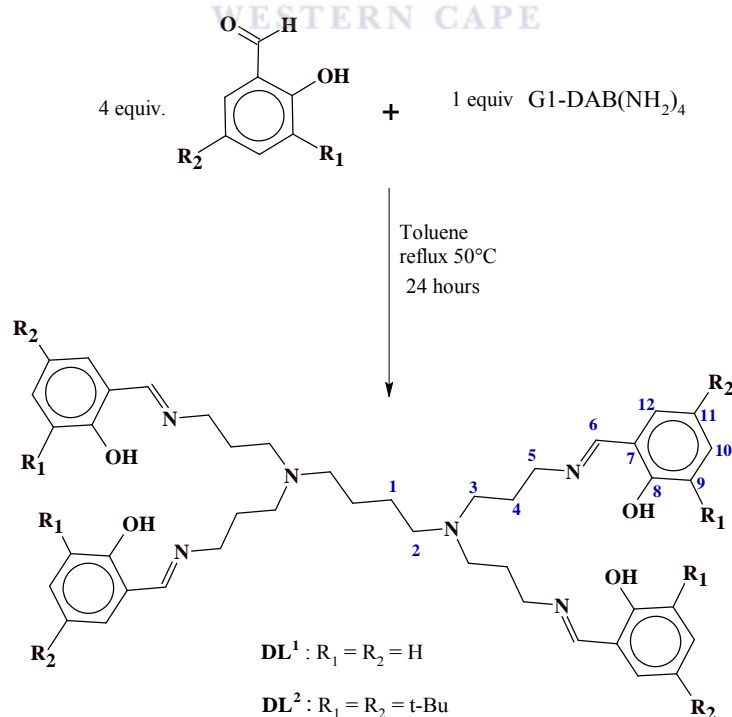
Scheme 3.1: *Synthesis of first generation salicylaldimine DAB dendrimers* **DL^1** *and* **DL^2**

3.2.1.1   <u>*^{1}H-NMR and {^{1}H} ^{13}C-NMR studies of the dendritic ligands*</u>

All the functionalised dendrimers prepared were characterized by ^{1}H-NMR and {^{1}H}^{13}C-NMR spectroscopy in CDCl$_3$. The spectra obtained for the ligands confirmed the symmetrical nature of the dendritic structures. Spectroscopic data obtained for both the first (G1) and second (G2) generation peripheral functionalised dendrimers are provided in Tables 3.1 and 3.2. Typical spectra obtained for the G1 and G2 systems are shown in Figure 3.5. Successful condensation of the NH$_2$ groups on the surface of the dendritic scaffold with the aldehyde was confirmed by the appearance of a sharp singlet at approximately 8.3 ppm in the spectra of all the ligands which is due to the <u>H</u>C=N proton.   The dendritic ligands containing no substituents on the aromatic ring originating from the aldehyde contained a broad singlet at δ13.57 ppm in the spectra of **DL**^{1} and the G2 analogue **DL**^{3} due to the exchangeable phenolic OH proton.   The resonance for this proton appears as a sharper singlet at δ13.92 ppm in the spectra of **DL**^{2} and **DL**^{4}.   The difference in appearance of the signal is ascribed to the electron donating ability of the *tert*-butyl groups in **DL**^{2} and **DL**^{4} which strengthens the O-H bond and thus reduces the exchangeability of this proton.   The presence of this signal in the spectra of all four ligands indicates the phenol-imine tautomer is dominant for the dendritic ligands.

The aromatic rings protons for **DL**^{1} and **DL**^{3} are observed as a set of two multiplets centred at approximately δ6.9 and δ7.2 ppm, whereas the aromatic protons for **DL**^{2} and **DL**^{4} are observed as a set of two doublets at approximately δ7.0 ppm and δ7.3 ppm. The CH$_2$ protons for the dendritic scaffold appear in the range δ1.4–3.6 ppm for all four ligands.   In the spectrum of **DL**^{1} (Figure 3.5) the proton signals of C1 and C2 (Scheme 3.1) appear as broad singlets.
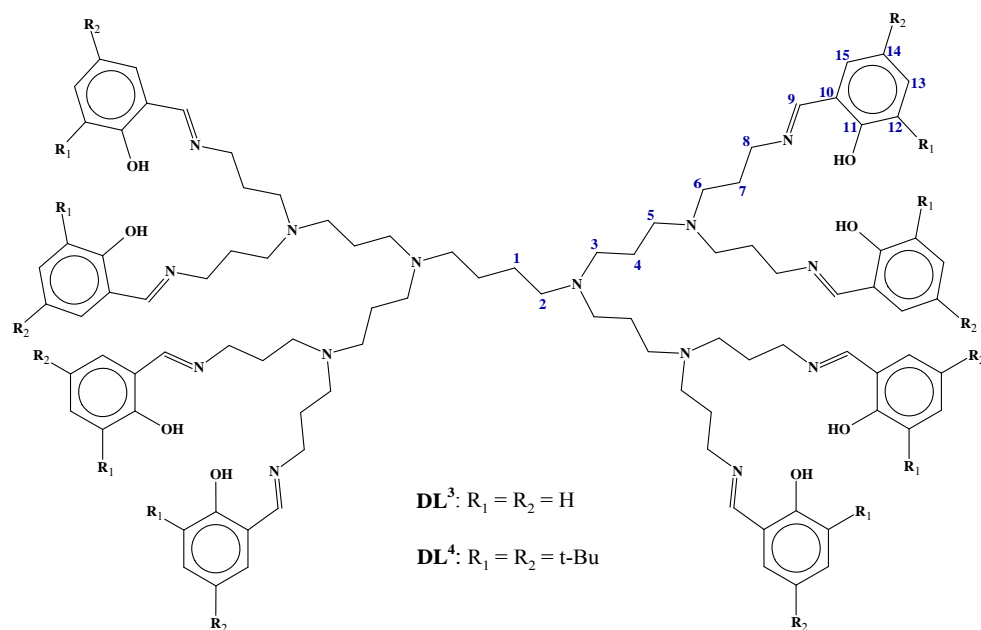
Figure 3.4: *General structure of second generation salicylaldimine DAB dendrimers.*
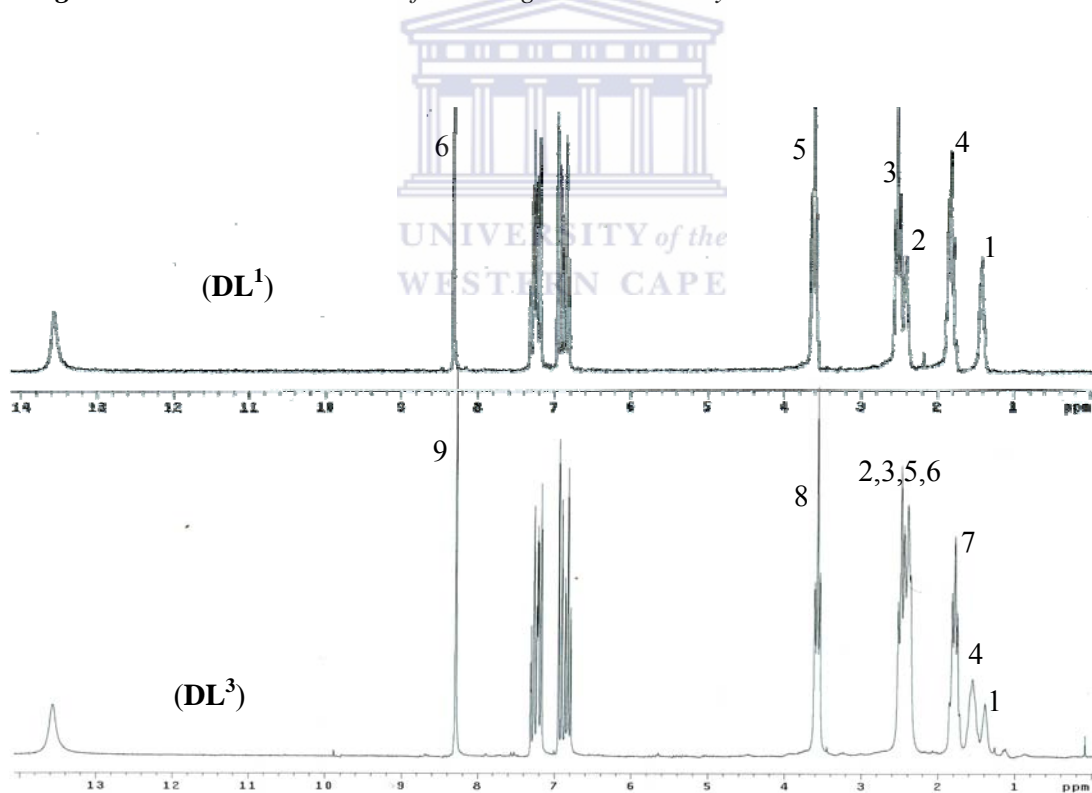
Figure 3.5: *¹H-NMR spectra of G1 (**DL¹**) and G2 (**DL³**) salicylaldimine functionalised poly(propyleneimine) dendrimers.*

The same broadening in the signals is observed for the proton signals of C1 and C4 in the spectrum of **DL**^{3} (Figure 3.5) as well as the proton signals of C6 due to overlap with the proton signals of C2, C3 and C5. The same phenomenon was observed by Schilf et al. in a NMR study conducted on G2-DAB systems containing the salicylaldimine functionality on the periphery [17]. Loss in fine structure was observed in proton signals of the dendritic framework as well as broadening of signals in the ^{13}C-NMR spectrum. The broadening of the signals was ascribed to the reduced mobility of the interior segment of the dendritic structure compared to the outer region of the dendritic framework which should be relatively more flexible. Signal broadening of the proton signals of the interior segment of PAMAM dendrimers were also observed by Haba et al. after polymerization of surface methacroyl groups incorporated on the surface of the dendritic structure which caused restricted molecular mobility of the interior segment of the dendritic structure [18]. The effect of signal broadening due to decreased mobility is also evident in the spectra of **DL**^{2} and **DL**^{4} which both show loss in fine structure of the signals of the protons of the dendritic framework. Both of these ligands contain two *tert*-butyl groups on the peripheral aromatic rings. In this case reduced mobility is ascribed to steric interactions of the bulky *tert*-butyl groups on the aromatic rings. The magnetically non-equivalent *tert*-butyl groups on the aromatic rings of **DL**^{2} and **DL**^{4} are observed as two singlets at δ1.40 ppm and δ1.29 ppm.

Similar to the proton NMR data the $\{^1H\}^{13}$C-NMR data confirms the symmetrical nature of the dendritic ligands which is evident in the ^{13}C-NMR spectra as seen from Figure 3.6 which shows the spectra of the G1 and G2 *tert*-butyl substituted dendritic ligands. The carbon signal for the HC=N group appears at approximately δ165 ppm in the spectra of all four ligands. The resonance of the carbon of the phenolic group

appears at approximately δ161 ppm for **DL**[1] and **DL**[3]. The resonance of this carbon is observed at δ158 ppm for ligands **DL**[2] and **DL**[4] and appears upfield relative to the signal observed in the spectra of ligands **DL**[1] and **DL**[3] due to electron donating ability of the *tert*-butyl groups. The other aromatic carbon signals appear in the range δ139 – 116 ppm for all four ligands. The carbon signals for the dendritic framework appear in the range δ57 – 25 ppm. The ^{13}C-NMR spectrum of ligand **DL**[4] also showed broadening of the carbon signals of C1, C2, C3, C4 and C5 (Fig 3.1) which once again is ascribed to restricted molecular mobility as previously mentioned and also observed by Schilf et al. [17].
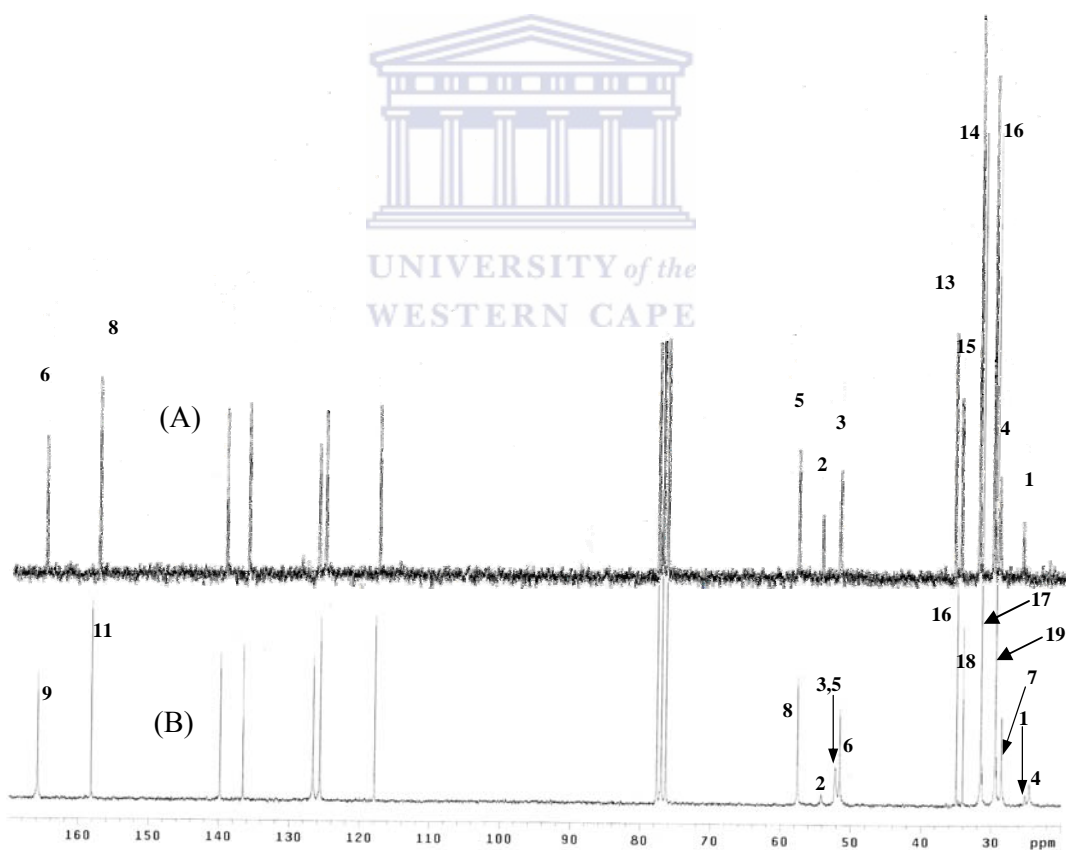
Figure 3.6: ^{13}C{^{1}H}NMR spectra of ligands **DL**[2] (A) and **DL**[4] (B) obtained in CDCl₃

Table 3.1: $\{^1H\}^{13}C$-NMR[a] shifts (δ in ppm) for first and second generation salicylaldimine functionalised dendritic ligands (**DL^n**).

Ligand	H$\underline{C}$=N	Ar-$\underline{C}$	$\underline{C}H_2$	$\underline{C}(CH_3)_3$	C($\underline{C}H_3)_3$
DL^1	164.77	161.26, 131.96, 131.04, 118.74, 118.33, 116.92	57.32, 53.96, 51.41, 28.48, 25.14	-	-
DL^2	165.79	158.21, 139.82, 136.64, 126.62, 125.65, 117.89	57.50, 54.10, 51.55, 28.64, 25.22	35. 00, 34.09	31.52, 29.46
DL^3	164.78	161.21, 131.96, 131.06, 118.71, 118.34, 116.89,	57.34, 54.07, 52.17, 52.05, 51.42, 28.45, 25.05, 24.52	-	-
DL^4	165.81	158.15, 139.81, 136.59, 126.63, 125.67, 117.84	57.60, 54.19, [b]52.22 51.57, 28.56, 24.62 24.54	34.99, 34.07	31.50, 29.44

[a] Spectra obtained in CDCl$_3$; [b] overlapping signals

3.2.1.2   *IR and UV-Vis Spectroscopic studies*

Infrared spectra of the dendritic ligands were obtained as dichloromethane solutions using a solution cell with sodium chloride windows. The ν(C=N) stretching mode for all the dendritic ligands is observed at ~1630 cm^{-1} (Table 3.3). This is significantly higher than what is observed for mono-functional salicylaldimine ligands such as those systems discussed in Chapter 2, where the band due to this functionality was observed in the region 1620 cm^{-1}. The band due to ν(C-O) is observed in the region 1275 – 1279 cm^{-1}, which is consistent with data obtained for mono-functional ligands.

Table 3.2: ^{1}H-NMR[a] shifts (δ ppm) for G1 and G2 salicylaldimine DAB dendritic ligands.

Ligand	O$\underline{H}$	$\underline{H}$C=N	Ar-$\underline{H}$	C$\underline{H}_2$	C(C$\underline{H}_3$)$_3$	C(C$\underline{H}_3$)$_3$
DL^1	13.57 (br s, 4H)	8.32 (s, 4H)	6.80 – 6.96 (m, 8H, J = 7.4 Hz); 7.19 – 7.32 (m, 8H, J 6.2 Hz)	1.41 (br s, 4H); 1.81 (t, 8H, J = 6.8Hz); 2.40 (br s, 4H); 2.51 (t, 8H, J =7.4Hz); 3.61 (t, 8H, J =6.6Hz)	-	-
DL^2	13.95 (s, 4H)	8.25 (s, 4H)	6.97 (d, 4H, J = 2.4 Hz); 7.27 (d, 4H, J = 2.0 Hz)	1.82(t, 8H, J =6.8Hz); 2.49(br s, 4H); 2.55(t, 8H, J =6.8Hz); 3.63(t, 8H, J =6.4Hz)	1.45 (s, 36H)	1.29 (s, 36H)
DL^3	13.57 (br s, 8H)	8.29 (s, 8H)	6.79 – 6.95 (m, 16H, J = 7.4 Hz); 7.17 – 7.31 (m, 16H, J = 7.8 Hz)	1.38(br s, 4H); 1.55(br s, 4H); 1.78(m, 16H, J =6.8Hz); 2.40(m, 40H, J =6.8Hz); 3.57(t, 16H, J =6.6Hz)	-	-
DL^4	13.92 (s, 8H)	8.33 (s, 8H)	7.05 (d, 8H, J = 2.0Hz); 7.31 (d, 8H, J = 2.0 HZ)	1.58(br s, 4H); 1.81(br m, 16H); 2.48(br m, 40H); 3.57(t, 16H)	1.43 (s, 72H)	1.29 (s, 72H)

[a] Spectra obtain in CDCl$_3$

s, singlet; d, doublet; t, triplet; m, multiplet

Table 3.3: Infrared and UV-Vis spectroscopic data for dendritic ligands.

Ligand	UV-Vis[a] λ_{max} (nm)	IR spectra (cm^{-1})[b]	
		$\nu(C=N)$	$\nu(C-O)$
DL[1]	228, 254, 315	1634	1279
DL[2]	231, 262, 328	1633	1275
DL[3]	229, 254, 315	1634	1279
DL[4]	231, 261, 328	1633	1276

[a] Obtained in dichloromethane

[b] Recorded as CH_2Cl_2 solutions with solution cell containing NaCl windows.

The UV-VIS absorption spectra of the dendritic salicylaldimine ligands were obtained in dichloromethane and the observed absorption bands are shown in Table 3.3. The spectra of all four ligands were composed of three bands which are fairly typical for Schiff bases absorption spectra [19]. The first two bands with absorption maxima at $\lambda_{max} = 228–231$ nm and $\lambda_{max} = 255–263$ nm are associated with intra-ligands $\pi \rightarrow \pi^*$ transitions of the benzene ring. The third absorption band observed at $\lambda_{max} = 314 – 329$ nm is associated with the transition due to $n \rightarrow \pi^*$, which involves the C=N chromophore.

In the case of ligands **DL**[2] and **DL**[4] the absorption peaks show bathochromic shifts in the positions of all three bands when compared to peaks positions observed for **DL**[1] and **DL**[3], which is as result of the presence of the *tert*-butyl substituents on the salicylaldimine backbone. It is well known that substituents on the aromatic rings of salicylaldimines, as well as the polarity of the solvent, influence the positions of the absorption peaks of the

first two transitions. This fact was demonstrated by Hammud et al. in a study investigating the influence of substituents as well as solvent polarity on the absorption bands for several salicylaldimine and benzaldimine systems [20]. Bathochromic shifts are generally associated with stabilization of the electronically excited state relative to the ground state in the case of Schiff bases.

3.2.1.3   *ESI-Mass spectrometry studies and elemental analysis*

The elemental analysis data obtained for the dendritic ligands are shown in Table 3.4 and were in agreement with proposed formulation shown in Scheme 3.1 and Figure 3.4. All four salicylaldimine functionalised dendritic ligands were characterised by electron spray ionization mass spectrometry which confirmed unambiguously the formulae of the expected dendritic compounds. Typical mass spectra obtained for the G1 and G2 ligands are shown in Figures 3.7 and 3.8 respectively. The observed parent ion m/z values for the ligands are provided in Table 3.4. The spectra of the first generation ligands, **DL**^{1} and **DL**^{2}, both show the presence of adducts due to [M+Na]$^+$ and [M+K]$^+$ and as a result very complex mass spectra for the first generation systems are obtained. These species are not observed in the spectra of the G2 ligands **DL**^{3} and **DL**^{4}, however multiply charged species (m/z where z = 2–4) for the G2 systems are observed. The fragmentation pattern for the two G1 ligands **DL**^{1} and **DL**^{2} were fairly similar. Both showed fragments due to the hydrolysis of the imine bond of one of the salicylaldimine units as well as the formation of a cyclic quaternary ammonium ion species due to an intramolecular nucleophilic substitution reaction. A similar cyclic quaternary ammonium species is observed in the spectra of the G2 ligands. A possible fragmentation mechanism for the formation of the

quaternary ammonium ion for G2 ligand **DL**[3] is provided in Figure 3.8. These fragmentation species are consistent with fragmentation patterns observed for $DAB(NH_2)_n$ dendrimers as well as other functionalised analogues [21, 22]

Table 3.4: Elemental analysis and ESI mass spectrometry data for dendritic ligands **DL**[n].

Ligand M.p. (°C)	Formula	[MH$^+$] (calcd) m/z	Anal Found (Calcd.)		
			C	H	N
DL[1] 52 – 53	$C_{44}H_{56}N_6O_4$	733.3 (733.9)	71.93 (72.10)	7.91 (7.70)	11.49 (11.47)
DL[2] 105 – 107	$C_{76}H_{120}N_6O_4$	1182.6 (1182.8)	77.43 (77.24)	10.17 (10.23)	6.71 (7.11)
DL[3] oil	$C_{96}H_{128}N_{14}O_8$	1607.05 (1607.1)	71.07 (71.79)	8.28 (8.03)	11.76 (12.21)
DL[4] 63 – 65	$C_{160}H_{256}N_{14}O_8$	2504.09 (2504.8)	76.18 (76.75)	10.35 (10.31)	8.03 (7.83)

3.2.2   Synthesis and characterization of copper and cobalt metallodendrimers

The G1 copper metallodendrimers **16** and **17** as well as their G2 analogues **20** and **21** were readily obtained by the reaction of the appropriate dendritic ligand with copper acetate monohydrate using stoichiometric amounts as shown in Scheme 3.2. All the copper(II) metallodendrimers precipitated from solution as green powders, which were isolated in yield of 63 – 75%.
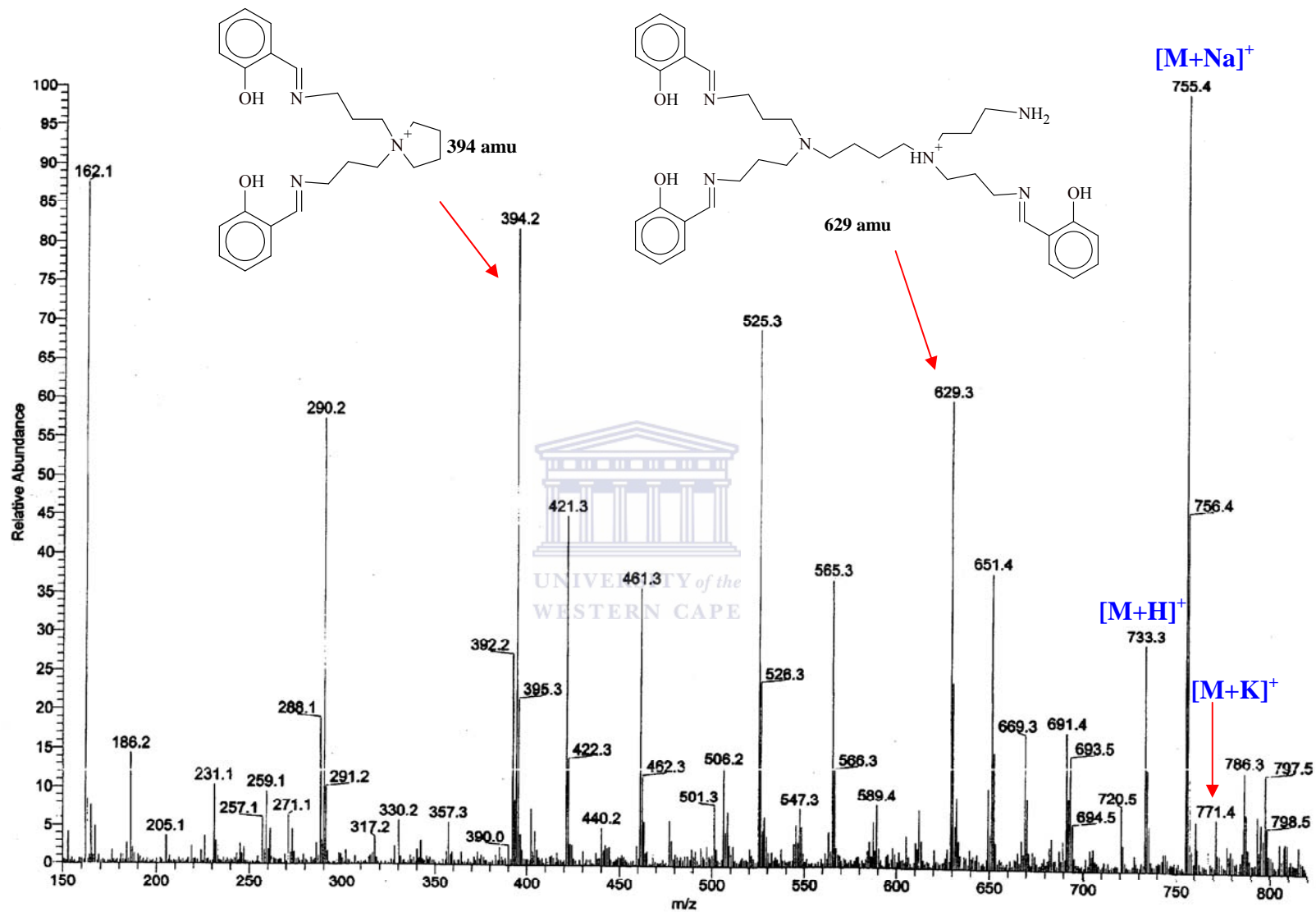
Figure 3.7: *ESI mass spectrum of the G1 ligand **DL¹** which shows adducts due to [M+H]⁺, [M+Na]⁺ and [M+K]⁺. Other significant fragments formed are also indicated.*
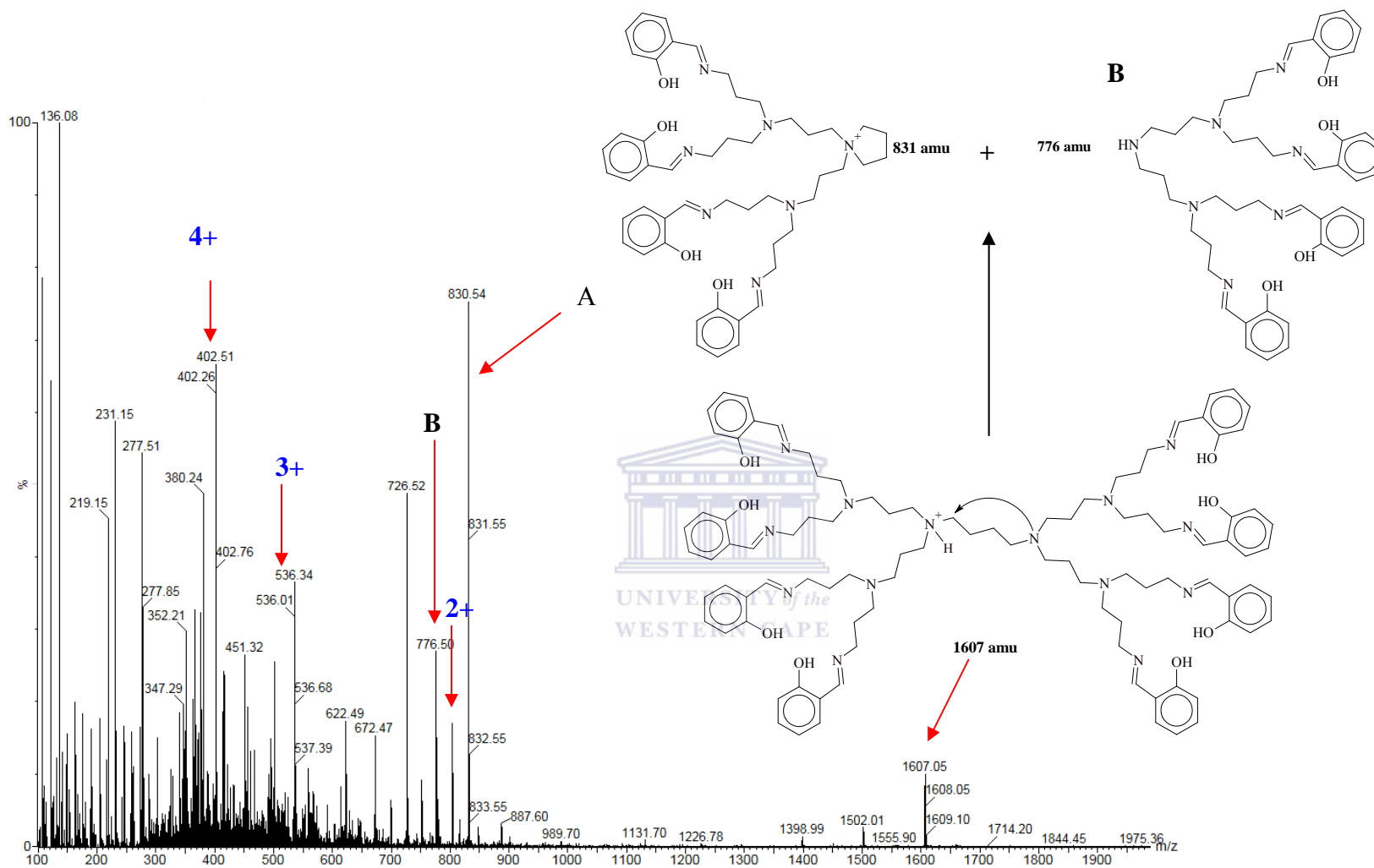
Figure 3.8: *ESI mass spectrum of the G2 ligand* **DL³**.

The synthesis of the cobalt metallodendrimers was performed using a slightly modified protocol as was used for the mononuclear *N*-(aryl)salicylaldimine cobalt complexes discussed in Chapter 2. The desired metallodendrimers were obtained by reacting the dendritic ligands with cobalt acetate tetrahydrate in the presence of sodium hydroxide. All four cobalt metallodendrimers were obtained as dark brown solids in yields of 60 – 70%.

The copper(II) complexes were observed to be very stable in solution as well as in the solid state. However the cobalt(II) complexes although stable in the solid state was prone to slow oxidation in solution a phenomenon also observed with the *N*-(aryl)salicylaldimine systems as mentioned in Chapter 2 [23]. The complexes based on both metals showed good solubility in dichloromethane and THF. Attempts to characterize these complexes with ^{1}H-NMR produced spectra with very broad and poorly defined peaks which was indicative of the paramagnetic nature of the complexes. Characterization of these metal complexes was thus performed with FT-IR, UV-Vis, elemental analysis, ESI mass spectrometry and thermogravimetric analysis (TGA).

3.2.2.1 *IR spectra and UV-Vis spectroscopy*

Infrared spectra of coordinated salicylaldimines generally show distinctive shifts in the bands due to ν(C=N) and ν(C-O). However the IR data obtained for Cu(II) and Co(II) salicylaldiminato metallodendrimers show only a slight shift in the position of the ν(C=N) band, on the other hand the band due to ν(C-O) shows a positive shift of ~47 cm^{-1} in the spectra of the metal complexes relative to the position observed in the spectra of the uncoordinated ligands [24].

16 : R$_1$ = R$_2$ = H; M= Cu
17 : R$_1$ = R$_2$ = t-Bu; M = Cu
18 : R$_1$ = R$_2$ = H; M= Co
19 : R$_1$ = R$_2$ = t-Bu; M = Co
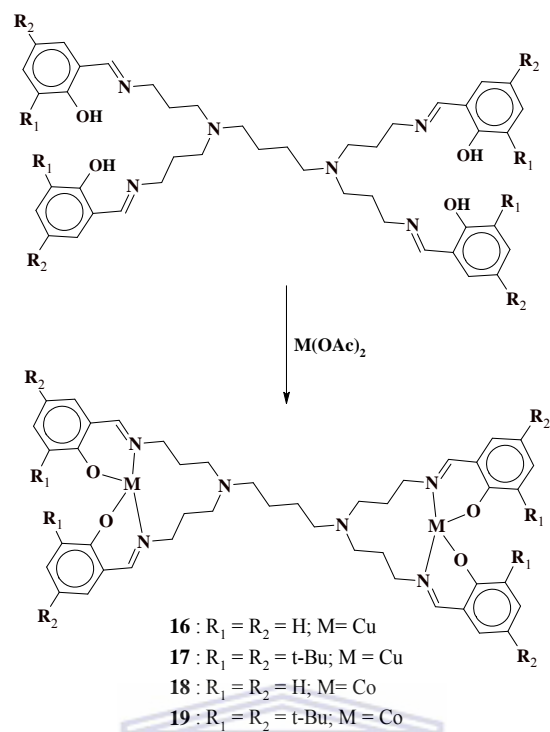
Scheme 3.2*: General procedure for the synthesis of G1 copper(II) and cobalt(II) metallodendrimers.*

20 : R$_1$ = R$_2$ = H; M = Cu
21 : R$_1$ = R$_2$ = t-Bu; M = Cu
22 : R$_1$ = R$_2$ = H; M = Co
23 : R$_1$ = R$_2$ = t-Bu; M = Co
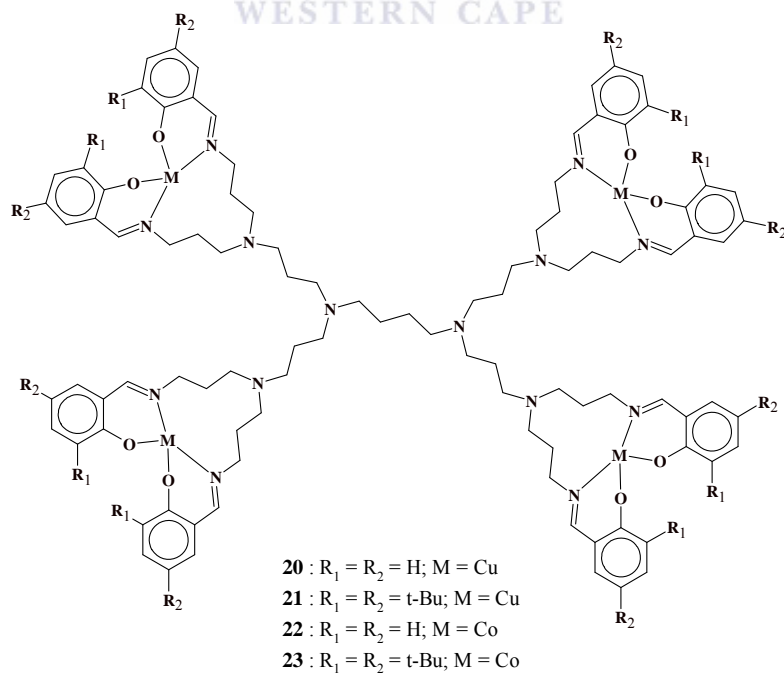
Figure 3.9*: General structure of G2 copper(II) and cobalt(II) metallodendrimers.*

Table 3.5: Infrared and UV-Vis spectroscopic data for copper(II) and cobalt(II) metallodendrimers.

Complex	UV-Vis λ_{max} (cm^{-1})	IR spectra (cm^{-1})[a]	
		ν(C=N)	ν(C-O)
16	241, 272[b], 304[b], 369	1634	1325
17	233, 280[b], 310[b], 377	1632	1326
20	237, 269[b], 304[b], 370	1634	1325
21	234, 277[b], 317[b], 377	1632	1325
18	239, 348	1630	1306
19	239, 359	1630	1319
22	239, 360	1634	1308
23	237, 358	1631	1321

[a]: Recorded as CH$_2$Cl$_2$ solutions with solution cell containing NaCl windows.

[b]: Shoulder

The UV/Vis spectra for the metallodendrimers were obtained in dichloromethane and the absorption peaks observed for the complexes are shown in Table 3.5. In the case of the copper metallodendrimers four bands are observed in the spectra of the investigated coordination systems. The first two absorption maxima observed in the range 233 -241 nm and 269-280 nm are assigned to intra ligand $\pi \rightarrow \pi^*$ transitions of the aromatic ring and the third band in the range 304-317 nm is assigned to the n $\rightarrow \pi^*$ transitions of the azomethine chromophore. A fourth band not observed in the spectra of the ligands in the range 369-377 nm was attributed to a metal to ligand charge transfer (MLCT) transition which involves electrons in the n orbital of the C=N functionality. The spectra of the investigated Co(II) metallodendrimers show only two broad bands with absorption maxima at 237-239 nm associated with the intra ligand $\pi \rightarrow \pi^*$ transitions and 348-360 nm associated with metal to ligand charge transfer (MLCT) transitions [24]

3.2.2.2 *Electron spray ionisation mass spectrometry*

The elemental analysis data obtained for the dendritic complexes are shown in Table 3.6. The data indicates that solvent molecules are included within the dendritic framework, which is a typical observation for dendritic complexes. All metallodendrimers synthesised were analysed with electron spray ionisation (ESI) mass spectrometry, which and confirmed the expected molecular weights of the obtained compounds. Observed m/z values for parent ions of the metallodendrimers are provided in Table 3.6. All copper dendrimers showed high mass ions due to $[MH]^+$, whereas for the cobalt complexes parent ions were observed. The fragmentation patterns for the complexes were very different compared to those of the dendritic ligands. The fragmentation pattern of G1 copper metallodendrimer **16** was observed to be much more complex compared to the fragmentations observed for the other G1 systems. The most abundant species (m/z 751) in the spectrum of **16** was a fragment produced due to the loss of a phenolic ring of one of the salicylaldimine units. This was followed by the loss of the oxygen of one of the remaining phenolic groups as H_2O, followed by the loss of the aromatic ring followed by loss of oxygen of one of the remaining phenolic groups as H_2O and then loss of one of the copper centres. Fragmentation patterns of the other G1 systems were comparatively simple.

The most abundant species in the mass spectra of dendrimers **17**, **18**, and **19** was the molecular ion peak of these particular compounds. Dendrimer **18** showed almost exclusively the presence of the molecular ion whereas for **17,** a fragment due to the loss of one copper centre was observed and for **19** a fragment due to the loss of one of the *tert*-butyl groups of the aromatic rings.

Table 3.6: Elemental analysis and ESI mass spectrometry data for copper and cobalt metallodendrimers.

Complex	Formula	$[M+H]^+$ (calcd.) m/z	Anal Found (calcd.)		
			C	H	N
16	$C_{44}H_{52}Cu_2N_6O_4 \cdot \frac{1}{2}H_2O$	857.2 (857.01)	60.88(60.51)	5.98(6.12)	9.53(9.63)
17	$C_{76}H_{116}Cu_2N_6O_4 \cdot 2EtOH$	1305.6 (1305.86)	68.71(68.78)	9.94(9.24)	6.28(6.02)
20	$C_{96}H_{120}Cu_4N_{14}O_8 \cdot 3CH_2Cl_2$	1853.7 (1853.25)	54.36 (54.79)	6.62(7.09)	9.94 (9.32)
21	$C_{160}H_{258}Cu_4N_{14}O_8 \cdot 4CH_2Cl_2$	2750.8 (2750.96)	63.07 (63.26)	8.72 (8.56)	5.49 (6.07)
18	$C_{44}H_{52}Co_2N_6O_4 \cdot H_2O$	[a]846.1 (846.79)	61.30(61.11)	6.90(6.29)	10.00(9.72)
19	$C_{76}H_{116}Co_2N_6O_4 \cdot \frac{1}{2}CH_2Cl_2$	[a]1295.6 (1295.64)	68.71(68.66)	8.87(8.81)	6.05(6.28)
22	$C_{96}H_{120}Co_4N_{14}O_8 \cdot 3CH_2Cl_2$	[a]1833.7 (1833.80)	56.46(56.93)	6.41(6.08)	9.09(9.39)
23	$C_{160}H_{258}Co_4N_{14}O_8 \cdot H_2O$	[a]2731.8 (2731.50)	69.76(69.89)	9.47(9.16)	6.69(7.13)
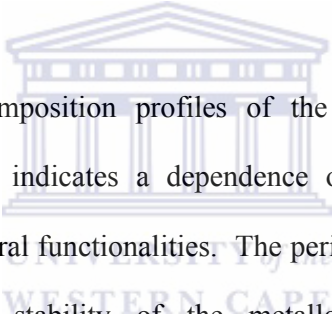
[a] represents $[M]^+$

The G2 systems showed relatively more complex fragmentation patterns. As for the ligands the spectra also showed adducts due to multiply charged species. Metallodendrimer **22** was the only system for which the parent ion was observed to be the most abundant species. All other G2 dendrimers showed a very low abundance of the parent ion of the metal complexes.

3.2.2.3   *Thermogravimetric analysis*

All metallodendrimers were analysed with thermogravimetric analysis (TGA). Thermograms obtained for the unsubstituted complexes (**16**, **18**, **20**, and **22**) and *tert*-butyl substituted complexes (**17**, **19**, **21**, and **23**) are provided in Figure 3.10 and Figure 3.11 respectively. The decomposition profiles obtained for the two different types of peripheral functionalised metallodendrimers (unsubstituted and *tert*-butyl substituted) were significantly different. However the thermograms obtained for a particular series of metallodendrimers were observed to be fairly similar. For instance the series of metallodendrimers **16**, **18**, **20** and **22** showed decomposition curves (Fig. 3.10) with several steps in the profile. In the case of the copper metallodendrimers **16** and **20** two step are observed which show roughly the same percentage mass loss for the two generations of dendrimers. The first stage of the decomposition, which occurs at 300°C, reflects a mass loss of approximately 20% in the initial mass. For metallodendrimer **16** this could possibly be due to the loss of one of the metal centres as well as two of the phenolic rings, while for **20** this could possibly be due to the loss of two metal centres and four phenolic rings. The loss of the phenolic ring from the Schiff base moiety as a free radical has been reported by El-Said [25]. The second stage occurs at 380°C and reflects a mass loss of approximately 23% and is also the final step in the decomposition, most likely to the metal oxide. The thermogram of the

unsubstituted Co(II) metallodendrimer **17** showed the decomposition of the complex to occur in three stages. However the G2 analogue of this complex (**21**) showed several overlapping steps in its thermogram. Thus for the unsubstituted cobalt systems the mechanism of decomposition appears to slightly more complex than for the analogous copper systems. The TGA curves obtained for the series of metallodendrimers **17**, **19** and **21** showed the decomposition to proceed via a single step process, while for the Co(II) metallodendrimer **23** a second step is observed at 400°C. In the case of **17**, **19** and **21** a mass loss of approximately 80% was observed which is attributed to decomposition of the dendrimeric ligands thus producing the corresponding metal oxides.

The difference in the decomposition profiles of the unsubstituted and tert-butyl substituted metal complexes indicates a dependence on the decomposition of the metallodendrimers on peripheral functionalities. The peripheral functional groups were also observed to increase stability of the metallodendrimers since onset of decomposition was observed to be at a higher temperature for the tert-butyl functionalised dendrimers compared to unfunctionalised counter parts. A similar observation was made by Newkome et al. in the TGA analysis of DAB metallodendrimers containing ruthenium terpyridine functionalities on the periphery of the dendrimers. Each ruthenium terpyridine unit contained different functional groups on the peripheral terpyridine units. The onset of decomposition was observed to be dependent on the nature of the functional groups on the periphery of the metallodendrimers [26].
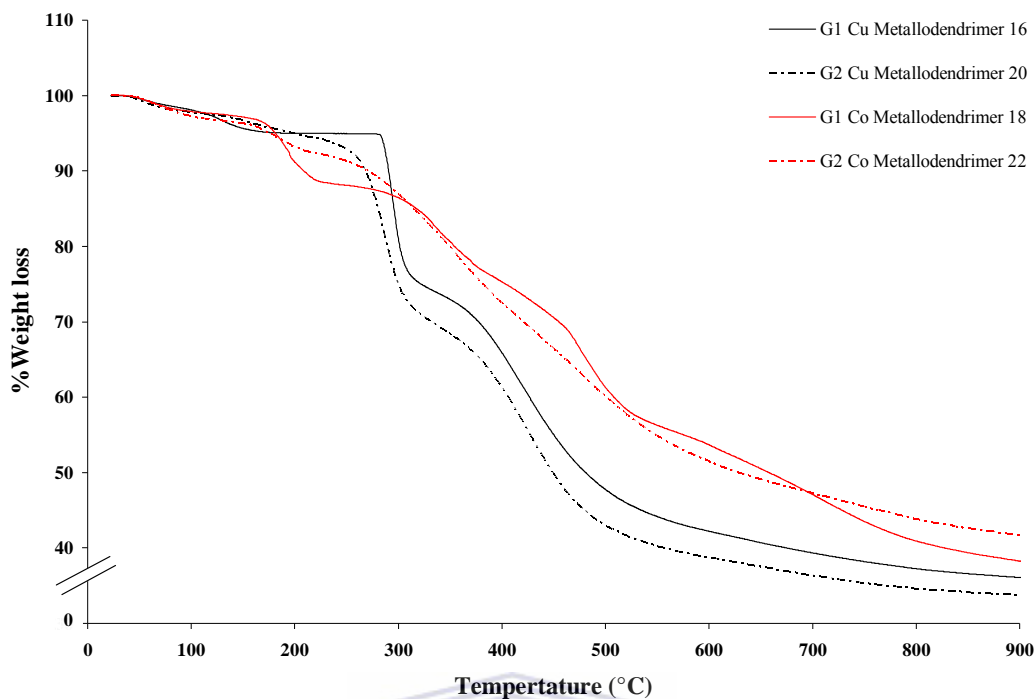
Figure 3.10*: Thermograms obtained for unsubstituted copper(II) and cobalt(II) metallodendrimers.*
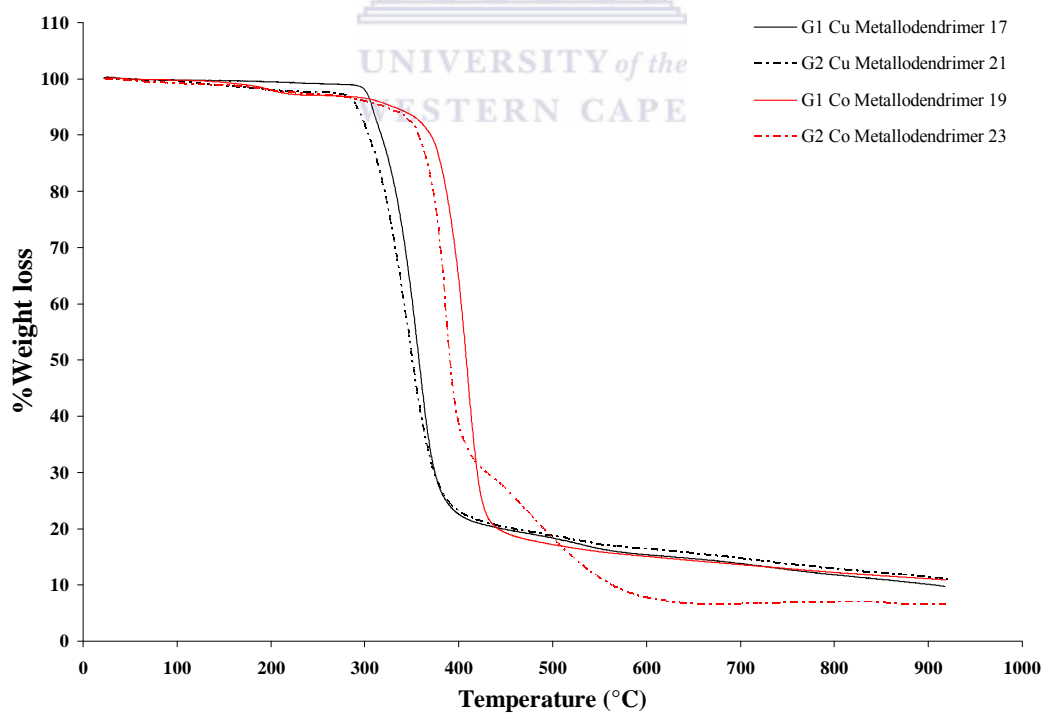
Figure 3.11*: Thermograms obtained for tert-butyl substituted copper(II) and cobalt(II) metallodendrimers.*

3.3   CONCLUSIONS

Two generation of peripheral functionalised salicylaldimine dendrimers were successfully obtained by modifying the surface groups of commercially available G1 and G2 poly(propyleneimine) dendrimers.   Copper(II) and cobalt(II) coordination systems of the dendritic ligands were readily obtainable. The dendritic ligands showed similar reactivity towards the two metal centers as observed for the bis-salicylaldimines discussed in Chapter two. The ligands readily coordinated to copper, however the target complexes of cobalt were only obtained in the presence of a base.   Eight new metallodendrimers were fully characterized using a range of analytical techniques.

3.3   EXPERIMENTAL

3.3.1   *Materials and Instrumentation*

All chemicals were of reagent grade and used as received. All solvents were dried over the appropriate drying agent and distilled prior to use. Reactions and manipulation of compounds were carried out using a dual vacuum/nitrogen line and standard Schlenk techniques unless stated otherwise. ^{1}H NMR (200 MHz) and ^{13}C NMR (50 MHz) spectra were recorded on a Varian XR200 spectrometer, using tetramethylsilane as an internal standard. Infrared spectra were recorded on a Perkin Elmer Paragon 1000PC FT-IR spectrophotometer as dichloromethane solutions using a solution cell with NaCl windows.   UV-Vis spectra were recorded on a GBC UV-Vis spectrometer. Microanalyses were performed by the University of Cape Town Microanalytical Laboratory.   Thermogravimetric analysis was performed by the University of Cape Town. Electron Spray Ionization mass spectrometry was performed by the University of Stellenbosch Mass Spectrometry Unit using a Walters Q-TOF Ultima instrument in the V-mode.

3.3.2 General procedure for the synthesis of first and second generation peripheral functionalised salicylaldimine dendrimers.

The synthesis of the dendritic ligands is described using the synthesis of ligands **DL**^{1} as an example. A round bottom flask was charged with G1 DAB-$(NH_2)_4$ (0.1 mmol) and toluene (20 mL). Salicylaldehyde (0.4 mmol) was added to the flask and the resulting yellow reaction mixture was stirred under reflux at 50°C for 24 hours. After the reflux period the solvent of the crude reaction mixture was removed with gentle heating. The yellow oily residue obtained was dissolved in dichloromethane (~10 mL) and this solution was extracted with deionised water (5 × 5 mL). The dichloromethane layer was dried over magnesium sulphate, filtered and the solvent of the filtrate removed under vacuum. Both first and second generation dendritic ligands were synthesized in a similar manner using the appropriate 2-hydroxybenzaldehyde and dendrimer. Purification of the ligands was performed by extracting dichloromethane solutions of the ligand with deionised water.
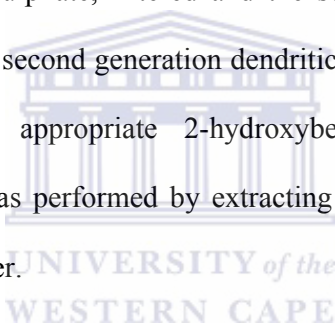
3.3.3 Synthesis of copper metallodendrimers

The synthesis of first and second generation copper metallodendrimers is described using the synthesis of metallodendrimer **16** as an example. Copper acetate monohydrate (1 mmol) and dendrimer ligand **DL**^{1} (0.5 mmol) was refluxed in methanol (20 ml) for 4 hours. During the reflux period a green solid precipitated from solution. The reaction mixture was cooled to 0°C for approximately 15 minutes and the solid isolated by vacuum filtration. A similar procedure was used to synthesise G2 copper(II) metallodendrimers. The metallodendrimers were recrystallized from a 1:2 dichloromethane/ethanol solvent system. The first and second generation metallodendrimers were obtained as light green solids in yields of 63 − 75%.

3.3.4   Synthesis of cobalt metallodendrimers

The synthesis of G1 and G2 cobalt metallodendrimers is described using the synthesis of metallodendrimers **18** as an example. Cobalt acetate tetrahydrate (1 mmol), sodium hydroxide and dendrimer ligand **DL**[1] (0.5 mmol) were refluxed in methanol (20 ml) for 4 hours. During this time period a brown solid precipitates from solution. The reaction mixture was cooled to 0°C for approximately 15 minutes and the solid isolated by vacuum filtration. The solid was dissolved in dichloromethane and filtered to remove impurities such as cobalt hydroxide and sodium hydroxide.   The solvent of the dichloromethane filtrate was removed under vacuum and the first and second generation metallodendrimers were obtained as brown solids in yields of 60 – 70%.

3.4   REFERENCES

1. D. A. Tomalia, P. R. Dvornic, *Nature* **1994**, *372*, 617.

2. D. A. Tomalia, *Prog. Polym. Sci.* **2005**, *30*, 294.

3. P. J. Flory*, J. Am. Chem. Soc*. **1952**, *74*, 2718.

4. D.A. Tomalia, D. M. Hedstrand, M. S. Ferrito, *Macromolecules* **1991**, *24*, 1435.

5. M. Gauthier, M. Moller, *Macromolecules* **1991**, *24*, 4548.

6. C. J. Hawker, J. M. J. Fréchet, *J. Am. Chem. Soc*. **1990**, 112, 7638.

7. H. Mekelburger, W. Jasworek, F. Vogtle, *Angew. Chem. Int. Ed. Engl*. **1992**, *31*, 1571.

8. S. Hecht, J. M. J. Fréchet, *Angew. Chem. Int. Ed*. **2001**, *40*, 74.

9. A. Caminade, J. Majoral, *Coord. Chem. Rev*. **2005**, 249, 1917.

10. G R. Newkome, E. He, C. N. Moorefield, *Chem. Rev*. **1999**, 99, 1689.

11. C. Liang, J. M. J. Fréchet, *Prog. Polym. Sci.* **200**5, *30*, 385.

12. H. P. Dijkstra, N. Ronde, G. P. M. van Klink, D. Vogt, G. Van Koten, *Adv. Synth. Catal.* **2003**, *345*, 364.

13. I. F. J. Vankelecom, *Chem. Rev*. **2002**, *102*, 3779.

14. R. van Heerbeek, P. C. J. Kamer, P. W. N. M. van Leeuwen, J. N. H. Reek, *Chem. Rev*. **2002**, *102*, 3717.

15. G. Smith, R. Chen, S. Mapolie, *J. Organomet. Chem*. **2003**, *673*, 111.

16. G. S. Smith, S. F. Mapolie, *J. Mol Catal. A Chem*. **2004**, *213*, 187.

17. W. Schilf, B. Kolodziej, E. Grech*, J. Mol. Struct*. **2006**, *791*, 93.

18. Y. Haba, A. Harada, T. Tagaishi, K. Kono, *Polymer* **2005**, *46*, 1813.

19. M. M. Campos-Vallette, K. A. Figueroa, R. Latorre, V. Manriquez, G. Diaz, J. Costamagna, M. Otero, *Vib. Spectrosc*. **1992**, *4*, 77.

20. H. H. Hammud, A. Ghannoum, M. S. Masoud, *Spectrochim. Acta A* **2006**, *63*, 255.

21. J–W. Weener, J. L. J. van Dongen, E. W. Meijer, *J. Am. Chem. Soc*. **1999**, *121*, 10346.

22. B. Baytekin, N. Werner, F. Luppertz, M. Engeser, J. Brüggemann, S. Bitter, R. Henkel, T. Felder, C. A. Schalley, *Int. J. Mass Spectrom*. **2006**, *249*,138.

23. K. Kurzak, I. Biernacka, B. Zurowska, *J. Solution. Chem*. **1999**, *28*, 133.

24. V. T. Kasumov, F. Köksal, *Spectrochim. Acta A* **2004**, *60*, 31.

25. A. I. El-Said, *J. Therm. Anal. Cal*. **2002**, *68*, 917.

26. G. R. Newkome, K. S. Yoo, S. Hwang, C. N. Moorefield, *Tetrahedron* **2003**, *59*, 3955.

CHAPTER 4

CATALYTIC OXIDATION OF PHENOL IN AQUEOUS MEDIA USING

MONO- AND MULTINUCLEAR SALICYLALDIMINE METAL COMPLEXES

CONTENT

4.1. INTRODUCTION

Oxidation reactions are widely used industrially in organic transformations and play a key role in the manufacture of intermediate chemicals for both the fine chemical and pharmaceutical chemical industries. Industrial oxidation processes often utilize oxidants which are environmentally harmful and because of increasing environmental concerns there have been intensive investigations into developing oxidation processes which utilize environmentally friendly oxidants such as molecular oxygen and hydrogen peroxide [1]. However suitable catalyst systems are required in order for these oxidants to be implemented effectively on an industrial scale. In recent years there has been increased interest in transition metal complexes based on porphyrins [2-3], phthalocyanines [4] and Schiff bases [5-7]. In addition the above systems have been extensively utilized as model compounds to study oxygen binding as well as the mechanistic aspects of oxidation processes catalyzed by enzymes such as cytochrome P-450 and peroxidases [8]. These enzymes are capable of selectively oxidizing various substrates using molecular oxygen and hydrogen peroxide. The aforementioned model complexes potentially provide a means of developing catalysts for oxidation processes, which are environmentally and economically sustainable [9].

Currently the direct oxidation of phenol to the dihydroxybenzenes, hydroquinone (HQ) and catechol (CT) using hydrogen peroxide is of significance due to the industrial importance of HQ and CT and the environmentally friendly nature of the process. There are several processes for the commercial production of these dihydroxybenzenes using hydrogen peroxide as oxidant, such as the Rhône-Poulenc and Hamilton processes [10]. However environmentally undesirable catalysts such as strong mineral acids and the Fenton reagent are used. Although a process utilizing a heterogeneous catalyst based on

titanium silicalite (TS-1) has been developed and implemented industrially, full commercial application has been limited due to the difficult synthesis of the catalyst and the associated high cost [11].

Wet air oxidation is a well known remediation method for treating water containing organic pollutants, such as phenol, in concentrations which makes other treatment options unviable [12]. This process has been extensively investigated in recent years due to the extreme conditions employed which result in high operation costs. Significant research has thus focussed on finding suitable catalysts to reduce the costs associated with the process conditions [13-16]. In addition to being a very effective water treatment method, catalytic wet air oxidation (CWAO) also holds great potential from a synthetic point of view. Recently Santos et al. showed that by controlling factors such as the pH of the reaction medium in the CWAO of phenol that the oxidation proceeds via two different pathways when employing a commercially available copper catalysts [17]. The investigation conducted by this group showed that under acidic conditions (pH 3.5) oxidation of phenol proceeds via the dihydroxybenzene intermediates, hydroquinone (HQ) and catechol (CT) with low mass organic acids as secondary intermediates in the oxidation process as shown in Scheme 4.1. It was also shown that oxidation under basic conditions (pH 8) did not include the formation of the dihydroxybenzenes (Scheme 4.2). Controlling parameters such as the pH of the reaction medium for CWAO of phenol provides an alternative route to the production of CT and HQ. This process has the added advantage of using water as the reaction medium and H_2O_2 and O_2 as oxidants, which makes this route very attractive form an environmental perspective.
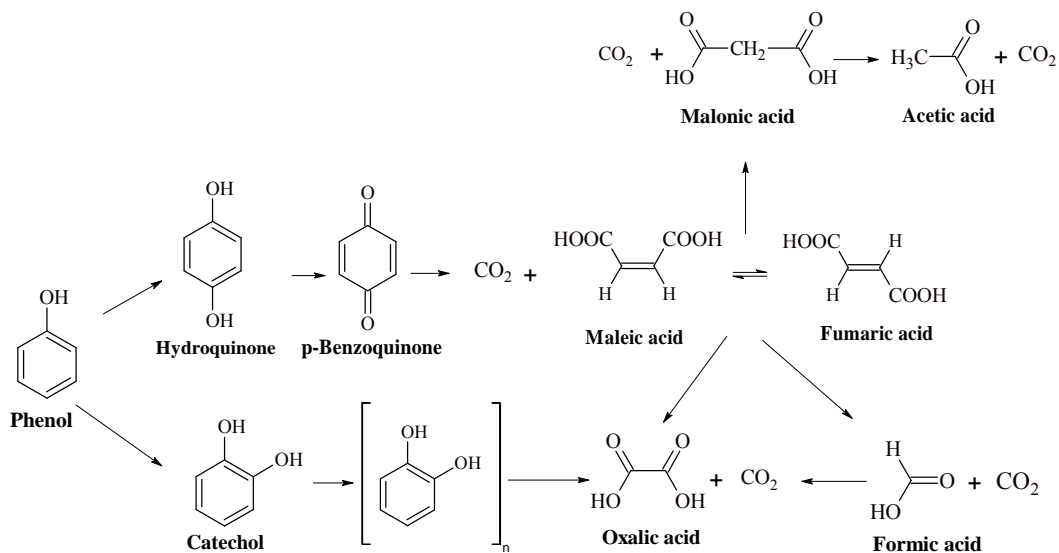
Scheme 4.1: *Oxidation pathway proposed by Santos et al. for phenol oxidation in aqueous media at pH 3.5 [12].*
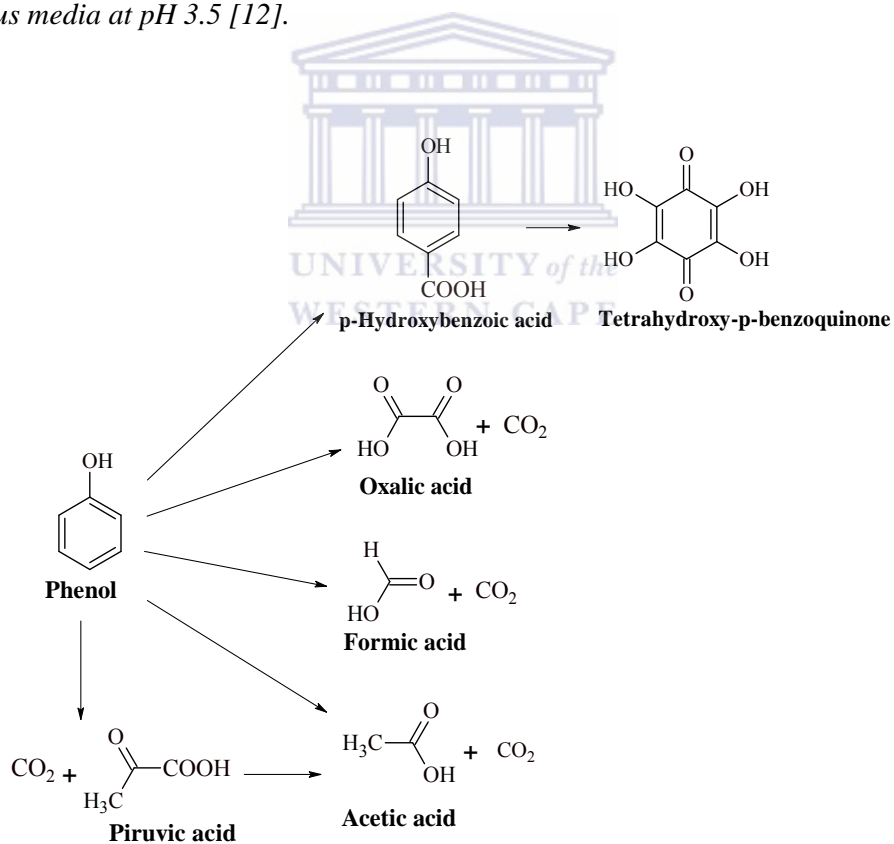
Scheme 4.2: *Oxidation pathway proposed by Santos et al. for phenol oxidation in aqueous media at pH 8 [12].*

In this chapter the catalytic activity of typical homogeneous catalysts based on *N*-(aryl)salicylaldimines as well as dendritic supported catalysts containing copper(II) and cobalt(II) as metal centres are investigated in the aqueous oxidation of phenol using hydrogen peroxide as oxidant. In this study the oxidation process is investigated under different pH values to determine to what extent this parameter has an effect on the activity of the catalysts and selectivity to HQ and CT.

4.2.   RESULTS AND DISCUSSION

4.2.1.   Hydroxylation of phenol using Cu(II) salicylaldiminato complexes.

The hydroxylation of phenol catalyzed by mononuclear complexes **1**, **3**–**5**, bimetallic complex **8** and Cu(II) metallodendrimers (**16**, **17**, **20**, and **21**) was studied in deionised water in the pH range 3–6 using appropriately buffered solutions. All reactions were performed under an oxygen atmosphere using 30% H_2O_2 (w/w) as oxidant. A substrate to metal ratio of 100:1 and a 1:1 mole ratio of phenol to H_2O_2 was used for all reactions. It should be noted that complex **8** as well as the metallodendrimers contain multiple metal centres, however the phenol to copper ratio of 100:1 was maintained irrespective of the catalyst used in the catalytic runs. Results for the hydroxylation reaction performed for the mononuclear and dendrimeric systems are shown in Table 4.1 and Table 4.2 respectively.

4.2.1.1 The effect of pH on phenol conversion

All the *N*-(aryl)salicylaldimine copper complexes (Fig. 4.1) evaluated were found to be active for the hydroxylation of phenol. The activity of the catalysts was tested over a range of pH values in order to evaluate to what extent the acidity of the medium affects phenol conversion.

1 : R = H; R$_1$ = H; R$_2$ = H; M = Cu
3 : R = H; R$_1$ = t-Bu; R$_2$ = t-Bu; M = Cu
4 : R = i-Pr; R$_1$ = H; R$_2$ = H; M = Cu
5 : R = i-Pr; R$_1$ = H; R$_2$ = Cl; M = Cu

9 : R = H; R$_1$ = H; R$_2$ = H; M = Co
11 : R = H; R$_1$ = t-Bu; R$_2$ = t-Bu; M = Co
12 : R = i-Pr; R$_1$ = H; R$_2$ = H; M = Co
13 : R = i-Pr; R$_1$ = H; R$_2$ = Cl; M = Co
14 : R = i-Pr; R$_1$ = t-Bu; R$_2$ = H; M = Co
15 : R = i-Pr; R$_1$ = t-Bu; R$_2$ = t-Bu; M = Co
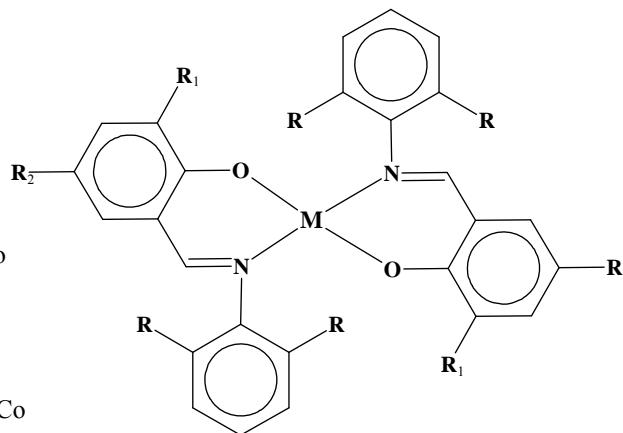
Figure 4.1*: Mononuclear copper(II) and cobalt(II) salicylaldiminato complexes evaluated in the hydroxylation of phenol.*
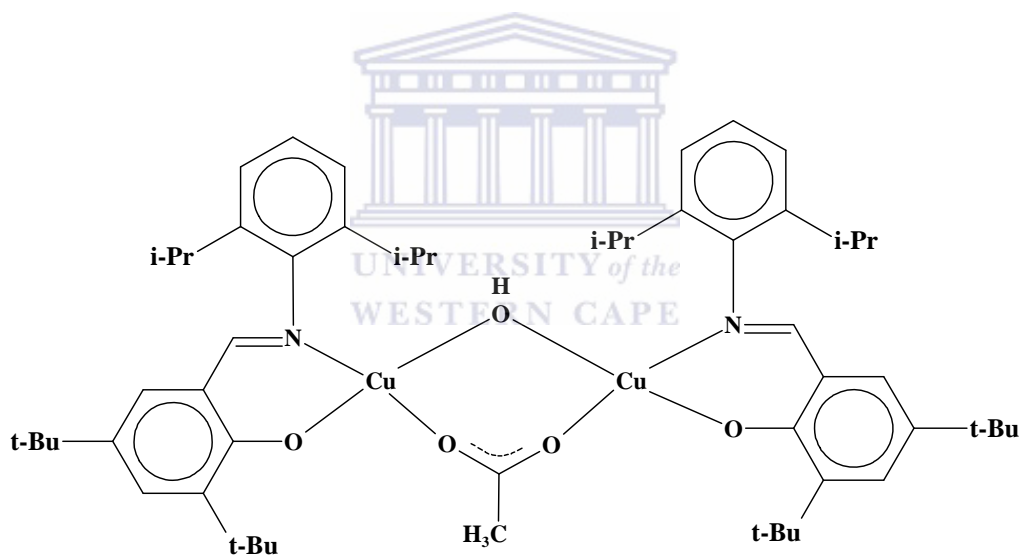
Figure 4.2*: Structure of bimetallic copper(II) complex **8** which was evaluated in the hydroxylation of phenol.*

(a)

16 : R$_1$ = R$_2$ = H; M= Cu
17 : R$_1$ = R$_2$ = t-Bu; M = Cu
18 : R$_1$ = R$_2$ = H; M= Co
19 : R$_1$ = R$_2$ = t-Bu; M = Co

(b)

20 : R$_1$ = R$_2$ = H; M = Cu
21 : R$_1$ = R$_2$ = t-Bu; M = Cu
22 : R$_1$ = R$_2$ = H; M = Co
23 : R$_1$ = R$_2$ = t-Bu; M = Co
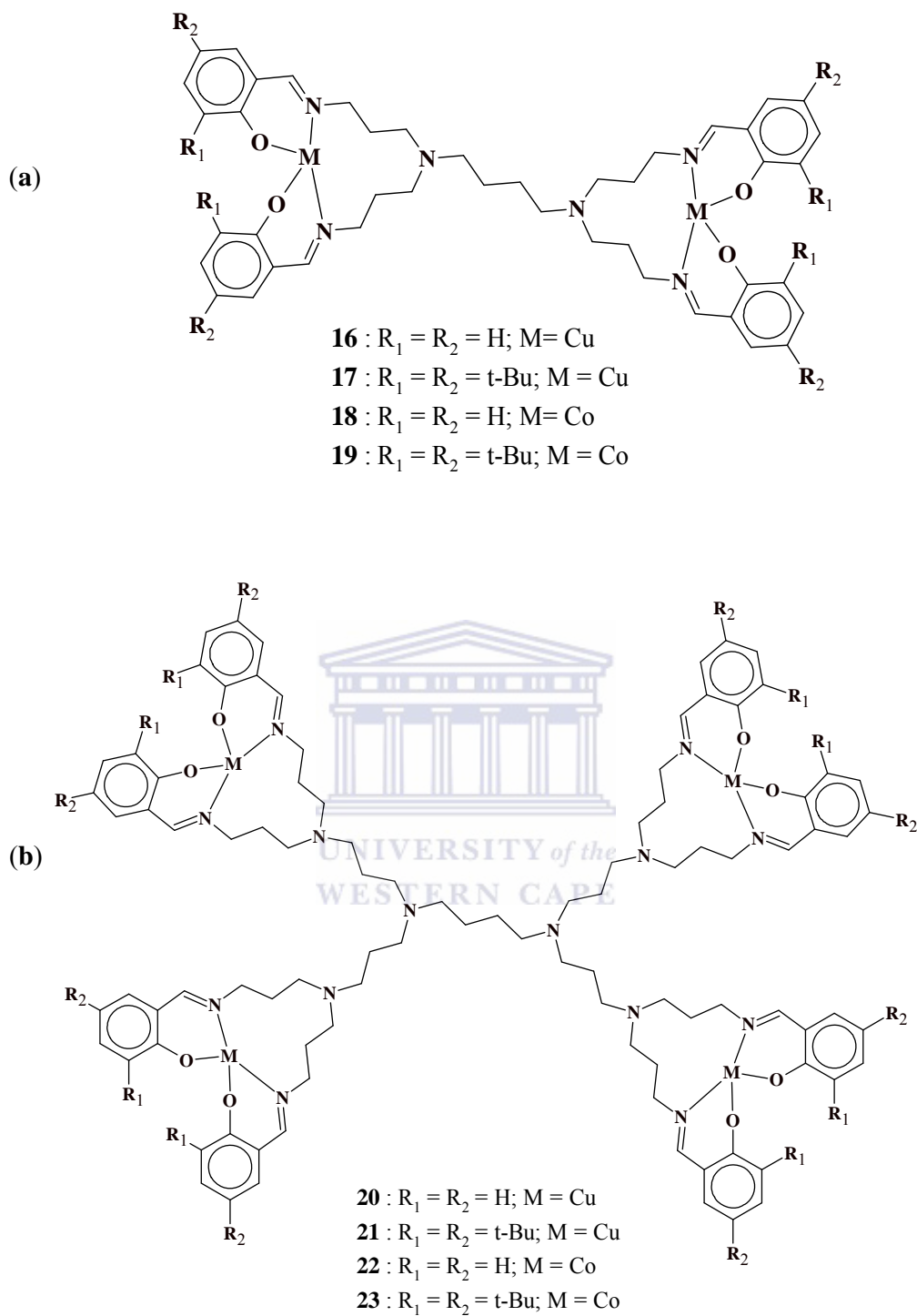
Figure 4.3: *G1 (a) and G2 (b) copper(II) and cobalt(II) salicylaldimine metallodendrimers evaluated in the hydroxylation of phenol.*

The performance of the catalysts under the various reaction conditions is graphically represented in Figure 4.4. It was found that the complexes perform better at moderately acidic pH values. Among the mononuclear complexes investigated, catalyst **3** showed the highest phenol conversion (74%) at pH 5. This is only slightly lower than the optimum phenol conversion (77%) observed with bimetallic catalyst **8**, which was obtained at pH 6. Generally the catalysts derived from bis-salicylaldimines exhibited optimum activity at pH 6, the exceptions being catalysts **1** and **3** which both showed optimum activity at pH 5. These two catalysts also exhibited a significant drop in activity at pH 3 indicating that they are much more sensitive to low pH conditions than catalysts **4**, **5** and **8**.

In the case of dendrimer supported catalysts the optimum activity for both G1 and G2 metallodendrimers were also observed at pH 6. The phenol conversions at pH 6 (71 – 78%) were comparable to conversions obtained with those for the tetra-coordinate *N*-(aryl)salicylaldimine Cu(II) catalysts at the optimum pH. There was no significant dendritic effect observed when comparing the results obtained for the two different generations of dendritic complexes in that very similar activities were observed. It was however found that the metallodendrimers were not as sensitive to pH changes as the bis-salicylaldimine catalysts. The two types of dendrimeric systems also behaved slightly differently (Figure 4.5). For instance the unsubstituted G1 dendrimer **16** shows a very significant drop in activity with a decrease in the pH whereas for the G2 system **20,** a very slight difference in activity is observed across the pH range investigated. In the case of the *tert*-butyl substituted systems this phenomenon is reversed with the G1 system **17** showing a slight drop in activity over the pH range, while the G2 system **21** shows quite a significant drop. The reason for this behaviour is not entirely clear but it

most likely involves the stability of the active intermediates formed under the different pH conditions. The activity of peroxidase enzymes have been shown to be inherently linked to the structural conformation of the enzyme which in turn has been shown to be transformed by changes in the pH of the reaction medium. These conformational changes undoubtedly also has an effect on the active intermediates formed during the catalytic process and it is thus necessary to control the acidity of the reaction medium for processes catalysed by peroxidases. Model compounds based on salens have been shown to behave in a similar manner to the peroxidase and thus for the Schiff base systems investigated here the stability of the active intermediate, which is widely proposed to be a metal peroxo species, is also expected to be affected by the pH of the reaction medium.

Reactions were also attempted in alkaline media but these showed no phenol consumption. The results obtained are in agreement with what has previously been reported in the literature for other metal mediated phenol hydroxylation processes [18]. The results can be explained in terms of the generally accepted reaction mechanism for the oxidation of aromatic hydrocarbons [19]. The accepted reaction pathway can basically be summarized by the steps outlined in Scheme 4.3. Thus the effectiveness of the hydroxylation process in acidic media can be explained in terms of some of the steps outlined in this Scheme. Acidic media enhances the metal-mediated decomposition of H_2O_2 to the hydroxyl radical, which is an important species in the hydroxylation of phenol [20, 21].
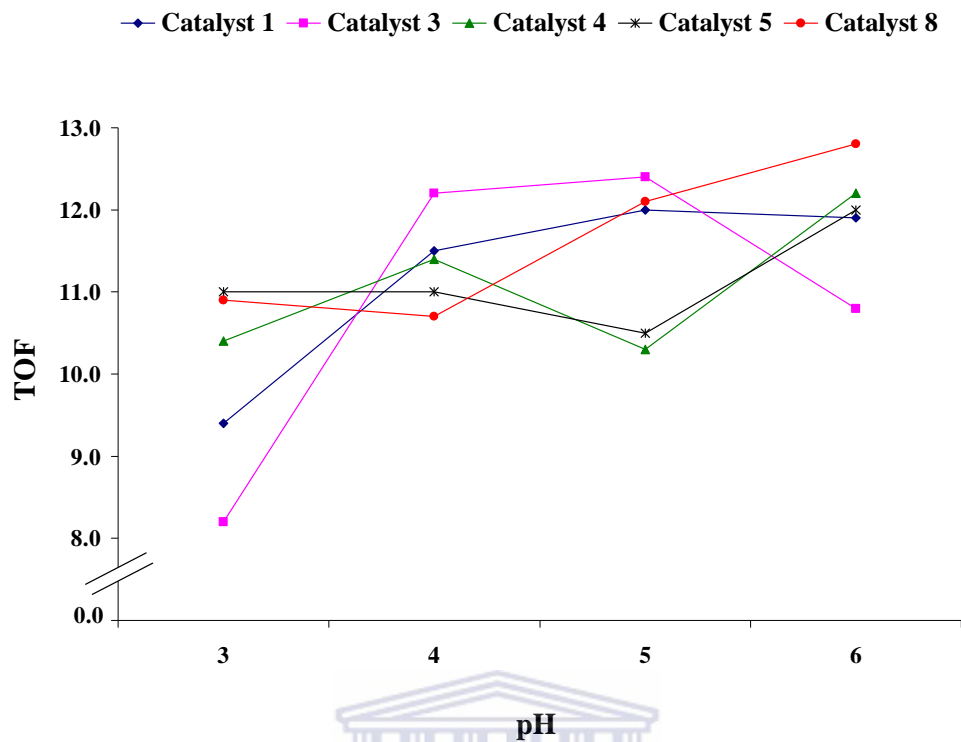
Figure 4.4*: Effect of pH on the activity of mononuclear copper(II) salicylaldiminato complexes.*
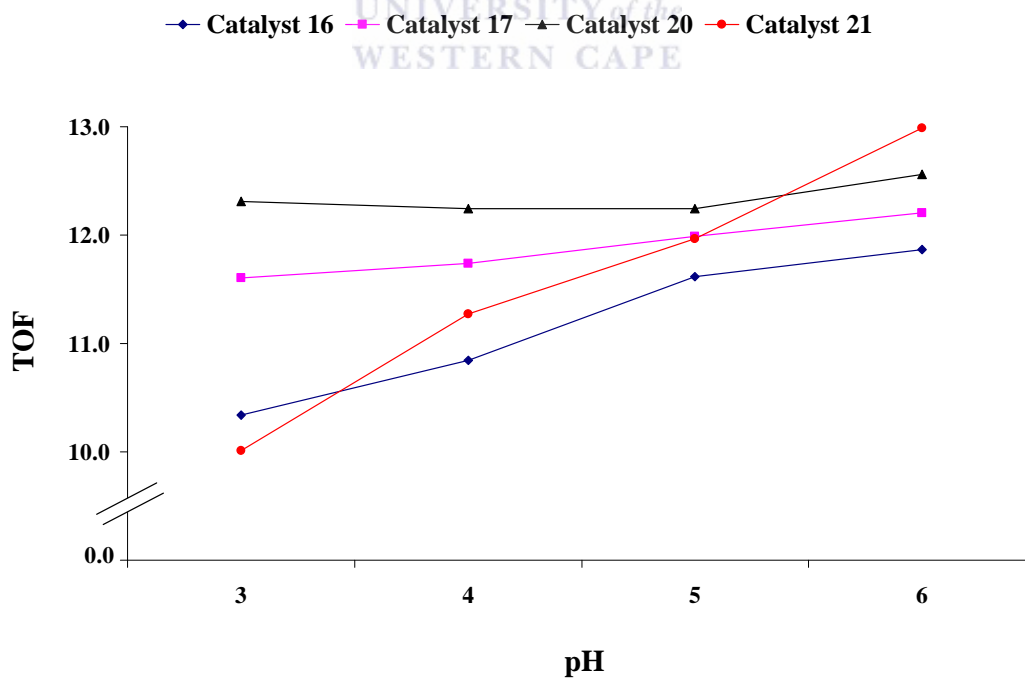
Figure 4.5*: Effect of pH on the activity of dendritic copper(II) salicylaldiminato complexes.*

Table 4.1: Effect of pH on the catalytic activity of complexes **1**, **3-4** and **8** [a].

Catalyst	pH	%W Dihydroxybenzenes[b]		%PhOH	TOF[c]
		HQ	CT	Conversion	
1	3	37.18	62.82	56	9.4
	4	40.99	59.01	69	11.5
	5	42.01	57.99	72	12.0
	6	37.02	62.98	71	11.9
3	3	38.13	61.87	49	8.2
	4	31.99	68.01	73	12.2
	5	37.86	62.14	74	12.4
	6	32.69	67.31	65	10.8
4	3	32.67	67.33	62	10.4
	4	34.39	65.61	68	11.4
	5	36.53	63.47	62	10.3
	6	35.77	64.23	73	12.2
5	3	37.45	62.55	66	11.0
	4	28.74	71.26	66	11.0
	5	33.63	66.37	63	10.5
	6	30.40	69.60	72	12.0
8	3	31.79	68.21	65	10.9
	4	28.24	71.76	64	10.7
	5	32.32	67.68	73	12.1
	6	39.11	60.89	77	12.8

[a] Reaction performed in 10 ml H_2O, Phenol:Cu = 100:1; 110°C at 1atm O_2 for 6h;
30% H_2O_2 as co-oxidant; Phenol:H_2O_2 = 1:1; [b] HQ = Hydroquinone; CT = Catechol
Product distribution given on a tar free basis; [c] TOF = (mol phenol consumed/mol Cu)/hour.

The decomposition of the peroxide is shown in step 2 (Scheme 4.3). This step is clearly enhanced in moderately acidic media by the removal of OH^- anions from the reaction mixture. Conversely, at alkaline pH, the high OH^- concentration shifts the equilibrium in step 2 to the left, thus lowering the hydroxyl radical concentration. This is what we observe, as all the catalysts are inactive at pH values above pH 7.

Table4.2: Effect of pH on activity and selectivity of Cu(II) metallodendrimers[a].

Catalyst	pH	%W Dihydroxybenzenes[b]		%PhOH Conversion	TOF[c]
		HQ	CT		
16	3	42.1	57.9	62	10.3
	4	40.3	59.7	65	10.8
	5	40.8	59.2	70	11.6
	6	35.7	64.3	71	11.9
17	3	41.7	58.3	70	11.6
	4	39.4	60.6	70	11.7
	5	41.5	58.5	72	12.0
	6	32.9	67.1	73	12.2
20	3	42.3	57.7	74	12.3
	4	36.7	63.3	73	12.2
	5	41.2	58.8	72	12.2
	6	36.1	63.9	75	12.6
21	3	42.6	57.4	60	10.0
	4	40.9	59.1	68	11.3
	5	42.1	57.9	68	12.0
	6	40.9	59.1	78	13.0

[a] Reaction performed in 10 ml H_2O, Phenol:Cu = 100:1; 110°C at 1atm O_2 for 6h;

30% H_2O_2 as co-oxidant; Phenol:H_2O_2 = 1:1; [b] HQ = Hydroquinone; CT = Catechol

Product distribution given on a tar free basis; [c] TOF = (mol phenol consumed/mol Cu)/hour.

In this study it was also found that too low a pH has a detrimental effect on catalyst activity. Thus the catalysts are ineffective at pH 2 and below, with no phenol hydroxylation being observed. At such low pH values there is an increase in the possibility of step 1 in Scheme 4.3 being retarded due to the high concentration of protons in the reaction medium. This ultimately causes the production of the hydroxyl ions (step 2) to be retarded which affects the overall hydroxylation process.

$$H_2O_2 \;+\; M^{n+}L_n \;\rightleftharpoons\; HO_2^- \;+\; H^+ \;+\; M^{(n-1)+}L_n \tag{1}$$

$$H_2O_2 \;+\; M^{(n-1)+}L_n \;\rightleftharpoons\; HO^{\bullet} \;+\; {}^-OH \;+\; M^{n+}L_n \tag{2}$$

(3)

(4a)

(4b)

$$H_2O_2 \;+\; M^{n+}L_n \;+\; HO^{\bullet} \;\rightleftharpoons\; H_2O \;+\; H^+ \;+\; M^{(n-1)+}L_n \tag{5}$$

$$H^+ \;+\; {}^-OH \;\rightleftharpoons\; H_2O \tag{6}$$
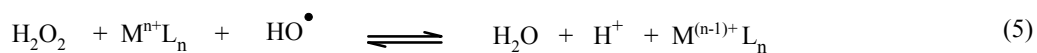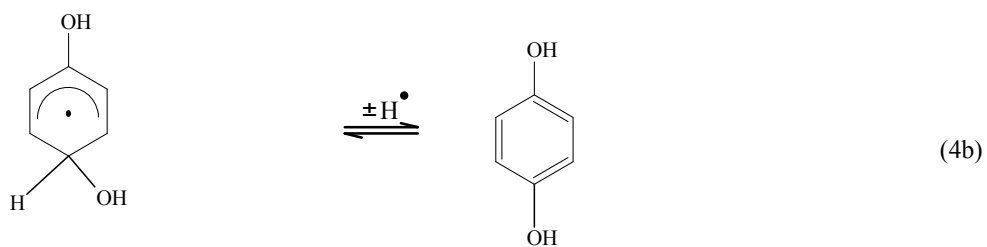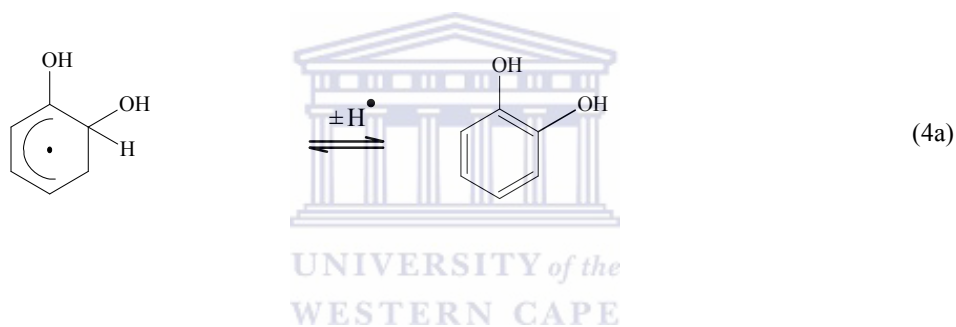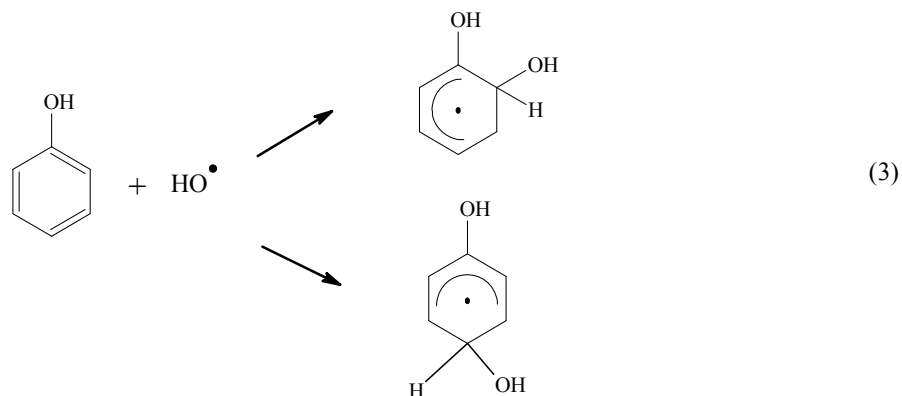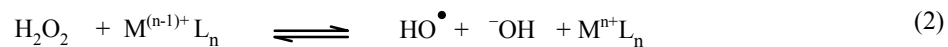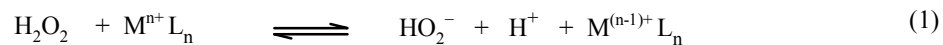
Scheme 4.3: *Proposed reaction pathway for phenol hydroxylation.*

4.2.1.2 The effect of pH on product selectivity

The major products observed under the conditions used were hydroquinone (HQ) and catechol (CT). In some instances trace quantities of benzoquinone (BQ) were also detected. In the case of all the catalysts investigated catechol is preferentially produced over hydroquinone. Both catalysts **5** and **8** show the best selectivity to CT at pH 4 with a ratio of CT:HQ of 2.3:1. However a general CT:HQ ratio of roughly 2:1 was observed with the majority of the catalysts investigated. The exception being complex **1**, which produces slightly higher levels of hydroquinone than the other catalysts. In the latter case the CT:HQ ratios are around 1.5:1. This product distribution is fairly typical for copper mediated phenol oxidation processes.

The metallodendrimers investigated showed a similar product distribution as complex **1**. The pH of the reaction medium is also observed to have an impact on the product selectivity for the various catalysts since it is observed that at certain pH values the different catalysts produce higher quantities of HQ. Thus while the pH of the reaction medium in aqueous phenol oxidations is important in determining the oxidation pathway as shown by Santos et al. [17], it also appears that the structure of the metal complex is important in determining product selectivity under different pH conditions. The predominance of catechol over hydroquinone is not unexpected for copper-mediated hydroxylation occurring *via* the free radical process. It has previously been reported that the hydroxylation occurs *via* a pathway which involves initial weak coordination of both phenol and H_2O_2 to the active site. The anchoring of the two reaction partners in close proximity leads predominantly to a *cis* arrangement, which in turn results in ortho-substitution of the phenol [22].

4.2.2 *Hydroxylation of phenol using Co(II) salicylaldiminato complexes*

The activities of bis-salicylaldimine cobalt(II) metal complexes (**9**, **11-15**) and dendritic immobilized complexes (**18**, **19**, **22** and **23**) were also investigated in the liquid phase hydroxylation of phenol. The structure of the complexes used in the catalytic runs are shown in Figure 4.1 and Figure 4.2. As for the copper catalysts the oxidation process was studied in de-ionized water, however the investigation focused on the two extreme pH values (3 and 6) for which the copper catalyst showed production of CT and HQ. The oxidation reactions were performed under an oxygen atmosphere using a 30% H_2O_2 (w/w) as oxidant using appropriately buffered solutions. A metal to substrate ratio of 1:100 and 1:1 mole ratio of phenol to H_2O_2 was used for all reactions. All the catalysts investigated were found to be active in the phenol oxidation process. In all reactions the major products detected were hydroquinone (HQ) and catechol (CT). However trace quantities of benzoquinone was also observed. In some cases viz. for complexes **12** and **13** no dihydroxybenzenes formation is observed at the higher pH value. Instead tar-like material was obtained, which is probably some sort of polymeric product. Phenol conversion and product selectivity for the mononuclear complexes and metallodendrimers are shown in Table 4.3 and Table 4.4 respectively.

4.2.2.1 *The effect of pH on phenol conversion*

The activity of the Co(II) mononuclear catalysts investigated using the two pH values are shown in Figure 4.6. Lower activity for all catalysts was observed using a more acidic medium (pH 3). An increase in activity is observed when the pH is increased to pH 6. This observation is consistent with results obtained for the copper catalysts investigated as well as for other Schiff base model complexes where the optimum activity of the catalysts was observed to be pH dependant [23, 24]. There also appears

to be a structure-reactivity effect since catalysts with bulky substituents on the aromatic rings (**11**, **14** and **15**) appeared to be slightly more active than those without bulky substituents (**9** and **12**). This is possibly due to the fact that the bulky substituents are exerting some stabilizing effect by preventing μ-oxo dimer formation. It has been reported previously that dimerization of the metal complex leads to deactivation [25]. In addition such stabilization by bulky ligands around the active centre is also consistent with what is observed for the peroxidase enzymes [26]. The most active mononuclear catalyst was found to be complex **14** at pH 6 which gave a phenol conversion of 67%. Catalyst **14** was however only slightly more active than catalyst **15**. The least active catalyst is complex **13**, which has an electron withdrawing Cl substituent on the aromatic ring. The electronegative chloride makes the oxidation of the Co centre more difficult. This slows down the formation of the Co (III) intermediate which is instrumental in the activation of the peroxide.

In the case of the metallodendrimers a significantly higher activity of the complexes was observed at pH 6 when compared to activities observed at pH 3 (Figure 4.7). However the performance of these catalysts was also slightly lower than their copper(II) analogues. In addition the activities of the dendritic catalysts were also observed to be comparable to that of the mononuclear cobalt(II) catalyst investigated. As for the copper systems, attempts to carry out the reactions in alkaline medium were not successful as no phenol consumption was observed at pH values greater than 7. Our results correspond with those previously reported for other metal-mediated phenol hydroxylation processes and can be accounted for via the generally accepted reaction pathway for the hydroxylation of phenol [23].
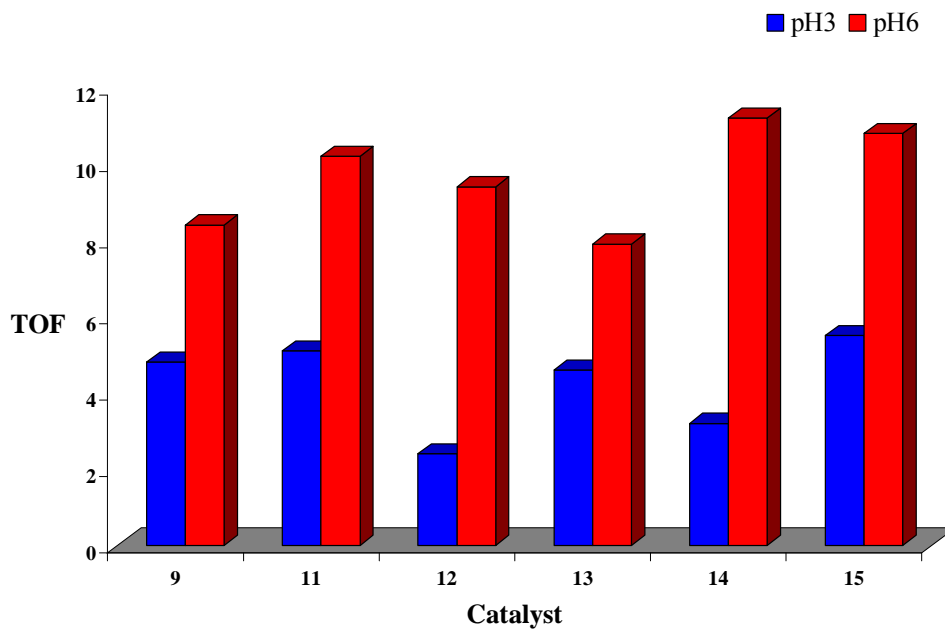
Figure 4.6*: Effect of pH on the activity of mononuclear cobalt(II) salicylaldiminato complexes.*
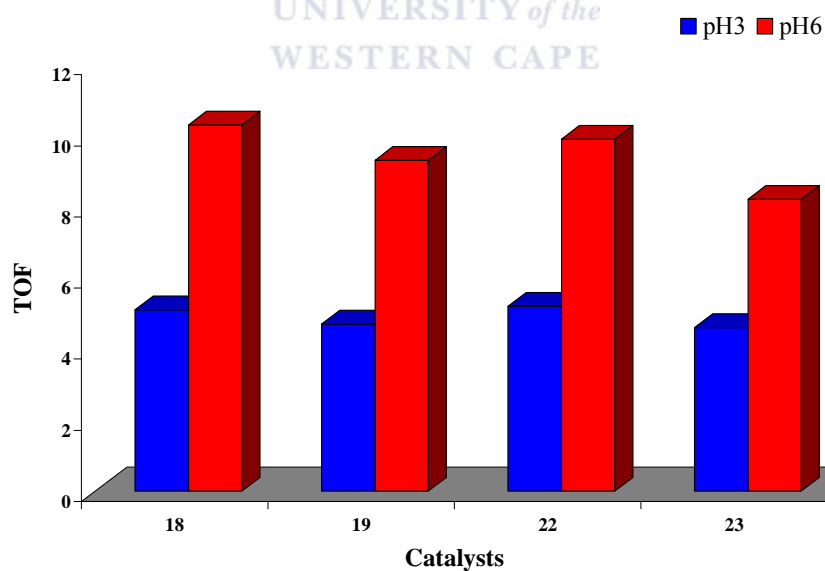
Figure 4.7*: Effect of pH on the activity of dendritic cobalt(II) salicylaldiminato complexes.*

Table 4.3: Effect of pH on the catalytic activity of complexes **9** and **11** - **15**[a].

Catalyst	pH	%W Dihydroxybenzenes[b]		%PhOH Conversion	TOF[c]
		HQ	CT		
9	3	-	100	29	4.8
	6	-	100	50	8.4
11	3	44.31	55.69	30	5.1
	6	28.26	71.74	61	10.2
12	3	39.55	60.45	15	2.4
	[d]6	-	-	56	9.4
13	3	33.91	66.09	28	4.6
	[d]6	-	-	47	7.9
14	3	36.18	63.82	19	3.2
	6	27.23	72.77	67	11.2
15	3	37.67	62.33	33	5.5
	6	28.51	71.49	65	10.8

[a] Reaction performed in 10 mL H_2O, Phenol:Co = 100:1; 110°C at 1atm O_2 for 6h;

30% H_2O_2 as co-oxidant; Phenol:H_2O_2 = 1:1; [b] HQ = Hydroquinone; CT = Catechol;

Product distribution given on a tar free basis; [c] TOF = (mol phenol consumed/mol Co)/hour.

[d] Neither CT nor HQ observed possibly due to preference of an alternate oxidation pathway.

Table 4.4: The effect of pH on the activity and selectivity of Co(II) metallodendrimers[a].

Catalyst	pH	%W Dihydroxybenzenes[b]		%Phenol Conversion	TOF[c]
		HQ	CT		
18	3	38.7	61.3	31	5.1
	6	14.45	85.55	62	10.3
19	3	37.1	62.9	28	4.7
	[d]6	-	-	56	9.3
22	3	37.0	63.0	31	5.2
	6	18.06	81.94	59	9.9
23	3	35.2	64.8	28	4.6
	[d]6	-	-	49	8.2

[a] Reaction performed in 10 ml H_2O, Phenol:Co = 100:1; 10°C at 1atm O_2;

30% H_2O_2 as co-oxidant; Phenol:H_2O_2 = 1:1; [b] HQ = Hydroquinone; CT = Catechol;

Product distribution given on a tar free basis; [c] TOF = (mol phenol consumed/mol Co)/hour.

[d] Neither CT nor HQ observed possible due to preference of an alternate oxidation pathway.

4.2.2.2 *The effect of pH on product selectivity*

The relative ratios of the two dihydroxybenzenes formed, were observed to be dependent on the nature of the catalyst as well as the pH of the reaction medium. Catalyst **9** selectively produced only catechol (CT) irrespective of the pH of the reaction medium. Both catalysts **14** and **15** produced HQ and CT roughly in a 1:2 ratio at low pH, while at pH 6 the amount of catechol is increased resulting in a final ratio of 1:3 (HQ:CT). A similar trend is observed for catalyst **11** which showed a higher selectivity to HQ at pH 3, however at pH 6 a ratio of 1:3 (HQ:CT) was observed indicating a preferential formation of CT under less acidic conditions. Both catalysts **12** and **13** produced the expected ratio of 1:2 (HQ:CT) at pH 3, however none of the dihydroxybenzenes are observed at pH 6. This is despite the fact that phenol

consumption of 56% and 47% respectively is observed, suggesting that the reaction medium is basic enough to promote another oxidation pathway which does not include the formation of the dihydroxybenzenes CT and HQ. The only products observed were intractable tar material which is believed to be some sort of polymer.

As for the mononuclear catalysts, the pH of the reaction medium also has an impact on the product distribution of the dihydroxybenzenes, CT and HQ, when using the metallodendrimers as catalysts. In addition the structure of the catalysts also has an impact on product distribution. In the case of the unsubstituted catalysts **18** and **22** a CT:HQ distribution of roughly 1.5:1 is observed, however an increase in the formation of CT is observed with a increase in pH resulting in a CT:HQ ratio of roughly 6:1 and 4.5:1 for catalysts **18** and **22** respectively at pH 6. The tert-butyl substituted catalysts **19** and **23,** however, only produce CT and HQ at pH 3 and neither of the two dihydroxybenzenes are observed at pH 6. Once again the nature of the catalyst system is observed to be as important as the pH of the reaction medium in terms of product selectivity.

4.2.3   *The effect of the nature of the metal on activity and product selectivity*

In general a slight dependence of the activity and product distribution on the nature of the metal centre of the catalyst was observed. The copper catalysts were observed to be much more active under similar conditions investigated for the cobalt catalysts. This dependence on the metal centre was also observed by Ray et al. while investigating bis(salicylaldimine) metal complexes containing copper, cobalt, and nickel anchored on inorganic supports. In the study conducted by Ray et al. the trend in activity of the catalysts was observed to decrease in the order Cu>Co>Ni [9]. The results obtained in

this investigation are in agreement with our observation since the copper catalysts were also observed to have superior activities compared to the cobalt catalysts. In the case of the copper catalysts the effect of pH is not as significant as was the case with the cobalt complexes as can be seen from Figures 4.8 and 4.9. Although the activities of the copper catalysts at pH 3 were slightly lower than activities observed at pH 6, the drop in activity was not as great as observed for the cobalt systems. In the latter case activities at pH 3 were approximately half those observed at pH 6 indicating that the cobalt catalysts are much more sensitive to very acidic pH values compared to the copper complexes.

The investigation conducted by Ray et al. [9] also showed a pronounced impact on the product distribution which depended on both the nature of the metal centre as well as the pH of the reaction medium. It was observed that a very similar ratio of HQ to CT was obtained with copper catalysts within the pH range studied, whereas cobalt and nickel catalysts appeared to be much more selective at different pH values producing one of the dihydroxybenzenes preferentially over the other [9]. This phenomenon is also observed in the catalytic experiments conducted here, which showed copper catalysts producing the dihydroxybenzenes in either a 1:2 or a 1:1.5 (HQ:CT) ratio over the pH range studied with little or no deviation from these distributions with change in pH. Although similar ratios to these are obtained for the cobalt catalysts at pH 3, under more basic conditions an increase in the formation of CT is observed which results in ratios of roughly 1:3 and 1:5 (HQ:CT) being obtained for the mononuclear catalysts and metallodendritic catalysts, respectively.

(A): pH 3

(B): pH 6
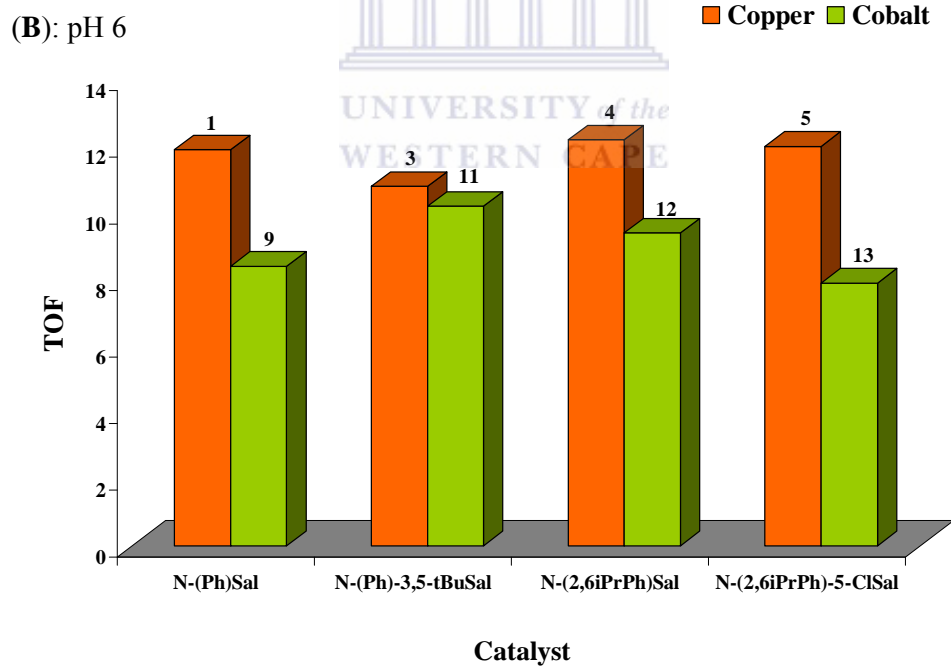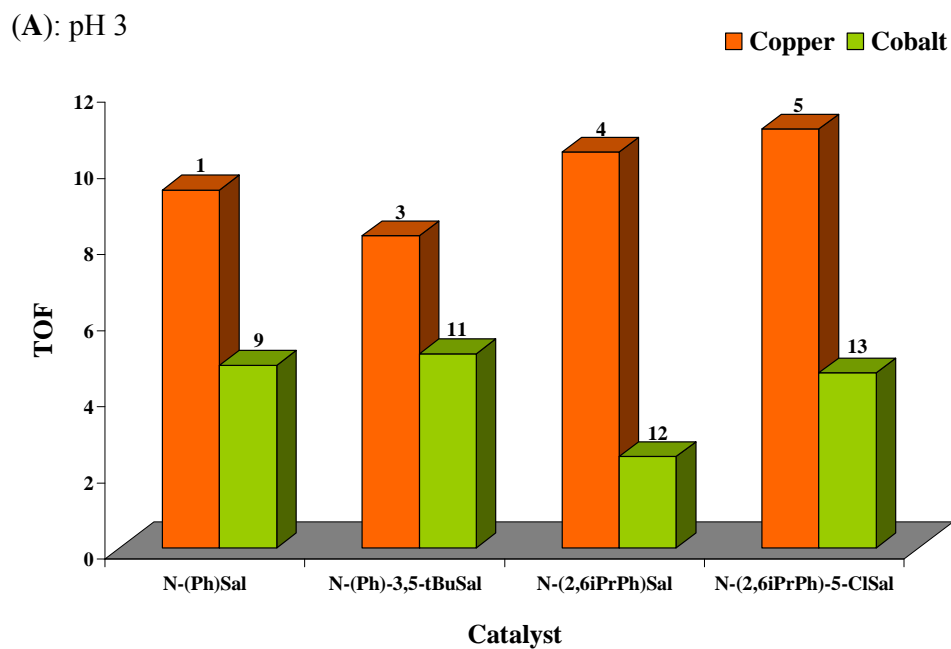
Figure 4.8*: Comparison of the activity of Cu(II) and Co(II) mononuclear complexes derived from the same N-(aryl)salicylaldimine ligands at pH 3 (A) and pH 6 (B). (x-axis indicates the ligand from which the metal complex is derived).*
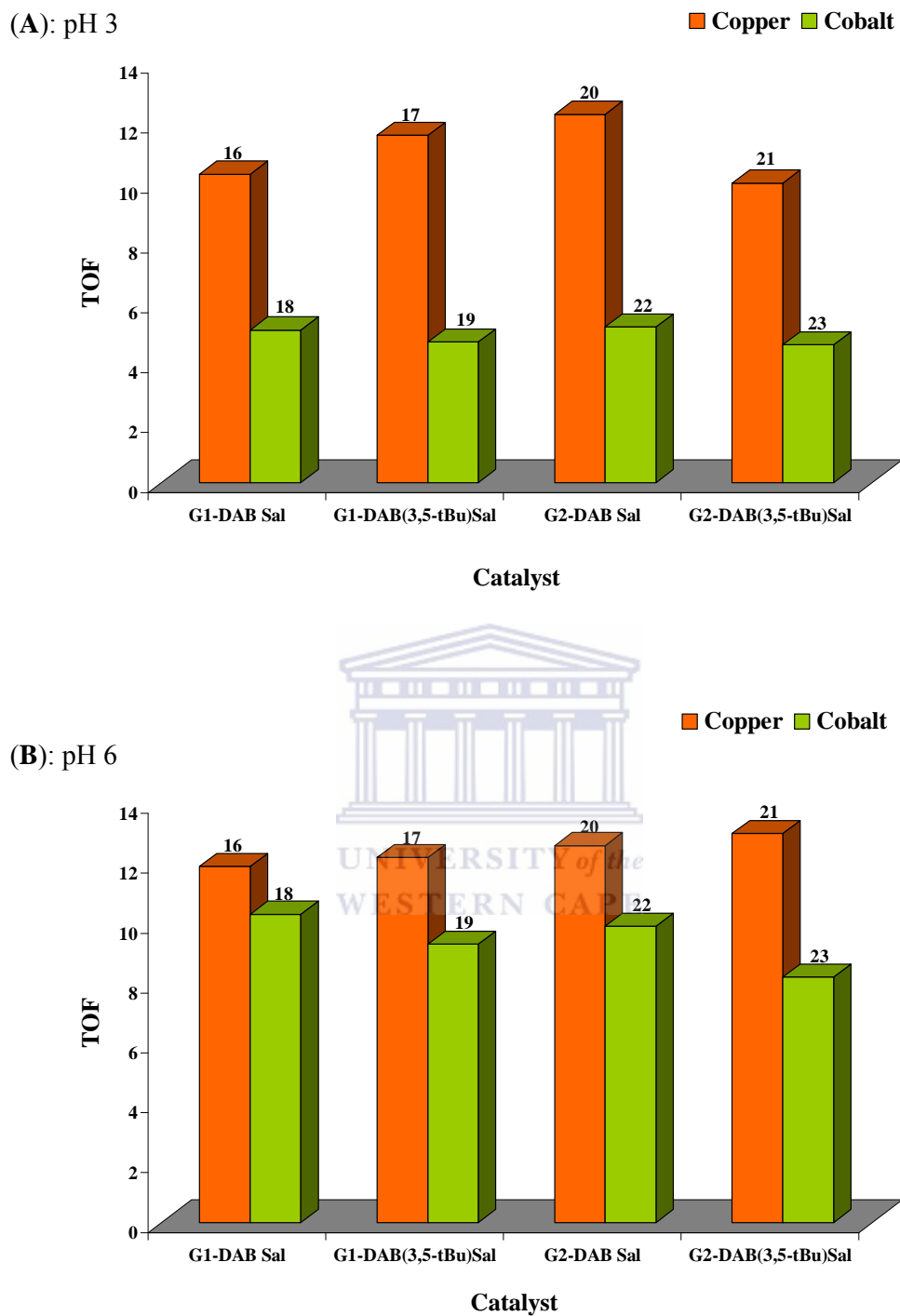
(A): pH 3

(B): pH 6

Figure 4.9*: Comparison of the activity of Cu(II) and Co(II) metallodendrimers derived from the same salicylaldimine dendritic functionalised ligands at pH 3 (A) and pH 6 (B). (x-axis indicates the ligand from which the metal complex is derived).*

4.2.4   *The effect of immobilization of complexes on activity and product selectivity.*

On comparing the performance of the mononuclear catalysts versus the dendritic immobilized systems of both copper and cobalt it was observed that under the conditions investigated the activities of the catalysts are in general comparable. However in the case of the copper catalysts it was found that the G2 catalyst **21** performed the best and the only catalyst derived from *N*-(aryl)salicylaldimines which produced comparable activity was bimetallic catalyst **8**. In the case of the cobalt systems mononuclear catalyst **14** produced the best overall activity and the G1 catalyst **18** was the only metallodendrimer which showed a comparable conversion. It was thus observed that the mononuclear cobalt systems performed slightly better than the dendrimeric systems.

For the copper catalysts it was found that the dendritic systems showed a higher formation of HQ than the mononuclear catalysts in the pH range investigated, the exception being **1** which showed a similar product distribution as the metallodendrimers. In the case of the cobalt catalyst, aside from **9**, which only showed the formation of CT it was observed that the product distribution of the dendritic immobilized catalysts was similar to that of the mononuclear catalysts. For instance at pH 3 the catalysts showed a 1:1.5 HQ to CT ratio, while at pH 6 either none of the two dihydroxybenzenes were produced or a higher selectivity to CT was observed.

4.3   CONCLUSIONS

The catalytic activity of copper(II) and cobalt(II) complexes derived form *N*-(aryl)salicylaldimines as well as those derived from peripheral functionalised dendritic salicylaldimine ligands were evaluated in the hydroxylation of phenol in aqueous media

under pH-controlled conditions. All the catalysts investigated were observed to be active for the oxidation process with the major products detected being HQ and CT. All the catalysts appeared to be more selective towards the formation of CT. In the case of the *N*-(aryl)salicylaldimine copper(II) catalysts a CT:HQ ratio of roughly 2:1 was observed for all catalysts except catalyst **1** which showed a slightly higher formation of HQ producing a CT:HQ distribution of 1.5:1. The copper(II) metallodendrimers also showed a higher formation of HQ resulting in a similar CT:HQ ratio as obtained for catalyst **1**. For the copper catalysts there was no significant pH effect observed in terms of catalyst activity and only a slight pH effect was observed favouring the formation of CT for all catalysts. The cobalt systems however showed a much more significant pH dependence of activity since the activity of the catalysts roughly doubled at pH 6 compared to activities observed at pH 3.
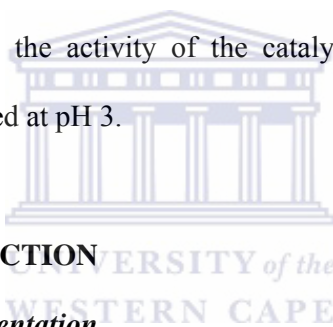
4.4   EXPERIMENTAL SECTION

4.4.1   *Material and Instrumentation*

Phenol, catechol, hydroquinone, benzoquinone and formic acid were purchased from Sigma-Aldrich Ltd and 30 % H_2O_2 (w/w) was obtained from Merck Chemicals Ltd. All chemicals were used without further purification. Oxidation reactions were performed on a 12 place RADLEY's Heated Carousel Reaction Station fitted with a reflux unit as well as a gas distribution system with glass reaction vessels. High-pressure liquid chromatography (HPLC) was performed on a HP 1090 liquid chromatograph equipped with a ZORBAX® C18 column of dimensions 4.6 x 150 mm and a UV detector using a solvent system consisting of 0.1% formic acid (v/v) and acetonitrile. The pH of the buffers was measured at 25 °C using a Metrohm Limited 744 pH meter.

4.4.2   General procedure for the hydroxylation of phenol

A 12 place RADLEY's Heated Carousel Reaction Station fitted with a reflux unit as well as a gas distribution system was used to perform the hydroxylation reactions. In a typical reaction, phenol (1 mmol) and the appropriate catalyst (0.1 mmol) was placed in a 50 mL glass reaction vessel followed by the appropriately buffered solution which was saturated with oxygen (10 mL) for approximately 15 minutes prior to use. The temperature of the reaction mixture was brought to 110 °C under an oxygen atmosphere and the mixture stirred at this temperature for 15 min. A 30% H_2O_2 (w/w) solution (1 mmol) was added and the reaction mixture was stirred at 110 °C under an oxygen atmosphere for a further 6 hours. The reaction mixture was cooled to room temperature and a 1 mL sample withdrawn, filtered through a syringe filter and diluted 20 times. The consumption of phenol and the oxidation products obtained were analyzed by HPLC. Detection of the products was performed with a dual wavelength UV detector (254 and 275 nm). The mobile phase used was a mixture of 0.1% formic acid solution and acetonitrile.

4.5   REFERENCES

1. C. J. Pereira, *Chem. Eng. Sci*. **1999**, *54,* 1959.

2. M. T. Hassenein, S. S. Gerges, M. A. Abdo, S. H. El-Khalafy, *J. Porphyrins Phthalocyanines* **2005**, *9*, 621.

3. D.C. Sherrington, *Pure & Appl. Chem.* **1988**, *60*, 401.

4. H-Q. Zeng, Q. Jiang, Y-F. Zhu, X-H. Yan, X-B. Lang, H-Y. Hu, Q. Liu, W-Y. Lin, C-C. Guo, *J. Porphyrins Phthalocyanines* **2006**, *10*, 96.

5. A. Zombeck, R. S. Drago, B. B. Corden, J. H. Gaul, *J. Am. Chem. Soc*. **1981**, *103*, 7580.

6. A. Haikarainen, J. Siplilä, P. Pietikainen, A. Pajunen, I. Mutikainen, *Bioorg. Med. Chem*. **2001**, *9*, 1633.

7. W. Zeng, Z. Mao, X. Wei, J. Li, Z. Hong, S. Qin, *J. Supramol. Chem.* **2002**, *2*, 501.

8. M. Stiborová, V. Suchá, M. Mikšanová, J. Páca Jr., J. Páca, *Gen. Physiol. Biophys*. **2003**, *22*, 167.

9. S. Ray, S. F. Mapolie, J. Darkwa, *J.Mol Catal. A: Chem*. **2007**, *267*, 143.

10. Kirk-Othmer Encyclopedia of Chemical Technology, 4th Edition, Volume 13, Page 996, Wiley Interscience Publications.

11. J. A. Martens, P. Buskens, P. A. Jacobs, A. V. D. Pol, J. H. C. van Hooff, C. Ferrini, H. W. Kouwenhoven, P. J. Kooyman H. van Bekkum, *Appl. Catal. A:Gen.*, **1993**, *99*, 7.

12. F. Luck, *Catalysis Today* **1999**, *53*, 81.

13. S. S. Lin, C. L. Chen, D. J. Chang, C. C. Chen, *Water Research* **2002**, *36*, 3009.

14. A. Cybulski, J. Trawczyński, *Appl. Catal. B: Environ*. **2004**, *47*, 1.

15. H. Zhang, X. Zhang, Y. Ding, L. Yan, T. Ren, J. Suo, *New J. Chem*. **2002**, *26*, 376.

16. W. Zhu, Y Bin, Z. Li, Z. Kiang, T. Yin, *Water Research* **2002**, *36*, 1947.

17. A. Santos, P. Yustos, A. Quintanilla, F. García-Ochoa, *Topics in Catalysis* **2005**, *33*, 1.

18. A. Dubey, V. Rives, S. Kannan, *J. Mol. Catal. A: Chem.* **2002**, *181*, 151.

19. Y.H. Hue, A. Gedeon, J.L Bonardet, N. Melush, J.B. D'Espinose, J. Fraissard, *Chem. Commun*. **1999,** 1967.

20. C. Liu, Y. Shan, X. Yang, X. Ye, Y. Wu, *J. Catal*. **1997**, *168*, 35.

21. L. Wang, A. Kong, B. Chen, H. Ding, Y. Shan, M. He, *J. Mol. Catal. A: Chem* **2005**, *230*, 143.

22. J.N. Park, J. Wang, K.Y. Choi, W.-Y. Dong, S.-J. Hong, C.W. Lee, *J. Mol. Catal. A: Chem.* **2006**, *247*, 73.

23. Q. Xie, J-Z. Li, X-G. Meng, C-W. Hu, X-C. Zeng, *Trans. Met. Chem.* **2004**, *29*, 388.

24. J. Zhang, Y. Tang, J-Q Xie, J-Z. Li, W. Zeng, C-W. Hu., *J. Serb. Chem. Soc.* **2005**, *70*, 1137.

25. Z-W. Yang, Q-X. Kang, H-C. Ma, C-L. Li, Z-Q. Lei, *J. Mol. Catal. A: Chem.* **2004**, *213*, 169.

26. E. Schön, D.A. Plattner, P. Chen, *Inorg. Chem.* **2004**, *43*, 3164.

27. K.C. Gupta , A.K. Sutar, *J. Mol. Catal. A: Chem.* **2007**, *272*, 64.

CHAPTER 5

CATALYTIC OXIDATION OF CYCLOHEXENE USING SALICYLALDIMINE COMPLEXES AS CATALYSTS

CONTENT

5.1.   INTRODUCTION

As mentioned in Chapter 1, catalysis is one of the key factors identified in developing *greener* chemical processes to diminish environmental impact and improve sustainability of current industrial chemical processes [1]. Recent years have thus seen considerable research efforts to develop suitable immobilized catalysts especially in the area of oxidation, which are able to utilise cheap oxidants such as hydrogen peroxide and molecular oxygen [2-5]. This strategy addresses two problems viz. catalyst-product separation and waste minimization by utilizing environmentally friendly oxidants. Developing catalysts which are able to produce oxygenated compounds with a high degree of selectivity remains an area of interest due to the complexity of oxidation processes and the limitations in controlling or terminating the oxidation at different stages. Achieving selectivity in the oxidation of organic substrates with peroxides is particularly difficult due to the fact that the reactions proceed via a radical mechanism which is generally described by the Haber-Weiss cycle [6]. Moreover the radical species generated during the oxidation process are highly reactive and thus achieving selective oxidation is not always possible.

The oxidation of cyclohexene has received considerable attention recently. This is most likely due to the propensity of this substrate to under go allylic oxidation as opposed to epoxidation particularly in the presence of peroxides. Cyclohexene is thus often used as a model substrate to investigate the activity and selectivity of transition metal complexes in the oxidation of substrates which typically show preferential attack at the allylic position as oppose to epoxide formation. It has widely been established that the reaction parameters such as the type of solvent, reaction temperature, oxidant to substrate ratio and the nature of the metal has a pronounced impact on the activity of the

catalyst as well as the distribution of the oxidation products. Recent investigations which have focussed on immobilized catalysts have also indicated that the nature of the support has an influence on the activity of the catalyst as well as product distribution.

It has been shown for oxidation processes catalysed by transition metal catalysts that the mechanism of oxygen transfer is very important to achieve selectivity. In order to achieve selective oxygen transfer it has widely been established that generation of an active transition metal intermediate such as the species depicted in Figure 5.1 is required. The mechanistic aspects of selective oxidation via metal-peroxo complexes have been extensively reviewed by Modena, Sherrington and Jørgensen [7-9]. Recently Yudanova also investigated the mechanistic aspects of oxygen transfer with metal-peroxo species using DFT methods [10].

Porphyrins, phthalocyanines and salicylaldimine metal complexes are very capable of generating the metal oxo species, especially in the presence of oxidants such as iodosylbenzene and sodium hypochlorite [11]. In the presence of peroxides these transition metal systems have also been reported to produce the metal-peroxo complex [12]. The ability of the metal to produce these active species generally depends on the ability of the ligand systems to stabilise these active intermediates. This in turn depends on the resistance of the ligand system itself to oxidation.

O‒OR   OR   O

M   M   M   M═O

         O   O   **oxo**

peroxy   **peroxo**
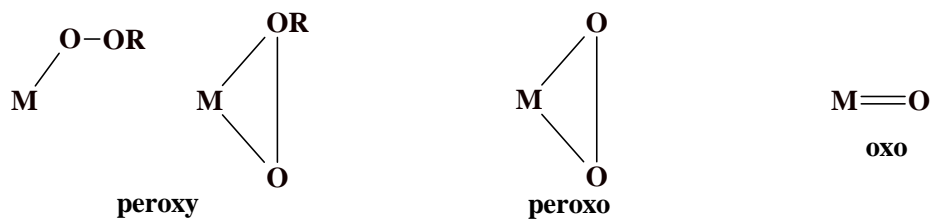
Figure 5.1: Active transition metal intermediates for selective oxygen transfer in oxidation processes.

In this chapter the oxidation of cyclohexene using typical mononuclear Co(II) complexes based on *N*-(aryl)salicylaldimines and multinuclear Co(II) complexes based on peripheral functionalised dendritic salicylaldimines is discussed. The efficiency of the dendrimer immobilized catalysts is also compared against typical mononuclear systems.
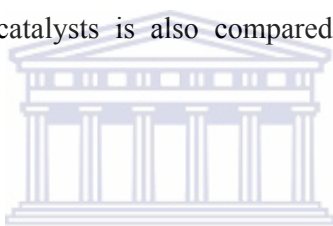
5.2.   RESULTS AND DISCUSSION

The catalytic oxidation of cyclohexene using H_2O_2 as oxidant under an oxygen atmosphere at ambient pressure was investigated using the mononuclear (Fig.5.2) and the multinuclear (Fig 5.8) complexes discussed in Chapter 2 and Chapter 3 as catalyst precursors. Due to the multinuclear nature of the metallodendrimers, the catalytic runs were performed in such a way as to ensure that the metal concentration was the same irrespective of the catalyst used. Initially a preliminary investigation of the mononuclear and dendrimeric cobalt catalysts was performed in acetonitrile, tetrahydrofuran (THF) and neat cyclohexene. This study was conducted under standard conditions which consisted of refluxing cyclohexene (10 mmol), 0.1 mol% Co(II) and 30% (w/w) H_2O_2 (10 mmol) at a temperature of 60°C for 6 hours. However the catalysts only exhibited good activity in THF and in neat cyclohexene and thus

subsequent investigations focused on the performance of the metal complexes in these two reaction media. The standard conditions employed in the preliminary investigation were also utilised to establish a base-line to investigate the effect of reaction parameters such as the oxidant to substrate ratio as well as the metal concentration on the performance of the catalysts as well as the distribution of oxidation products. The consumption of cyclohexene as well as the oxidation products formed in the catalytic runs were analysed and quantified with gas chromatography (GC) using toluene as internal standard. The major products detected under the conditions of analysis for the oxidation process were the oxygenated compounds 2-cyclohexene-1-ol (**2**) and 2-cyclohexene-1-one (**3**) with the epoxide, cyclohexene oxide (**1**) observed as a minor product often in trace quantities (Scheme 5.1).
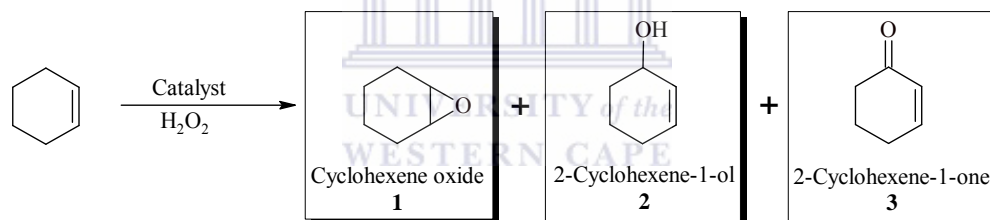
Scheme 5.1: *Oxidation products obtained in the oxidation of cyclohexene.*

5.2.1. *Catalytic oxidation of cyclohexene using mononuclear catalysts.*

The cobalt(II) *N*-(aryl) salicylaldiminato complexes investigated (**9-15**) in the oxidation of cyclohexene showed good activity under the base-line conditions as can be seen from Table 5.1 and Table 5.2 which show the results obtained for reactions performed in neat cyclohexene and THF respectively. Data in these tables also illustrate the effect of changing the cyclohexene to H_2O_2 ratio to 3:1 as well as increasing the Co(II) concentration to 0.2 mol%. The performance of the catalysts under the different

reaction conditions are also graphically represented in Figure 5.3 and Figure 5.4 , which show the activity of the catalyst in neat cyclohexene and THF respectively.

1 : R = H; R$_1$ = H; R$_2$ = H; M = Cu
2 : R = H; R$_1$ = H; R$_2$ = Cl; M = Cu
3 : R = H; R$_1$ = t-Bu; R$_2$ = t-Bu; M = Cu
4 : R = i-Pr; R$_1$ = H; R$_2$ = H; M = Cu
5 : R = i-Pr; R$_1$ = H; R$_2$ = Cl; M = Cu
6 : R = i-Pr; R$_1$ = t-Bu; R$_2$ = H; M = Cu
7 : R = i-Pr; R$_1$ = t-Bu; R$_2$ = t-Bu; M = Cu

9 : R = H; R$_1$ = H; R$_2$ = H; M = Co
10 : R = H; R$_1$ = H; R$_2$ = Cl; M = Co
11 : R = H; R$_1$ = t-Bu; R$_2$ = t-Bu; M = Co
12 : R = i-Pr; R$_1$ = H; R$_2$ = H; M = Co
13 : R = i-Pr; R$_1$ = H; R$_2$ = Cl; M = Co
14 : R = i-Pr; R$_1$ = t-Bu; R$_2$ = H; M = Co
15 : R = i-Pr; R$_1$ = t-Bu; R$_2$ = t-Bu; M = Co
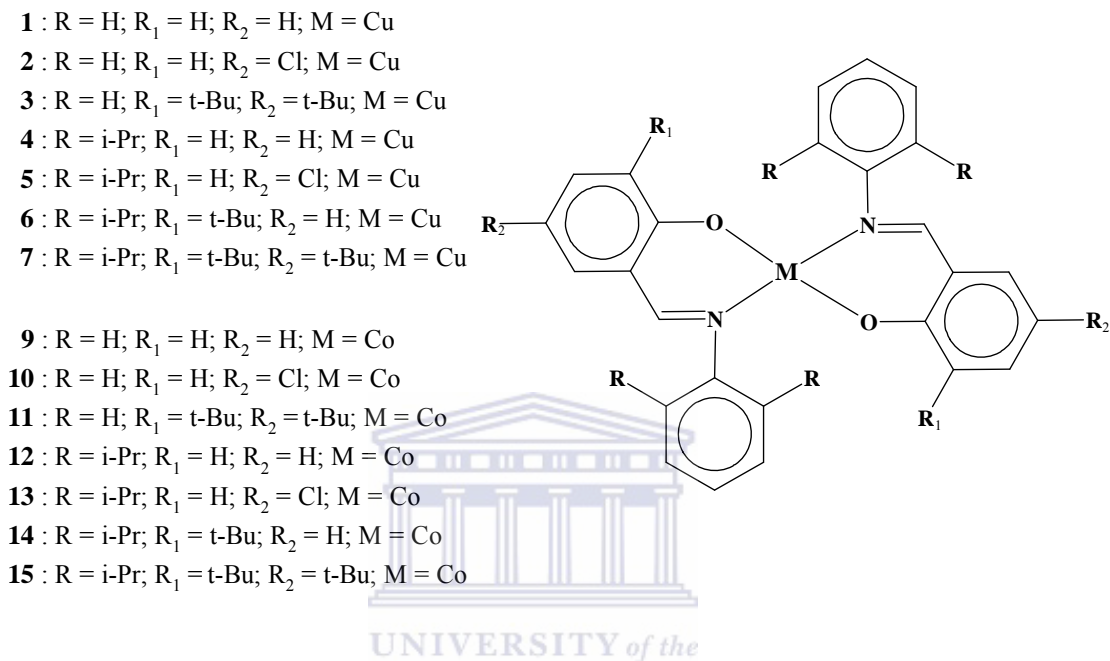
Figure 5.2: Salicylaldiminato metal complexes evaluated in the oxidation of cyclohexene.

5.2.1.1.   *Catalyst activity.*

It can clearly be seen that the catalysts performed very differently under the various reaction parameters in the two reaction media investigated (Fig. 5.3 and Fig. 5.4). In the case where the reactions were carried out in neat cyclohexene the catalysts generally performed the best under the base-line conditions with catalyst **10** being the most active resulting in a substrate conversion of 73%. However the activity of the catalyst when a higher metal loading (0.2 mol%) was used, was only slightly lower than activities observed under the base-line conditions. In fact catalyst **11** showed the same activity

when the reaction was performed with 0.1 mol% Co(II) as when performed with 0.2 mol%. Co(II). It was also observed that catalyst **15** showed slightly better activity with a loading of 0.2 mol% Co(II). Reactions where the oxidant to substrate ratio was reduced to 1:3 showed a significant drop in activity for all the catalysts.

In the presence of peroxides, transition metal catalysts are known to exhibit Fenton type chemistry which can generally be summarized by the two equations in Scheme 5.2 [13]. In the event that the metal is unable to return to its original oxidation state the decomposition of the peroxide is stoichiometric since a catalytic cycle cannot be formed. The catalytic nature of this process thus depends on returning the metal centre to its original oxidation state as described by Equation 5.2.2. For cobalt catalysts the ability of the metal to switch between the oxidation states Co^{II}/Co^{III} is well known and thus the oxidation processes mediated by the cobalt catalysts investigated here are expected to decompose hydrogen peroxide by the equations described in Scheme 5.2.

In the cases where the reactions were performed in neat cyclohexene, the observation that such a significant drop in activity when the hydrogen peroxide to substrate ratio was reduced, suggests that the decomposition of hydrogen peroxide is perhaps largely stoichiometric. The slight drop in activity in the case where 0.2 mol% Co(II) was used could be attributed to catalyst deactivation possibly due to dimerization as a result of the higher catalyst loading. The slightly higher activity observed with **15** is most likely due to the fact that deactivation of the catalyst via dimerization does not occur as readily due to steric constraints imposed by the highly substituted ligand systems. The stoichiometric nature of the decomposition reaction thus also explains the significant drop in activity when the amount of oxidant is reduced. This indicates that for the

oxidation reactions investigated in neat cyclohexene that the decomposition of the hydrogen peroxide is an important step in the oxidation process.

$$H_2O_2 + M^{n+} \longrightarrow HO^{\bullet} + OH^- + M^{(n+1)+} \qquad (5.2.1)$$

$$H_2O_2 + M^{(n+1)+} \longrightarrow HO_2^{\bullet} + H^+ + M^{n+} \qquad (5.2.2)$$
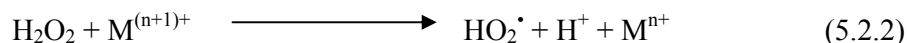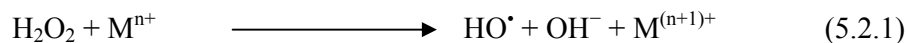
Scheme 5.2*: Metal catalyzed hydrogen peroxide decomposition.*

The oxidation could also be catalyzed by a metal-peroxo species and thus it is possible that the active species in this process are both the radicals produced by hydrogen peroxide decomposition as well as a metal-peroxo complex. In the case of catalyst **15** the higher activity of the catalyst could also possibly be due to the generation of stable metal-peroxo species. However the dependence of the activity of the process on the amount of hydrogen peroxide present indicates that for reactions performed in neat cyclohexene the radical process is perhaps the dominant pathway.
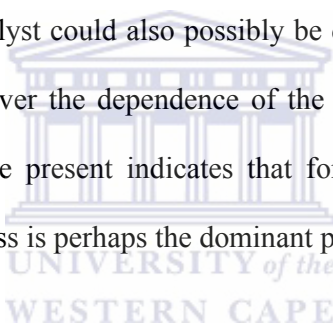
The trend in the performance of catalysts **10**, **12** and **13** when the reactions were studied in THF under the different conditions was essentially the same as that in neat cyclohexene. Catalyst **10** was still amongst the best performing catalysts. However catalyst **13** showed a vast improvement in activity in THF under the base-line conditions as well as under the other conditions investigated. All the other mononuclear catalysts showed deviation from the trend observed in neat cyclohexene. In THF catalyst **15** was observed to be the most active amongst the investigated complexes. The best activity for this catalyst (**15**) was observed with a reduced oxidant to substrate ratio, however the activity observed with the base-line conditions was only slightly lower. In the case of **9** it was found that the complex performed the best with a reduced oxidant to substrate ratio. In addition, for this catalyst, better activity was also observed

with a metal loading of 0.2 mol% than with the lower metal loading of 0.1 mol%. Catalyst **11** exhibited its best activity with a catalyst loading of 0.2 mol% and it was observed that with a oxidant to substrate ratio of 1:3 better activity than with the base-line conditions was obtained. The difference in the performance of the catalyst in THF as compared to neat cyclohexene is possibly due to the better solubility of hydrogen peroxide in the solvent which should allow for easier formation of the metal-peroxo intermediate.

In order to evaluate the effect of the nature of the metal centre on activity and product selectivity copper analogues of the cobalt systems were also investigated. The activities of the copper systems were evaluated by performing the catalytic runs under the same conditions as the base-line reaction used for the cobalt catalysts (10 mmol cyclohexene, 0.1 mol% Cu and 10 mmol 30% H_2O_2 (w/w)) in THF for 6 hours. Results obtained for the catalytic experiments conducted for the mononuclear copper complexes (**1-7**) are shown in Table 5.3.

In general the activity of many of the copper catalysts was observed to be slightly lower than the cobalt analogues. However for catalysts **1**, **4** and **6** slightly better activity was observed than analogous cobalt systems. It is generally expected that the decomposition reaction of hydrogen peroxide with a copper system should be slower since it has a lower redox potential than cobalt. It is known that metals with a higher redox potential switch between oxidation states more easily and thus decomposition of H_2O_2 occurs faster [14]. Thus the observation that comparable activity is observed supports the proposal that in THF oxidation occurs via a metal-peroxo species to a much greater extent than in cyclohexene. Thus the slightly better activity observed with some of the

copper complexes may be due to the fact that the metal-peroxo species formed are slightly more stable than analogous cobalt complexes.

5.2.1.2. *Distribution of oxidation products.*

The oxidation products produced under the different reaction parameters for the reactions performed in bulk was predominantly the allylic oxidation products. Thus the oxidation products formed also indicate that the oxidation proceeds via a radical pathway. The oxidation of cyclohexene via a radical mechanism is well established for peroxide and is expected to occur as depicted by the mechanism shown in Scheme 5.3. However under aerobic conditions this mechanism has also been shown to be operable [15]. Moreover the observed oxidation products could also be formed via a metal-peroxo species as proposed by Mukerjee et al. [16]. Reaction mechanisms which depict the formation of the oxidation products are shown in Schemes 5.4 and 5.5.
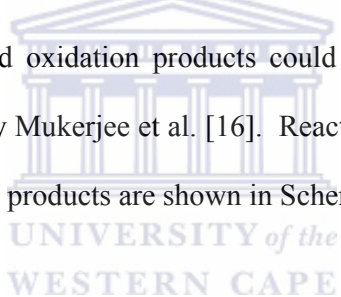
In neat cyclohexene the major product formed was the ketone and only catalysts **11** and **14** were observed to form small quantities of epoxide (Fig. 5.5). When the oxidant to substrate ratio was reduced the catalyst still produced the ketone as major product, however higher levels of alcohol were observed and all the catalysts except **15** produced the epoxide. This indicates that under a reduced hydrogen peroxide content oxidation may also proceed via the metal-peroxo species. When the catalyst loading was increased it was once again observed that higher quantities of alcohol was formed and the formation of the epoxide is also observed for catalysts **10**, **12** and **13**.

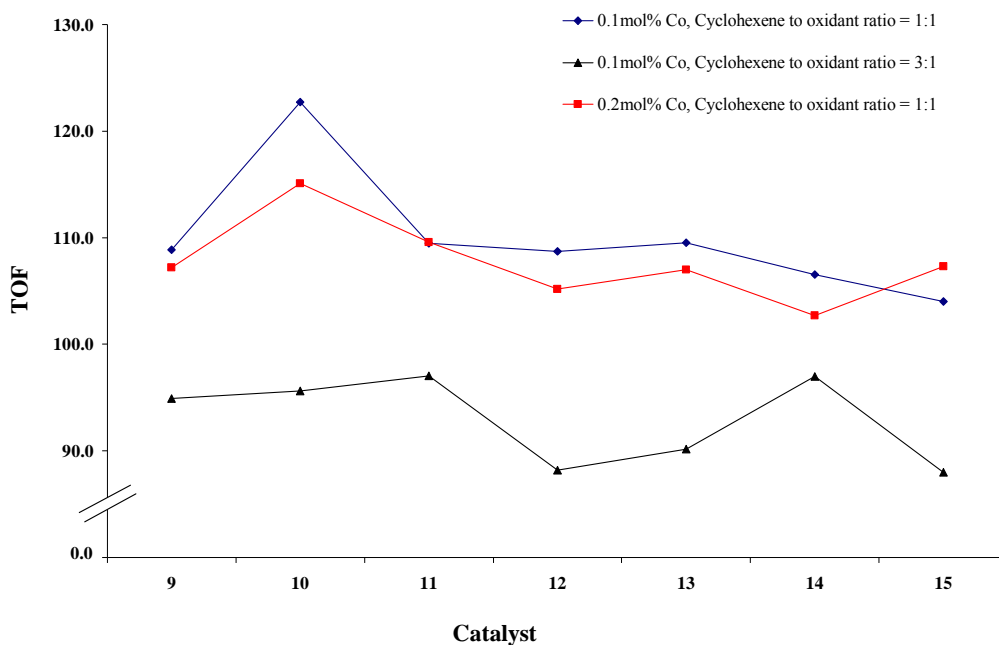***Figure 5.3****: The effect of reaction parameters on activity of catalysts **9-15** for reactions performed in neat cyclohexene.*
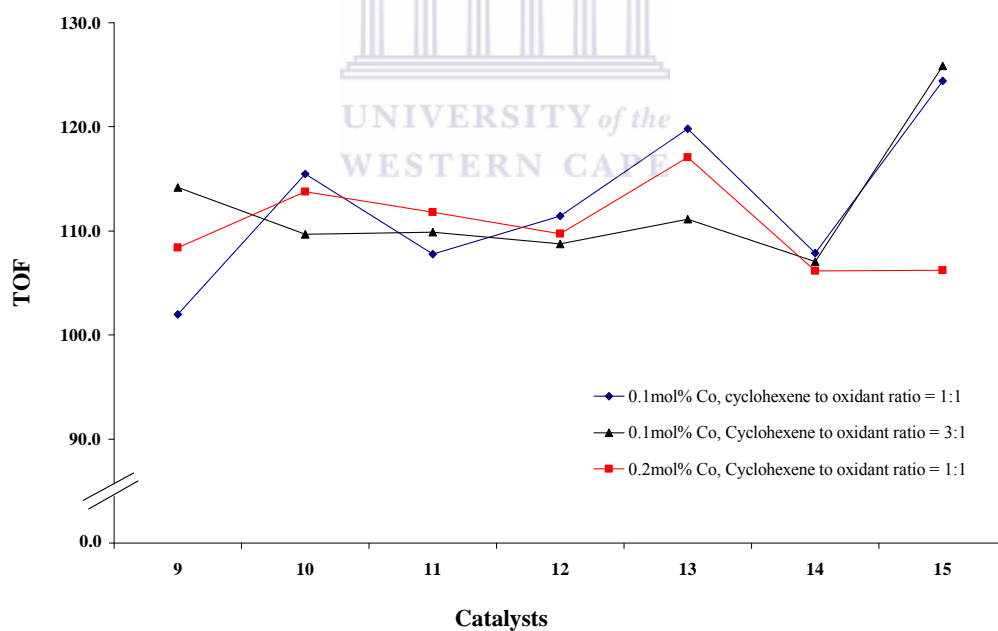

Figure 5.4*: The effect of reaction parameters on activity of catalysts **9-15** for reactions performed in THF.*

Table 5.1: Evaluation of mononuclear cobalt complexes in neat cyclohexene[a].

Entry	Catalyst	%Conversion	%Selectivity			TOF[e]
			Oxide[f]	Alcohol[g]	Ketone[h]	
1[b]		65.3	0	30	70	108.9
2[c]	**9**	57.0	2	27	71	94.9
3[d]		64.3	0	31	69	107.2
4[b]		73.6	0	38	62	122.7
5[c]	**10**	57.4	2	30	68	95.6
6[d]		69.0	1	26	73	115.1
7[b]		65.7	1	27	72	109.5
8[c]	**11**	58.2	4	30	66	97.0
9[d]		65.7	0	30	70	109.6
10[b]		65.2	0	31	69	108.7
11[c]	**12**	52.9	6	35	59	88.2
12[d]		63.1	5	39	56	105.2
13[b]		65.7	0	29	71	109.5
14[c]	**13**	54.1	4	33	63	90.1
15[d]		64.2	2	25	73	107.0
16[b]		63.9	1	24	75	106.5
17[c]	**14**	58.2	4	39	57	97.0
18[d]		61.6	0	39	61	102.7
19[b]		62.4	0	36	64	104.0
20[c]	**15**	52.8	0	45	55	88.0
21[d]		64.4	0	48	52	107.3

[a] Reactions performed in neat cyclohexene at 60°C for 6 hours under O_2 atmosphere (1atm)

[b] 0.1 mol% Co; Cyclohexene:H_2O_2 ratio = 1:1

[c] 0.1 mol% Co; Cyclohexene:H_2O_2 ratio = 3:1

[d] 0.2 mol% Co; Cyclohexene:H_2O_2 ratio = 1:1

[e] TOF = mmol substrate converted per mmol cobalt per hour

[f] Cyclohexene oxide; [g] 2-Cyclohexene-1-ol; [h] 2-Cyclohexene-1-one

Table 5.2: Evaluation of mononuclear cobalt complexes using THF as solvent[a].

Entry	Catalyst	%Conversion	Selectivity			TOF
			Oxide[f]	Alcohol[g]	Ketone[h]	
1[b]		61.2	5	48	47	102.0
2[c]	**9**	68.5	5	41	53	114.2
3[d]		65.0	6	41	54	108.4
4[b]		69.3	5	33	62	115.5
5[c]	**10**	65.8	4	38	58	109.7
6[d]		68.3	6	40	54	113.8
7[b]		64.7	5	39	56	107.8
8[c]	**11**	65.9	5	44	51	109.9
9[d]		67.1	6	47	47	111.8
10[b]		66.9	5	39	57	111.4
11[c]	**12**	65.3	4	43	53	108.8
12[d]		65.8	6	43	51	109.7
13[b]		71.9	4	34	62	119.8
14[c]	**13**	66.7	5	44	52	111.1
15[d]		70.2	6	41	53	117.1
16[b]		64.7	5	37	58	107.9
17[c]	**14**	64.2	5	52	43	107.1
18[d]		63.7	0	59	41	106.2
19[b]		74.6	6	44	50	124.4
20[c]	**15**	75.5	5	52	44	125.8
21[d]		63.7	5	53	42	106.2

[a] Reactions performed using 2 mL THF as solvent at 60°C for 6 hours under O_2 atmosphere (1atm)

[b] 0.1 mol% Co; Cyclohexene:H_2O_2 ratio = 1:1

[c] 0.1 mol% Co; Cyclohexene:H_2O_2 ratio = 3:1

[d] 0.2 mol% Co; Cyclohexene:H_2O_2 ratio = 1:1

[e] TOF = mmol substrate converted per mmol cobalt per hour

[f] Cyclohexene oxide; [g] 2-Cyclohexene-1-ol; [h] 2-Cyclohexene-1one

Table 5.3: Evaluation of copper(II) mononuclear and metallodendritic catalysts in the oxidation of cyclohexene[a].

Catalyst	%Conversion	%Selectivity			TOF[b]
		Oxide[c]	Alcohol[d]	Ketone[e]	
1	62.2	6	53	41	103.6
2	62.3	5	51	44	103.8
3	62.0	0	56	44	103.3
4	68.4	5	46	49	114.0
5	62.2	0	52	48	103.7
6	67.2	5	50	45	112.1
7	62.2	0	54	46	103.6
16	61.5	8	57	35	102.5
17	70.6	12	50	37	117.6
20	61.1	9	55	36	101.8
21	63.9	8	51	42	106.5

[a] Reactions performed using 2 mL THF as solvent at 60°C for 6 hours under O_2 atmosphere (1atm) with 0.1 mol% Cu and a cyclohexene:H_2O_2 ratio = 1:1

[b] TOF = mmol substrate converted per mmol cobalt per hour

[c] Cyclohexene oxide; [d] 2-Cyclohexene-1-ol; [e] 2-Cyclohexene-1one

The distribution of oxidation products supports the proposal that the oxidation process occurs via two different mechanisms simultaneously. In the case of a radical pathway the oxidation products are expected to be primarily ketone and alcohol, whereas for the process via the metal-peroxo species all three oxidation products shown in Scheme 5.2 could be expected.

The oxidation products obtained for the reactions performed in THF were also mostly the allylic oxidation products. However a very different picture is observed when comparing the product distribution under the different reaction conditions to the distribution of oxidation products observed for reactions performed in neat cyclohexene. Under the base-line conditions, as for the neat reactions, the ketone is still observed to

be the major oxidation product. However higher levels of alcohol are observed and all the catalyst are also observed to produce the epoxide. The amount of epoxide produced by the catalysts was observed to be fairly similar. The observed product distribution supports the suggestion that when the reactions are performed in THF the oxidation perhaps proceeds via the metal-peroxo species to a greater extent. The investigation conducted by Mukerjee et al. [16] showed that when the reactions were performed with hydrogen peroxide the ketone was also formed in higher levels than the alcohol due to further oxidation of the alcohol. Thus for the reactions performed in THF it is possible that further oxidation does not occur as readily as when the reactions were performed neat, thus leading to higher levels of alcohol being observed.
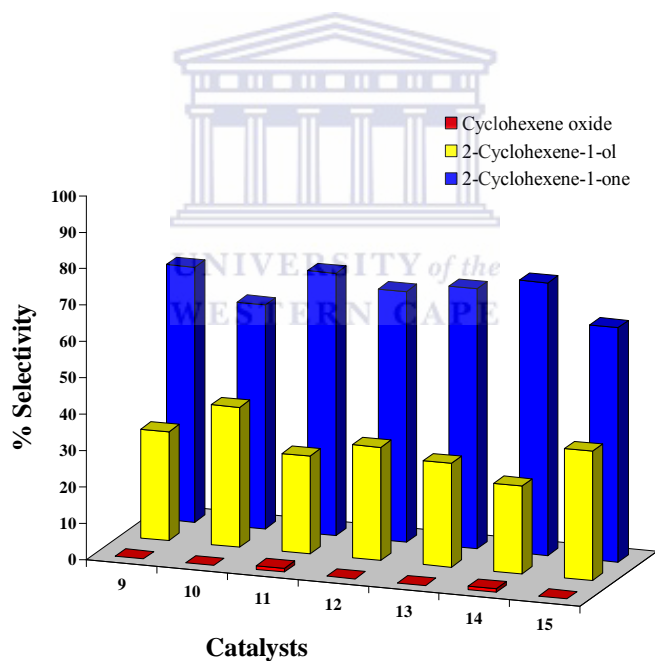

Figure 5.5: Product distributions for mononuclear Co(II) catalysts for reactions performed with 0.1 mol% Co and a 1:1 cyclohexene to H_2O_2 ratio in neat cyclohexene.
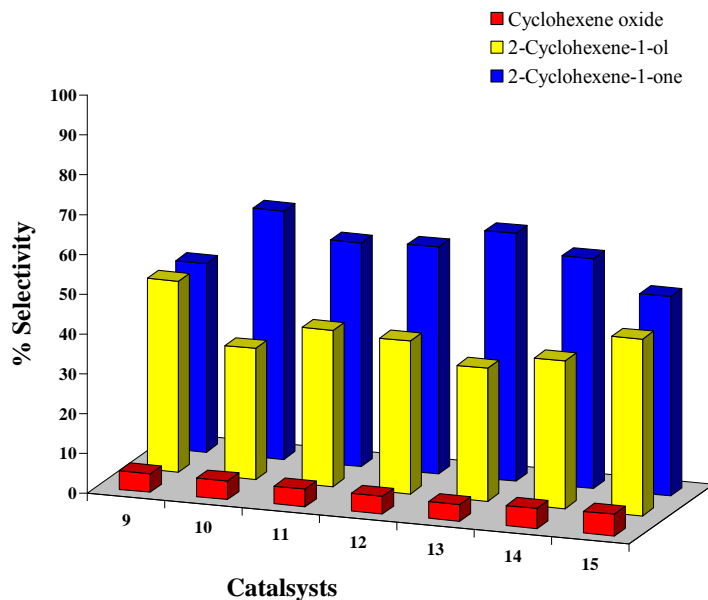
Figure 5.6: Product distributions for mononuclear Co(II) catalysts for reactions performed with 0.1 mol% Co and a cyclohexene to H_2O_2 ratio of 1:1 using THF as solvent.
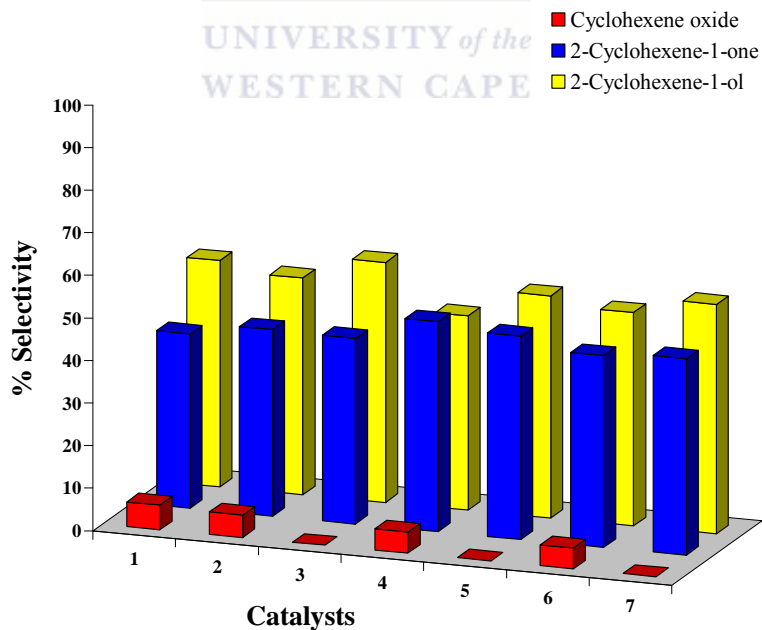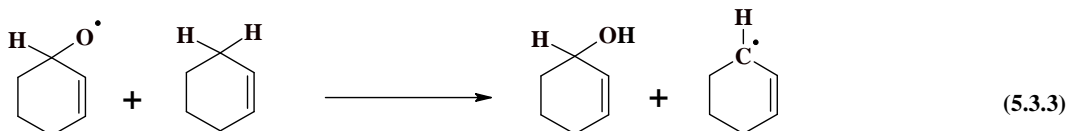

Figure 5.7: Product distributions for mononuclear Cu(II) catalysts for reactions performed with 0.1 mol% Cu and a 1:1 cyclohexene to H_2O_2 ratio using THF as solvent.
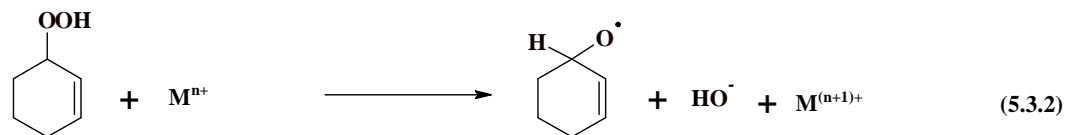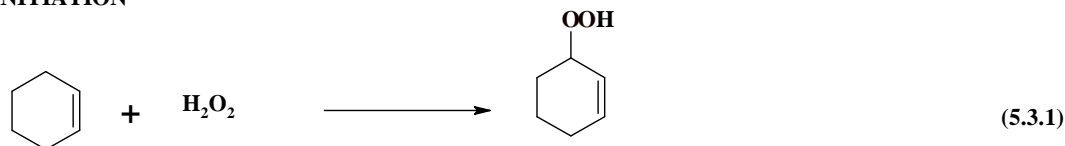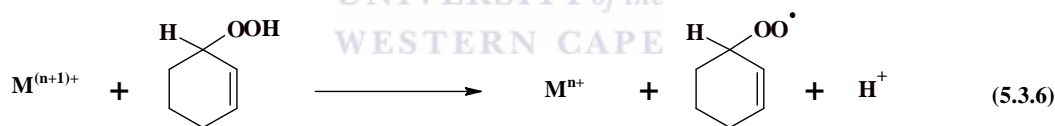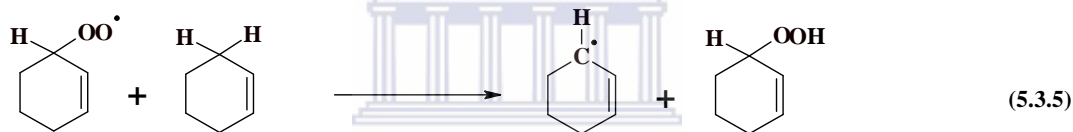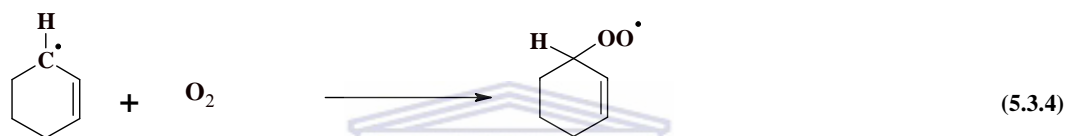
INITIATION

$$ (5.3.1) $$

$$ (5.3.2) $$

$$ (5.3.3) $$

PROPAGATION

$$ (5.3.4) $$

$$ (5.3.5) $$

$$ (5.3.6) $$

TERMINATION

$$ (5.3.7) $$
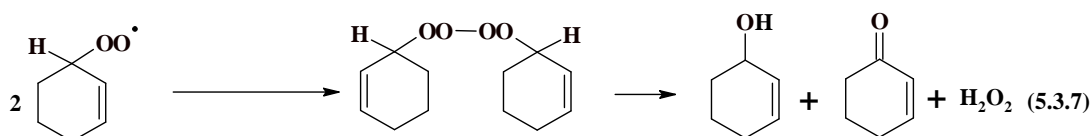
Scheme 5.3: *Free radical mechanism for the oxidation of cyclohexene [15].*

Pathway A

Pathway B

O
N = Salicylaldimine ligand
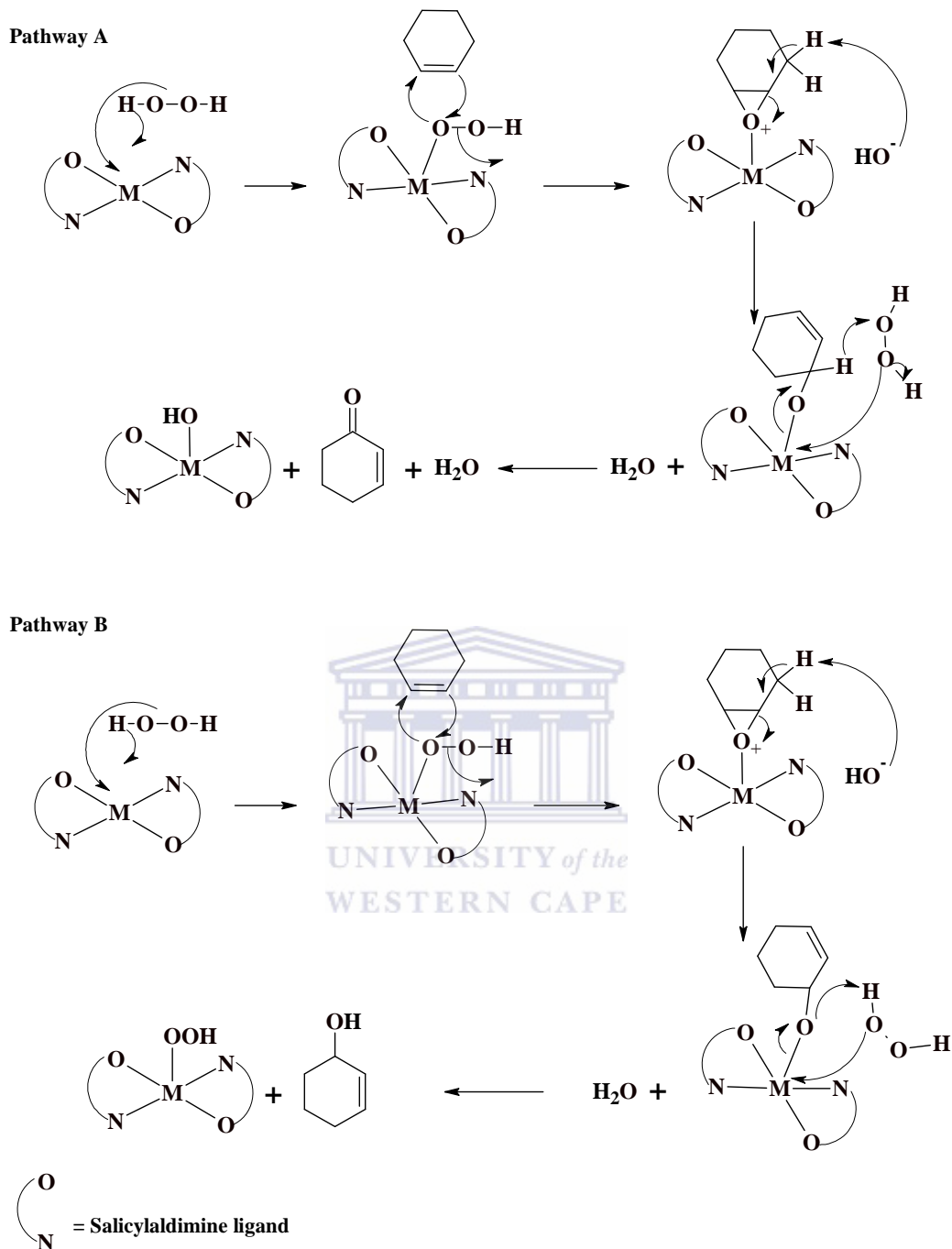
Scheme 5.4: Possible reaction mechanism for the allylic oxidation of cyclohexene which shows the formation of 2-cyclohexene-1-one (Pathway A) and 2-cyclohexene-1-ol (Pathway B) [16].

Pathway C

Pathway D
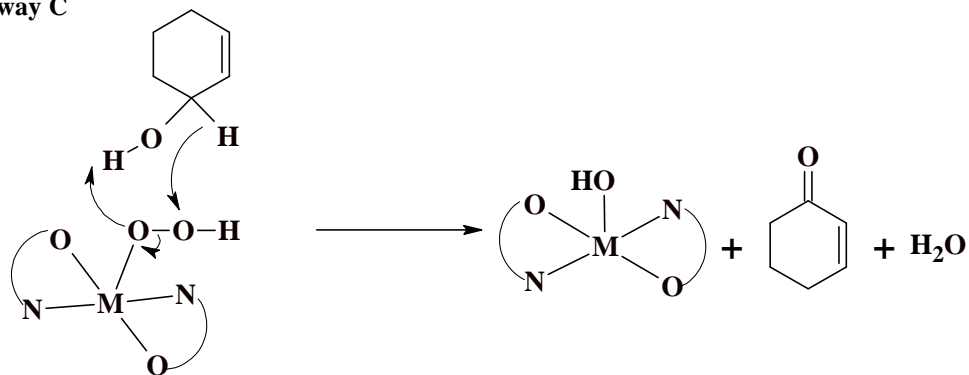
= **Salicylaldimine ligand**
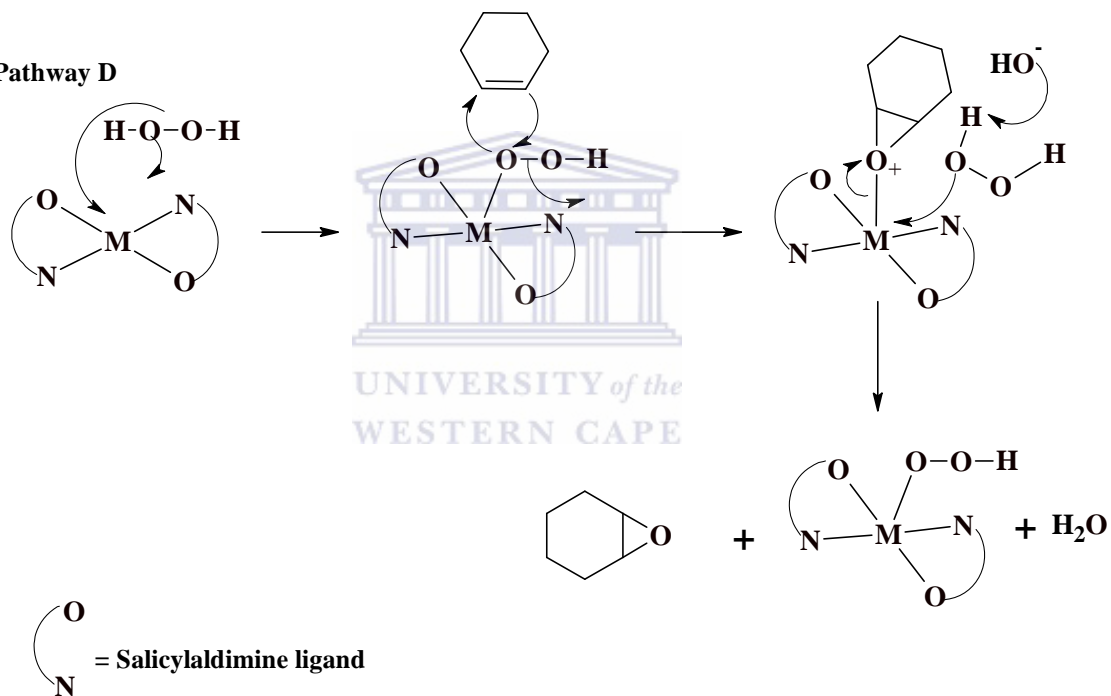
Scheme 5.5: Possible reaction mechanism which depicts the further oxidation of 2-cyclohexene-1-ol to 2-cyclohexene-1-one (Pathway C) and the formation of the epoxide via a metal-peroxo species [16].

In the case where the hydrogen peroxide to substrate ratio was reduced for the reactions performed in THF it was observed that the levels of alcohol formed were higher than for the reactions performed under the base-line conditions. Both catalysts **14** and **15** showed higher levels of alcohol than ketone. When the metal loading was increased the amount of alcohol formed was once again observed to be slightly higher than for the base-line reactions and catalysts **14** and **15** were found to produce higher quantities of alcohol than ketone. Thus as for the neat reactions an increase in the amount of alcohol with changing the oxidant content and metal loading is also observed. However the majority of the catalysts showed roughly the same levels of epoxide. The exception was catalyst **14** which did not show any epoxide formation with a higher metal loading (entry 18, Table 5.2).
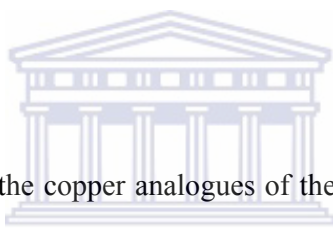
The reaction performed with the copper analogues of the cobalt systems also produced predominantly the allylic oxidation products. However it was observed that the copper catalysts showed better selectivity to the alcohol oxidation product with the ketone being formed to a lesser extent. Several of the catalysts viz. **1**, **2**, **4** and **6** were also observed to produce the epoxide. All three catalysts (**1**, **4** and **6**) which showed slightly better activity than their cobalt counter-parts are amongst the systems producing the epoxide. The distribution of the oxidation products supports the proposal that the oxidation occurs via the metal-peroxo species to a greater extent than the radical pathway. The different product distribution observed is most likely due to the fact that oxidation of the alcohol to the ketone occurs at a much slower rate than with cobalt.

5.2.2.   *Catalytic oxidation of cyclohexene using multinuclear catalysts.*

The Co(II) metallodendrimers were investigated using similar conditions to those utilised in the study conducted with mononuclear Co(II) complexes. As was the case for the mononuclear systems, the metallodendrimers were evaluated using various reaction conditions as well as in different solvents. The solvents investigated were acetonitrile, THF and cyclohexene. The performance of the multinuclear catalysts was observed to be similar to the mononuclear systems. In acetonitrile the catalysts were observed to be completely inactive and while good activity was observed in neat cyclohexene and THF. Thus variation in reaction parameters were also investigated in these two solvents for the metallodendrimers. Results obtained for catalysts **18**, **19**, **22** and **23** which were obtained in cyclohexene and THF are shown in Tables 5.3 and 5.4 respectively.

5.2.2.1.   <u>Catalyst activity.</u>

The activity of the catalysts under the various reaction conditions in neat cyclohexene is graphically represented in Figure 5.9. In the case of catalysts **18** and **22** the optimum activity is observed under the base-line conditions. A decrease in activity is observed when the metal loading is increased to 0.2 mol%. The reverse is observed for catalysts **19** and **23**. For both these catalysts the best activity was observed with a metal loading of 0.2 mol%.

As for the mononuclear catalysts it was found that the cobalt metallodendrimers also show a significant drop in activity with a reduced hydrogen peroxide content. Therefore in the case of the metallodendrimers the activity of the catalysts also appears to be linked to the amount of hydrogen peroxide present. Thus once again it would appear that the decomposition of hydrogen peroxide is largely stoichiometric when the reactions were performed in neat cyclohexene. The mechanism of oxidation thus also

possibly proceeds primarily via a radical mechanism. Investigations conducted by Yang et al. [18] showed Mn PAMAM metallodendrimers to be active for the oxidation of cyclohexene in the neat reaction medium using molecular oxygen as oxidant. Thus it is possible that oxygen also plays a role in the oxidation process for the catalysts investigated in this thesis.

Table 5.4: Evaluation of dendritic cobalt complexes in neat cyclohexene[a].

Entry	Catalyst	%Conversion	Selectivity			TOF
			Oxide[f]	Alcohol[g]	Ketone[h]	
1[b]		64.5	0	25	75	107.5
2[c]	**18**	53.6	3	19	77	89.3
3[d]		59.9	0	26	74	99.9
4[b]		61.9	0	31	69	103.1
5[c]	**19**	56.6	7	32	61	94.4
6[d]		64.1	10	30	60	106.9
7[b]		69.1	0	25	75	115.2
8[c]	**22**	52.4	0	20	80	87.3
9[d]		62.2	19	17	64	103.6
10[b]		60.3	0	28	72	100.5
11[c]	**23**	50.5	4	23	73	84.2
12[d]		64.7	3	21	75	107.8

[a] Reactions performed in neat cyclohexene at 60°C for 6 hours under O_2 atmosphere (1atm)

[b] 0.1 mol% Co; Cyclohexene:H_2O_2 ratio = 1:1

[c] 0.1 mol% Co; Cyclohexene:H_2O_2 ratio = 3:1

[d] 0.2 mol% Co; Cyclohexene:H_2O_2 ratio = 1:1

[e] TOF = mmol substrate converted per mmol cobalt per hour

[f] Cyclohexene oxide; [g] 2-Cyclohexene-1-ol; [h] 2-Cyclohexene-1one

16 : R$_1$ = R$_2$ = H; M= Cu
17 : R$_1$ = R$_2$ = t-Bu; M = Cu
18 : R$_1$ = R$_2$ = H; M= Co
19 : R$_1$ = R$_2$ = t-Bu; M = Co

20 : R$_1$ = R$_2$ = H; M = Cu
21 : R$_1$ = R$_2$ = t-Bu; M = Cu
22 : R$_1$ = R$_2$ = H; M = Co
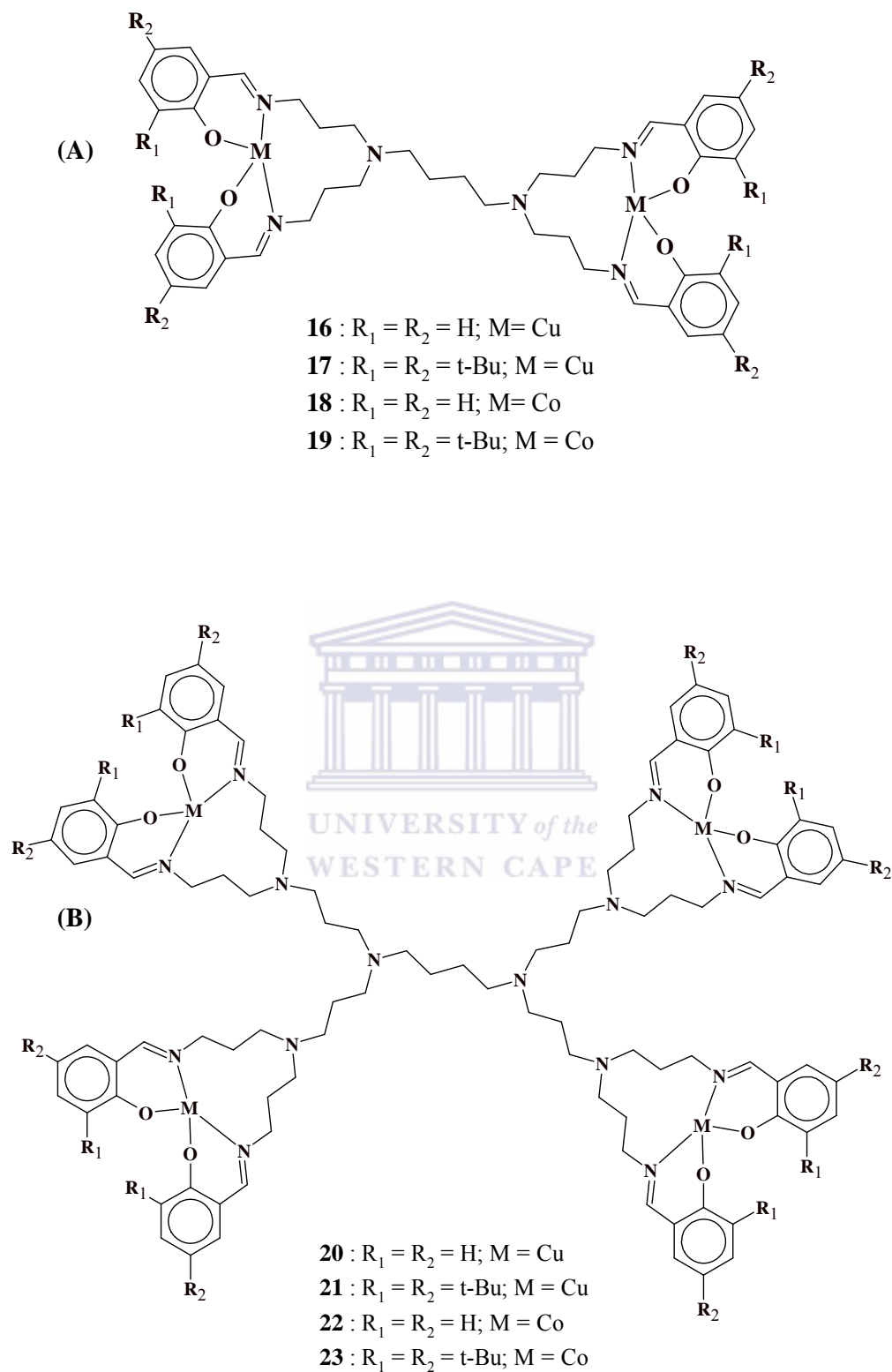**23** : R$_1$ = R$_2$ = t-Bu; M = Co

Figure 5.8*: First (A) and second (B) generation metallodendrimers evaluated in the oxidation of cyclohexene.*

When the reactions were performed in THF the trend in activity of the catalysts were observed to be completely different (Fig 5.12) to the trend observed in neat cyclohexene. It was also found that the catalysts performed much better in THF than in neat cyclohexene. This fact was exemplified by the observation that a conversion of 77% was obtained with catalyst **19** under the base-line conditions. Both G2 catalysts **22** and **23** also exhibit optimum activity under the base-line conditions in THF. Catalyst **18** on the other hand performed the worst of the dendritic catalysts investigated under all the conditions.

Table 5.5: Evaluation of dendritic cobalt complexes using THF as solvent[a].

Entry	Catalyst	%Conversion	Oxide[f]	Alcohol[g]	Ketone[h]	TOF
				Selectivity		
1[b]		64.1	8	40	52	106.8
2[c]	**18**	65.2	4	49	47	108.7
3[d]		67.7	8	43	49	112.9
4[b]		77.8	0	29	71	129.6
5[c]	**19**	72.4	5	39	57	120.7
6[d]		68.8	5	37	58	114.6
7[b]		76.0	4	32	64	126.7
8[c]	**22**	70.4	4	47	49	117.3
9[d]		69.6	4	50	46	116.0
10[b]		71.8	5	35	60	119.6
11[c]	**23**	68.3	4	38	58	113.8
12[d]		63.0	5	40	55	105.0

[a] Reactions performed using 2 mL THF as solvent at 60°C for 6 hours under O_2 atmosphere (1atm)

[b] 0.1 mol% Co; Cyclohexene:H_2O_2 ratio = 1:1

[c] 0.1 mol% Co; Cyclohexene:H_2O_2 ratio = 3:1

[d] 0.2 mol% Co; Cyclohexene:H_2O_2 ratio = 1:1

[e] TOF = mmol substrate converted per mmol cobalt per hour

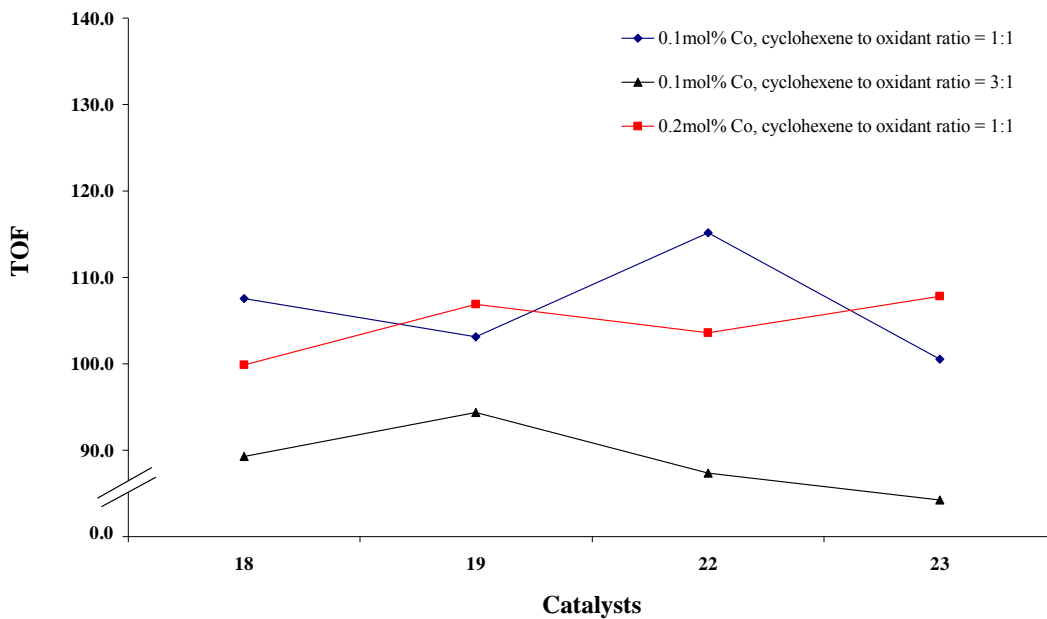[f] Cyclohexene oxide; [g] 2-Cyclohexene-1-ol; [h] 2-Cyclohexene-1one

Figure 5.9: The effect of reaction parameters on activity of dendritic catalysts for reactions performed in neat cyclohexene.
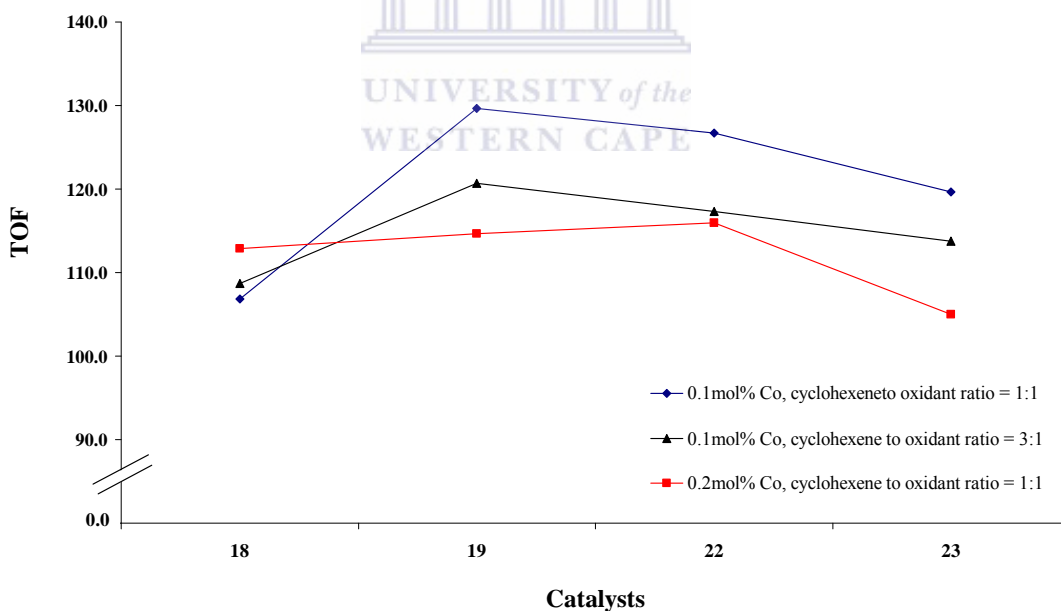

Figure 5.10: The effect of reaction parameters on activity of dendritic catalysts for reactions performed in THF.

In the case where the oxidant to substrate ratio was reduced the activities of the catalysts were lower than those observed under the base-line conditions, however virtually the same trend in activity was observed with catalyst **19** still performing the best. It was found that many of the catalysts showed the lowest activity when the metal loading was increased to 0.2 mol%. In addition it was observed that there is a distinct change in the trend in the activity of the catalysts for reactions performed in THF as compared to those carried out in neat cyclohexene. Under the conditions of higher metal loading **22** showed the best activity, while **18** and **19** showed slightly lower activities. Catalysts **23** showed quite a dramatic drop in activity in comparison to its performance under other reaction conditions as compared with the other dendritic systems investigated. The fact that **19**, **22** and **23** showed lower activity with a metal loading of 0.2 mol% is possibly due to the increased solubility of the complexes in THF and thus deactivation in solution plays a much more significant role as compared to when the reactions were performed in neat cyclohexene, where the solubility of the complexes were relatively poor in comparison.

In order to investigate the influence of the metal centre on the activity of the catalyst, copper analogues were also investigated under the base-line conditions in THF. Results obtained for these complexes are shown in Table 5.3. As for the mononuclear copper catalysts it was found that the copper metallodendrimers were also slightly less active than their cobalt counter-parts. The best activity was observed with catalyst **17**, the copper analogue of cobalt catalyst **19**, which exhibited the best performance under similar conditions amongst the metallodendrimers investigated. The activity of G1 and G2 catalysts **16** and **20** were roughly the same, while catalyst **21** performed slightly better than these two catalysts. Thus in the case of the metallodendrimers it also

appears that the reaction possibly proceeds via the metal-peroxo species since only a slight drop in activity to their cobalt counter part was observed. As mentioned previously, copper has a lower redox potential than cobalt and thus the copper catalysts are expected to decompose H_2O_2 slower since it is known that metals with higher redox potentials switch between oxidation states more easily and thus decompose H_2O_2 faster.

5.2.2.2. *Distribution of oxidation products.*

As was the case for the mononuclear catalysts the major product using the dendritic catalysts were observed to be the ketone and alcohol, although in some instances the epoxide is also observed. The distribution of the oxidation products observed for the base-line reactions are shown in Figure 5.11 and Figure 5.12 for reactions performed in cyclohexene and THF respectively. In the case of the neat reactions only ketone and alcohol were observed with none of the catalysts producing the epoxide under the base-line conditions. Thus the product distribution supports the idea that the oxidation proceeds largely via a radical pathway.

However for reactions performed in bulk when the oxidant to substrate ratio was reduced to 1:3 all the catalysts except **22** produced the epoxide which suggests that with a low oxidant content the oxidation possibly proceed via pathway C as shown in Scheme 5.5 to a greater extent. In the case where the catalytic reactions were performed with a higher metal loading all the catalysts except **18** produced the epoxide. For catalyst **22** the amount of epoxide produced was observed to be slightly higher than the amount of alcohol produced (entry 9, Table 5.3). Thus the distribution of oxidation products obtained for reactions performed in neat cyclohexene with a metal loading of

0.2 mol% also suggests that pathway C (Scheme 5.5) occurs to a greater extent under these experimental conditions.

The product distribution for the reactions performed in THF also showed the ketone to be the major product under the base-line conditions, however catalysts **18**, **22** and **23** also formed the epoxide. However when the oxidant ratio was reduced and the metal loading was increased the levels of alcohol formed were observed to increase for all the catalysts. This may possibly be due to fact that further oxidation of the alcohol to the ketone may not occur as readily under these conditions. The copper metallodendrimers produced the alcohol oxidation product in slightly higher quantities than the ketone. This was also the case for the mononuclear copper catalysts. The copper metallodendrimers were also observed to produce the epoxide in levels slightly higher than what was observed for the mononuclear systems.
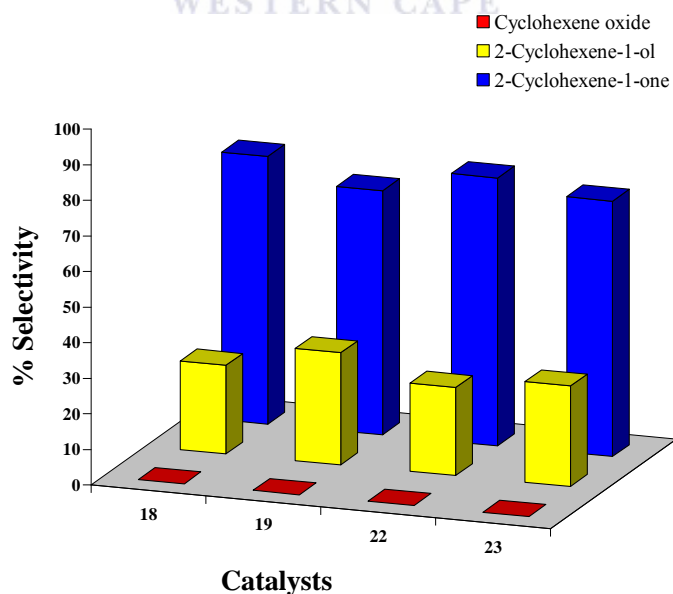

Figure 5.11: *Product distributions for Co(II) metallodendritic catalysts for reactions performed with 0.1mol% Co and a 1:1 cyclohexene to H$_2$O$_2$ ratio in neat cyclohexene.*

160

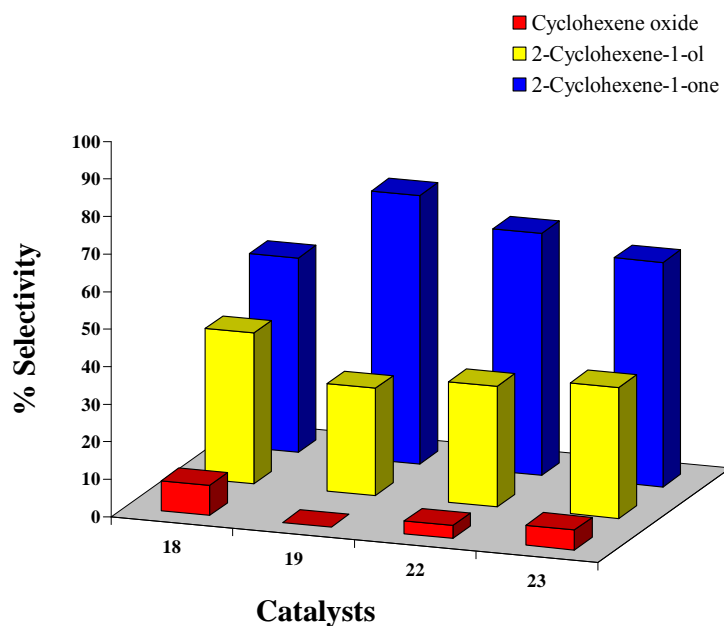***Figure 5.12****: Product distributions for Co(II) metallodendritic catalysts for reaction performed with 0.1 mol% Co and a 1:1 cyclohexene to H$_2$O$_2$ ratio using THF as solvent.*
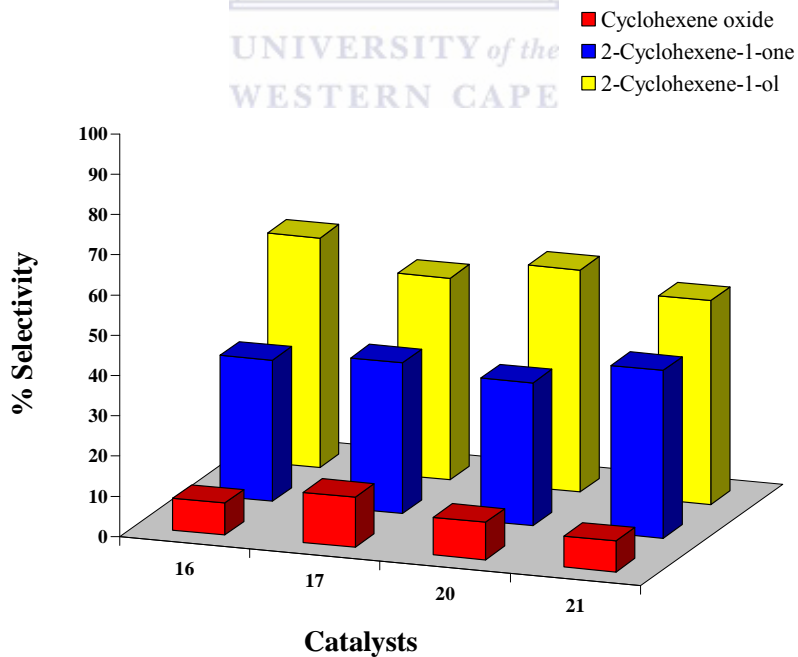

Figure 5.13*: Product distributions for Cu(II) metallodendritic catalysts for reactions performed with 0.1 mol% Cu and a 1:1 cyclohexene to H$_2$O$_2$ ratio using THF as solvent.*

5.2.3.   The effect of solvent on catalyst activity and selectivity.

The activity of the mononuclear and dendrimeric metal complexes was observed to be significantly different in the reaction media investigated. The inactivity of the metal complexes in acetonitrile could possibly be due to coordination of the solvent to the metal centre which thus prevents the formation of the active oxidation species. It has also been shown by Niasari et al. [19] that the solvent has a profound effect on the activity of salen based catalysts in cyclohexene oxidations. It was shown that the efficiency of the catalysts in the different reaction media decreased in the order cyclohexene > dichloromethane > chloroform > methanol > acetonitrile. A similar observation was made by Kanmani et al. [20] for the epoxidation of cyclohexene, however the study conducted showed benzene to be the best solvent and tetrahydrofuran the worst. The different behaviour of the catalysts in the different reaction media could possibly also be due to the fact that hydrogen peroxide is more soluble in THF and thus the interaction with the metal centre occurs to a greater extent. Alternatively the stability of the metal-peroxo intermediate could be different in the two reaction media. This could lead to a difference in activity of the catalysts and could also account for the difference in the distribution of oxidation products.

5.2.4.   The effect of the nature of the metal on catalyst activity and selectivity.

In general it was observed that majority of the cobalt catalysts performed better than their copper counter-parts. However catalysts **1**, **4** and **6** show slightly higher activity than analogous cobalt complexes investigated under similar conditions. Research conducted by the group of Salavati-Niasari also indicated that the nature of the metal centre is a factor in developing highly activity catalysts in their investigation of

bis(salicylaldiminiato) hydrazone metal complexes in the oxidation of cyclohexene with *tert*-butyl hydroperoxide [19]. A decrease in catalyst activity was observed in the order Mn>Co>Cu>Ni indicating copper(II) analogues also showed lower activity than cobalt systems. A similar trend was also observed by Karandikar et al. in a study which investigated the activity of Cu and Co catalysts in the oxidation of olefins with *tert*-butyl hydroperoxide [21].

The nature of the metal also appears to have an effect on the type of oxidation products formed. Both mononuclear and multinuclear copper systems show the preferential formation of the alcohol oxidation product as can be seen from Figure 5.7 and Figure 5.13. Studies conducted by Mukerjee et al. with copper systems also showed higher selectivity to the alcohol when hydrogen peroxide was used as oxidant [16]. It was also observed that the alcohol was subsequently converted to the ketone as the reaction progressed. However when tert-butyl peroxide was used the ketone was observed to be the preferred product. It thus possible that the oxidation of the alcohol to the ketone occurs to a lesser extent in the case of the copper catalysts or alternatively the rate of oxidation of the alcohol to the ketone might be slower.

5.2.5. *The effect of the catalyst immobilization on catalyst activity and selectivity.*

Several investigations have shown that improved catalysts activity is often observed when comparing immobilized catalysts with their homogeneous counter-parts. This improved performance is widely attributed to site-isolation of the coordination systems thus minimizing certain deactivation pathways of the catalysts.

In general only a slight difference in activity was observed in the activities of the mononuclear catalysts and dendritic immobilized systems. In addition it was found that the two different classes of coordination systems exhibit similar trends in activity when the reactions were performed in cyclohexene. Both mononuclear and multinuclear catalysts showed a significant drop in activity with a low oxidant to substrate ratio, while only a slight difference in activity was observed when the metal loading was increased from 0.1 mol% to 0.2 mol%. However when the reactions were performed in THF the trend in activity observed for the mononuclear catalysts appeared to be different to that observed for the metallodendrimer catalysts. It was also observed that the mononuclear systems showed slightly better activity than the dendritic systems when the reactions were performed in cyclohexene.
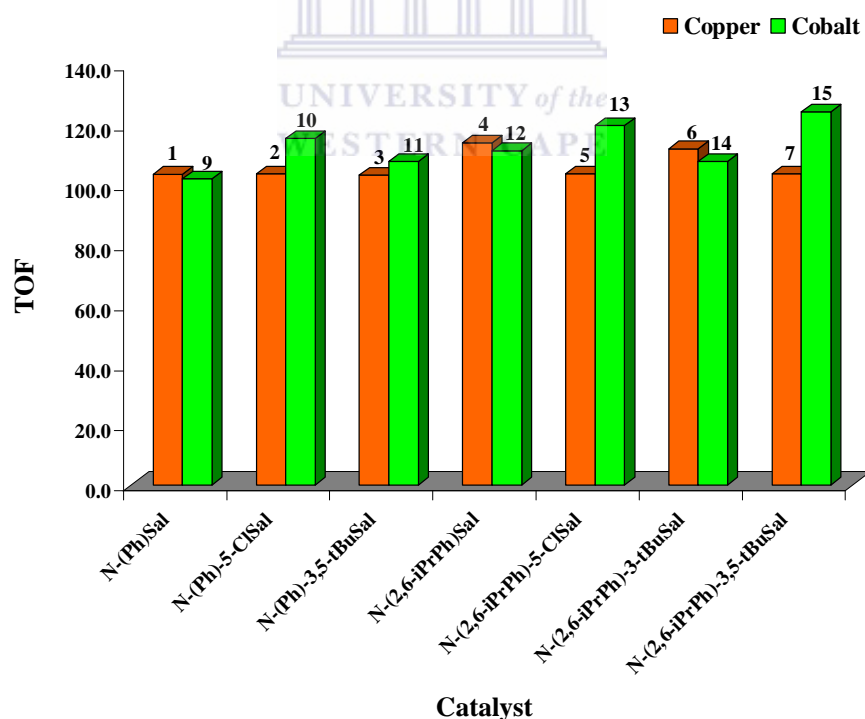

Figure 5.14: *Comparison of the activity of mononuclear Cu(II) and Co(II) complexes.*
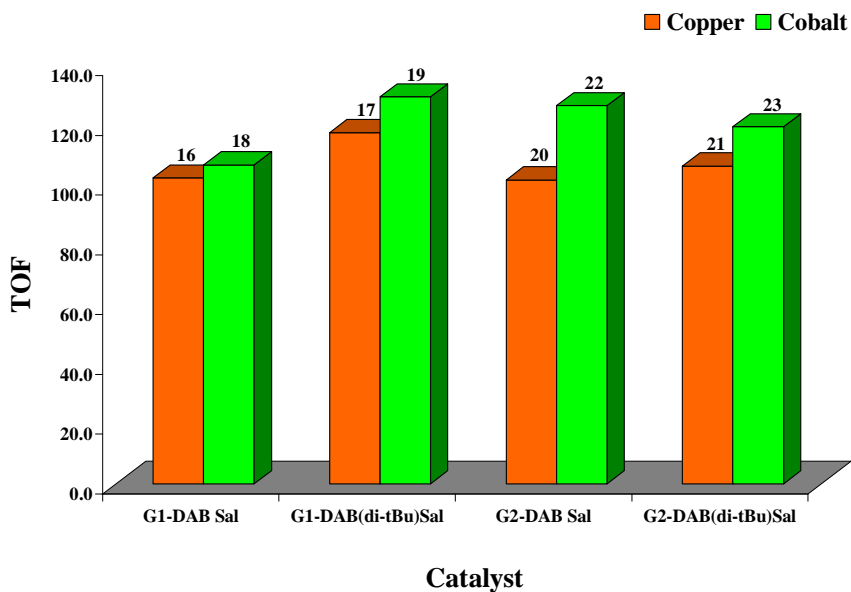
Figure 5.15*: Comparison of the activity of dendritic Cu(II) and Co(II) complexes.*

However the dendritic catalysts on the other hand showed better activity than the mononuclear catalysts when the reactions were performed in THF. This indicates that the influence of the solvent is slightly different for the two classes of catalysts. The superior performance of the dendritic catalysts in THF may allude to the fact the dendritic ligands are able to stabilise the active intermediate to a greater existent than the monofunctional ligands.

A difference in the activity of the two generations of dendrimeric catalysts was also observed. In the case of the unsubstituted G2 metallodendrimers catalysts, **22** exhibited slightly better activity than **18** in both solvents investigated. The exception was observed with a low oxidant to substrate ratio when the reactions were performed in neat cyclohexene. Catalyst **18** shows a slightly higher activity than **22**. The difference in the performance of the two generations may indicate a slight positive dendritic effect for the unsubstituted catalysts with increase in generation. The superior activity of **22** is

possibly due to greater distribution of active sites. However in the case of the *tert*-butyl substituted complexes G1 catalyst **19** showed slightly better activity than G2 system **23** in the two solvents under various reaction conditions. The only instance where comparable activity was observed for **19** and **23** was with a 0.2 mol% metal loading in neat cyclohexene. In this case there appears to be a slight negative effect on activity which might be due to steric interactions in the case of **23**, since the coordination spheres are closer together than in the G1 system and thus the *tert*-butyl groups might prevent the substrate from accessing the metal sites during the oxidation process.

5.3. CONCLUSIONS

It was found that for catalytic experiment performed in acetonitrile the catalysts were completely inactive in this solvent. However all the metal complexes investigated were found to show good activity when the oxidation reactions were performed in neat cyclohexene or in THF. Comparable activity of the catalysts was observed in the reaction media investigated and it was found that the solvent as well as the reaction conditions have an impact on the activity and product selectivity. The major oxidation product formed for all catalysts was 2-cyclohexene-1-one. However it was found that an increase in the formation of the alcohol was observed when the metal loading was increased as well as when the oxidant to substrate ratio was reduced.

5.4. EXPERIMENTAL

5.4.1. *Materials and instrumentation*

Cyclohexene, 2-cyclohexene-1-ol, 2-cyclohexene-1-one were purchased from Sigma-Aldrich Ltd. Cyclohexene oxide was purchased form Fluka. Acetonitrile was purchased

from BDH chemicals Ltd and toluene and 30 % H_2O_2 (w/w) were purchased from Merck Chemicals Ltd. Oxidation reactions were performed on a 12 place RADLEY's Heated Carousel Reaction Station fitted with a reflux unit as well as a gas distribution system with glass reaction vessels. GC analyses were performed on a Varian CP-3800 with a HP PONA column. Oxidation products were identified using authentic samples. Conversion and product yields were determined using toluene as internal standard.

5.4.2.   *Catalytic cyclohexene oxidation*

A 12 place RADLEY's Heated Carousel Reaction Station fitted with a reflux unit as well as a gas distribution system was used to perform the oxidation reactions. In a typical reaction, cyclohexene (10 mmol) and the appropriate catalysts (0.1 mol % M) were placed in a 50 mL glass reaction vessel followed by solvent (2 ml). This reaction mixture was brought to a temperature of 60°C under an oxygen atmosphere (1atm). The reaction mixture was stirred under these conditions for approximately 5 minutes after which the reaction was initiated by adding 30% (w/w) H_2O_2 (10 mmol). The resulting reaction mixture was stirred for a period of 6 hour at 60°C under an oxygen atmosphere (1atm). After this time 1 ml of the reaction mixture was withdrawn which was analysed with gas chromatography using toluene (0.2 ml) as internal standard.

5.5.   REFERENCES

1. P. T. Anastas, M. M. Kirchhoff, T. C. Williamson, *Appl. Catal. A: Gen.* **2001**, *221*, 3

2. Z. P. Pai, A. G. Tolstikov, P. V. Berdnikova, G. N. Kustova, T. B. Khlebnikova, N. V. Selivanova, A. B. Shangina, V. G. Kostrovskii, *Russ. Chem. Bull. Int. Ed.* **2005**, *54*, 1847.

3. M. Zimowska, A. Michalik-Zym, J. Połtowicz, M. Bazarnik, K. Bahranowski, E. M. Serwicka, *Catal. Today* **2007**, *124*, 55.

4. M. Cardoso, A. R. Silva, B. de Castro, C. Freire, *Appl. Catal A: Gen.* **2005**, *285*, 110.

5. K. C. Gupta, A. K. Sutar, *J. Mol. Catal. A:Chem.* **2008**, *280*, 173.

6. D. E. De Vos, M. Dams, B. F. Sels, P. A. Jacobs, *Chem. Rev.* **2002**, *102*, 3615.

7. F. Di Furia, G. Modena, *Pure & Appl. Chem.* **1982**, *54*, 1853.

8. D. C. Sherrington, *Pure & Appl. Chem.* **1988**, *60,* 401.

9. K. Jorgensen, *Chem. Rev.* **1989**, *89*, 431.

10. I. V. Yudanova, *J. Struct. Chem.* **2007**, *48*, S111.

11. E. N. Jacobsen, L. Deng, Y. Furukawa, L. E. Martínez, *Tetrahedron* **1994**, *50*, 4323.

12. M. Selke, M. F. Sisemore, J. Selverstone-Valentine, *J. Am. Chem. Soc.* **1996**, *118*, 2008.

13. C. Masters, *Homogeneous Transition-Metal Catalysis: A Gentle Art* **1981**, Chapman & Hall, London, 172.

14. S. Seelan, A. K. Sinha, *Appl. Catal. A: Gen.* **2003**, *238*, 201.

15. R. Wang, Z. Duan, Y. He, Z. Lei, *J. Mol. Catal. A: Chem.* **2006**, *260*, 280.

16. S. Mukherjee, S. Samanta, B. C. Roy, A. Bhaumik, *Appl. Catal. A: Gen.* **2006**, *301*, 79.

17. Z-W. Yang, Q-Z. Kang, H-C. Ma, C-L. Li, Z.-Q. Lei, *J. Mol. Catal. A: Chem.* **2004**, *213*, 169.

18. M. Salavati-Niasari, A. Amiri, *Appl. Chem. A: Gen.* **2005**, *290*, 46

19. A. S. Kanmani, S. Vacheesan, *J. Mol. Catal. A: Chem.* **1999**, *150*, 95.

20. P. Karandikar, K. C. Dhanya, S. Deshpande, A. J. Chandwadkar, *Catal. Commun.* **2004**, *5*, 69.

CHAPTER 6

SUMMARY

___

Chapter 1 of this thesis provides a brief literature survey of the current status of the application of salicylaldimine metal complexes as homogeneous catalysts as well as heterogenised catalysts. Several different classes of salicylaldimine complexes are discussed and their use in a range of catalytic applications are summarized in this chapter. In addition this chapter also provides a brief overview of the strategies employed to immobilized salicylaldimine catalysts as well as the application of these immobilized systems in some catalytic processes. This part of the thesis thus provides some background for one of the main objectives of this research project viz. the investigation into the use of previously unexplored salicylaldimine complexes as homogeneous as well as dendrimer immobilized catalysts in two catalytic processes (phenol hydroxylation and alkene oxidation) with the intent of identifying suitable catalysts for *greener* chemical processes.

Chapter 2 describes the synthetic approach to several new salicylaldimine ligands and their related metal complexes. From the results reported in this chapter, it can clearly be seen that all ligands and their copper and cobalt complexes have been successfully characterized. Similarly in Chapter 3 the preparation of 8 new dendritic metal complexes is also reported. Once again a comprehensive suite of characterization data for all complexes prepared is presented in this chapter. Characterization techniques employed include, IR and UV-Vis spectroscopy, mass spectrometry, elemental analysis

and thermogravimetric analysis. All of these techniques confirmed the nature of the metal complexes prepared.

Chapter 4 describes the evaluation of the Cu(II) and Co(II) complexes as catalysts in the hydroxylation of phenol to produce catechol (CT) and hydroquinone (HQ). The catalytic reactions were performed in aqueous media over a range of pH values using hydrogen peroxide as oxidant. All the metal complexes evaluated were active for the oxidation process. The Cu(II) complexes were evaluated in the pH range 3-6 and showed good activity producing both CT and HQ, however CT was observed as the major product. Most of the mononuclear Cu(II) catalysts produced CT and HQ in a ratio of approximately 2:1, which is the typical product distribution of copper catalysts reported in literature. However the Cu(II) metallodendrimers exhibited as slightly higher formation of HQ producing CT and HQ roughly in a 1.5:1 ratio. The investigation of the Cu(II) complexes in the pH range showed only a slight influence of the pH on the activity of the catalyst and product distribution. The Co(II) complexes were only investigated at pH values 3 and 6 and were found to be slightly less active than the Cu(II) complexes under these conditions. The Co(II) complexes were also observed to produce both CT and HQ, with CT once again being produced as the major product. However for the Co(II) complexes a much more significant influence of the pH on the activity of the catalysts as well as the distribution of the oxidation products was observed.

In Chapter 5 the performance of the Cu(II) and Co(II) complexes were evaluated in the oxidation of cyclohexene using hydrogen peroxide as oxidant under aerobic conditions. All the catalysts investigated were found to active for the oxidation process producing

the allylic oxidation products 2-cyclohexene-1-one (ketone) and 2-cyclohexene-1-ol (alcohol) as major products and the epoxide, cyclohexene oxide as a minor product or in trace quantities. All the catalysts were observed to produce the ketone in higher quantities than the alcohol. However it was found that the reaction conditions such as the solvent, oxidant to substrate ratio and the metal loading has an influence on the activity of the catalysts and the distribution of oxidation products.

The successful application of the investigated metal complexes in the oxidation of phenol and cyclohexene is thus described, however further optimization of the process conditions is still required and thus future studies should be focused on a more comprehensives study of reaction conditions. In addition, kinetic as well as mechanistic studies to probe the role of the complexes in the processes investigated should also be performed as this will perhaps provide a clearer picture of oxygen transfer to the substrates as well as the nature of the actives species involved in this process for future catalyst development. Future investigation should also include ultrafiltration studies to determine the suitability of the dendrimeric catalysts for continuous catalytic processes.
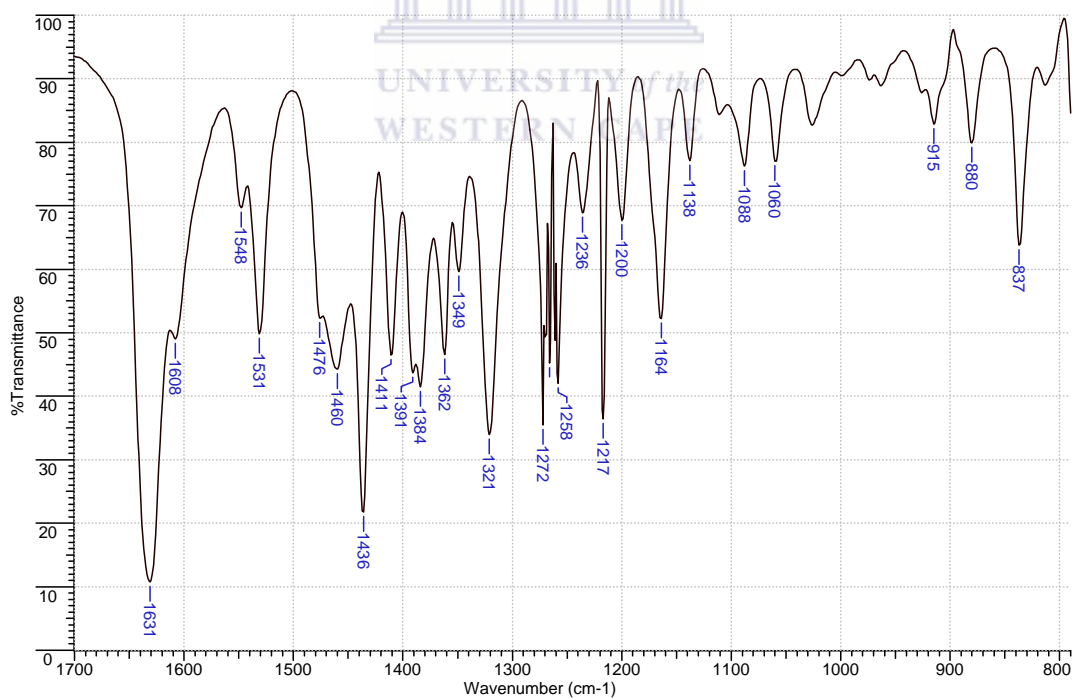
APPENDIX
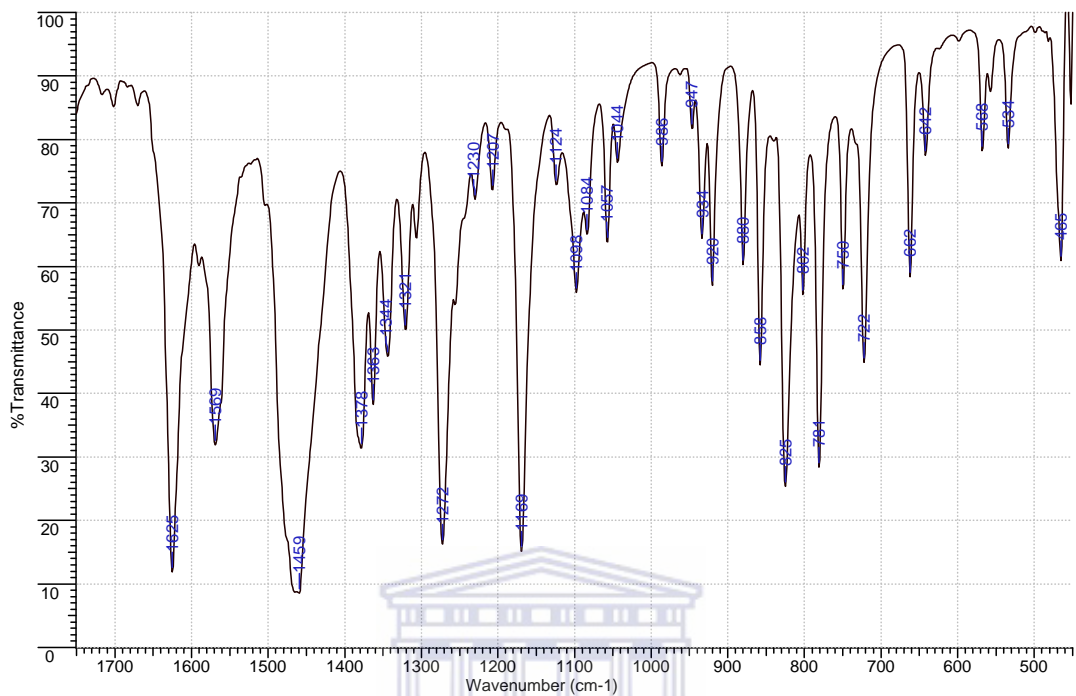
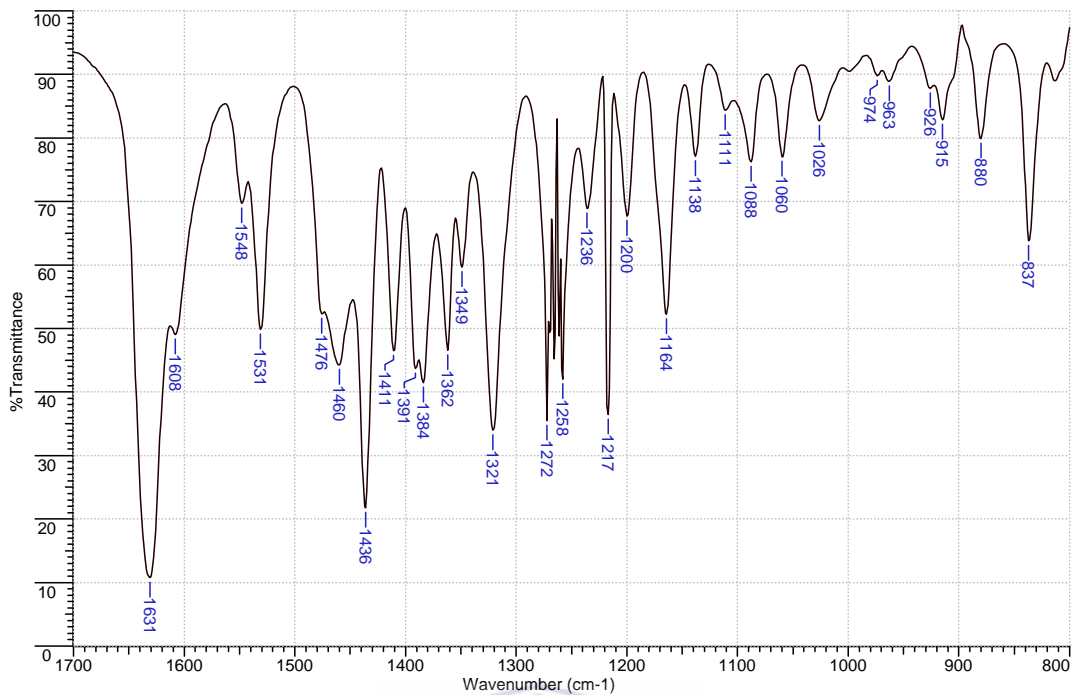*Infrared spectrum of N-(aryl)salicylaldimine ligand **HL**[5]*
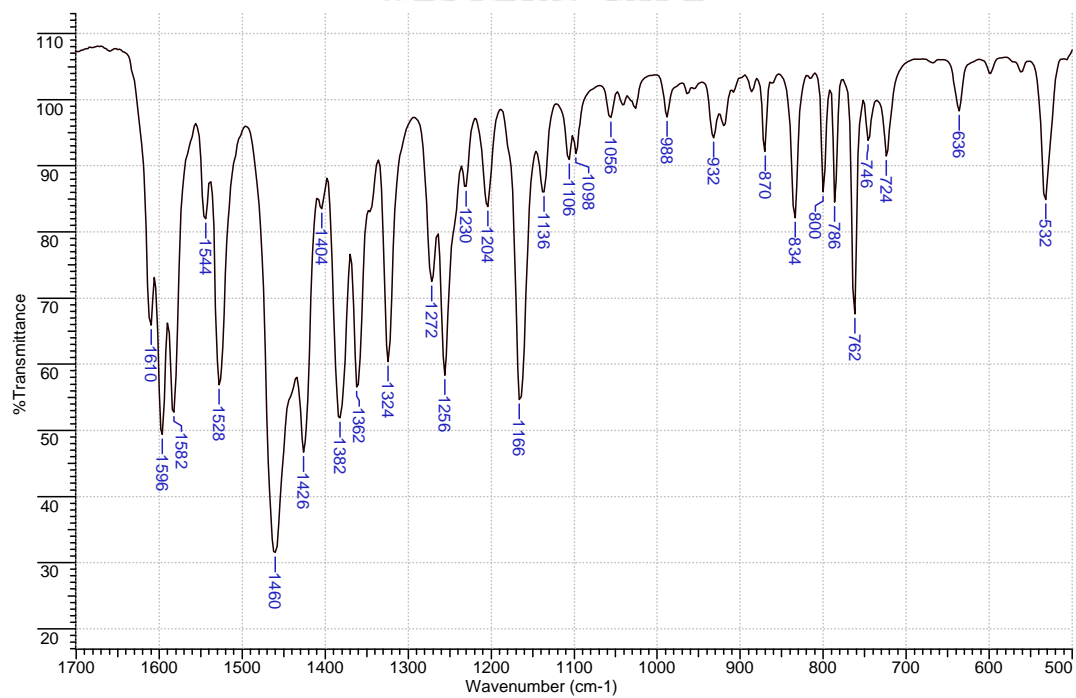
*Infrared spectrum of copper(II) salicylaldiminato complex **7**.*
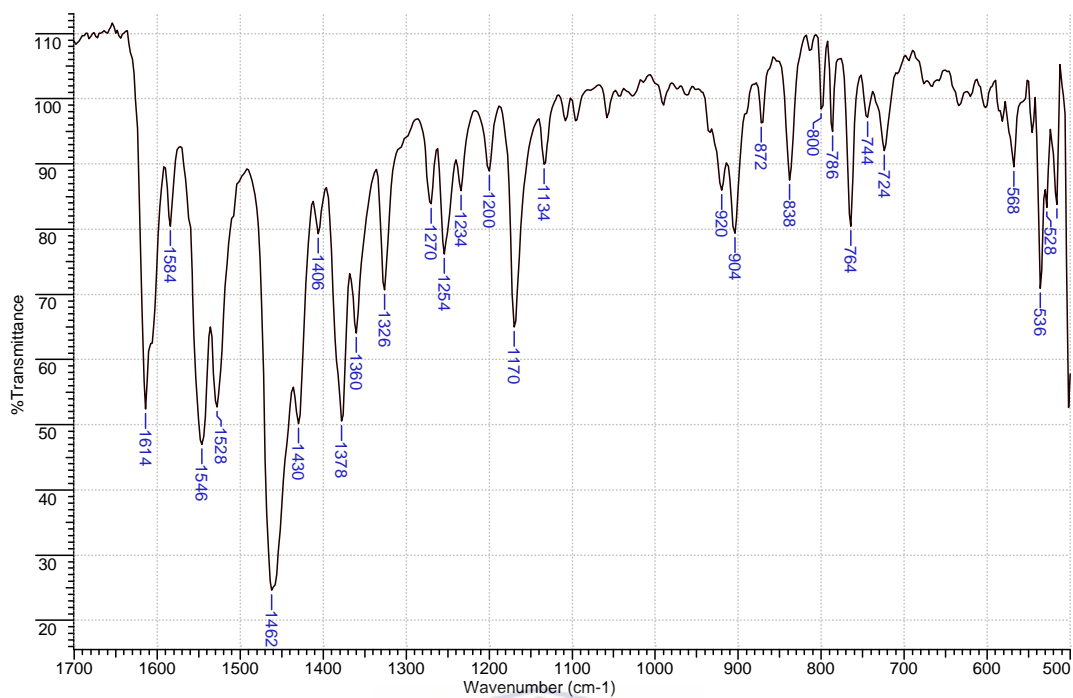
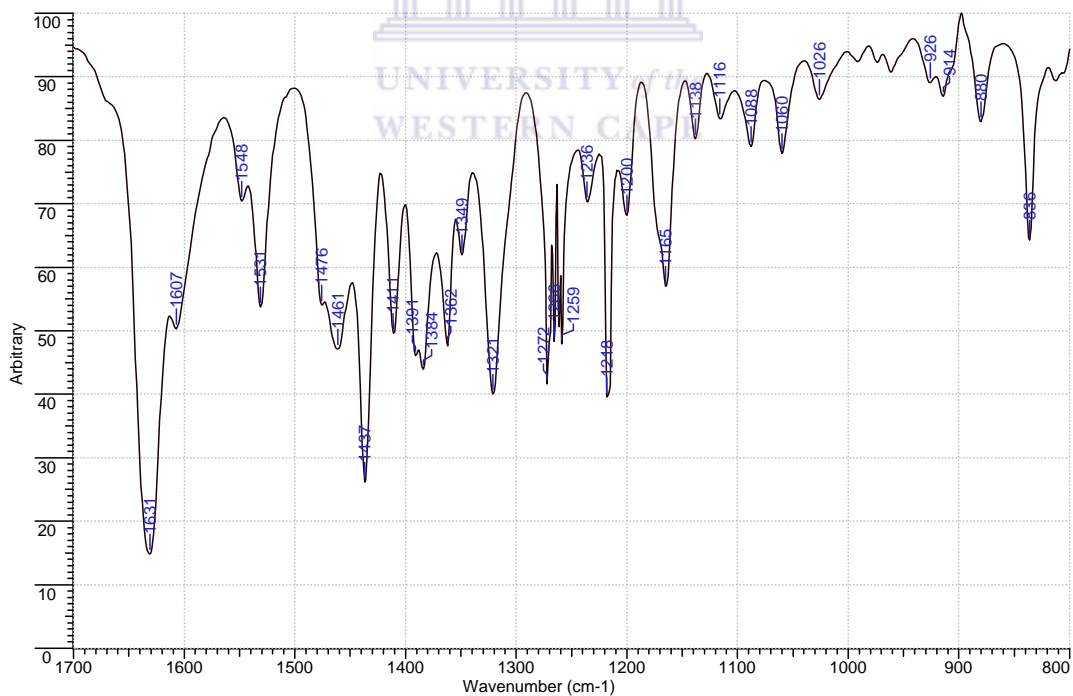*Infrared spectrum of bimetallic copper(II) complex 8.*
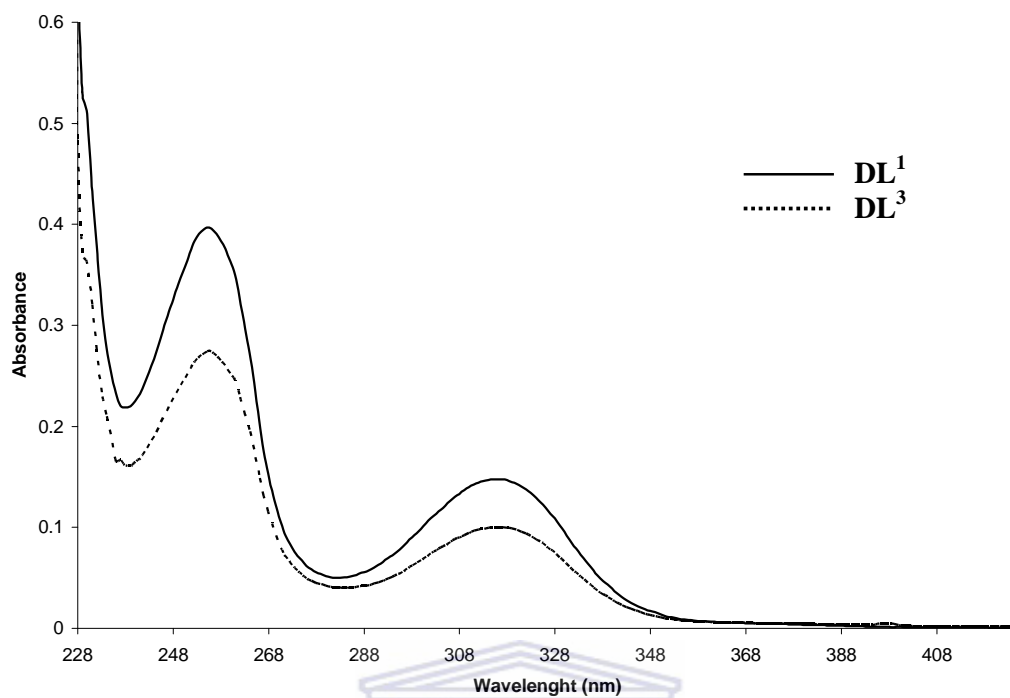

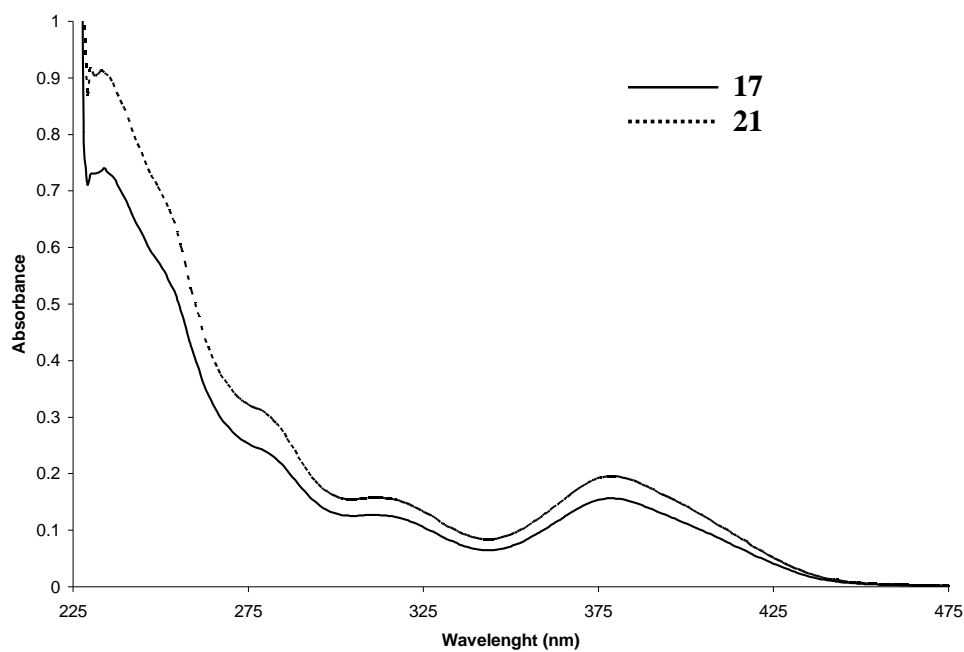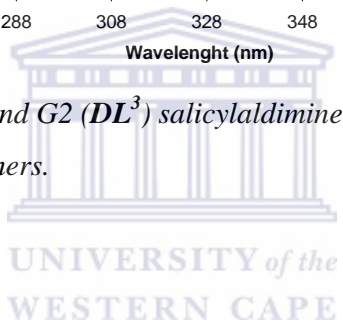*Infrared spectrum of G2 salicylaldimine functionalized poly(propyleneimine) dendrimer*

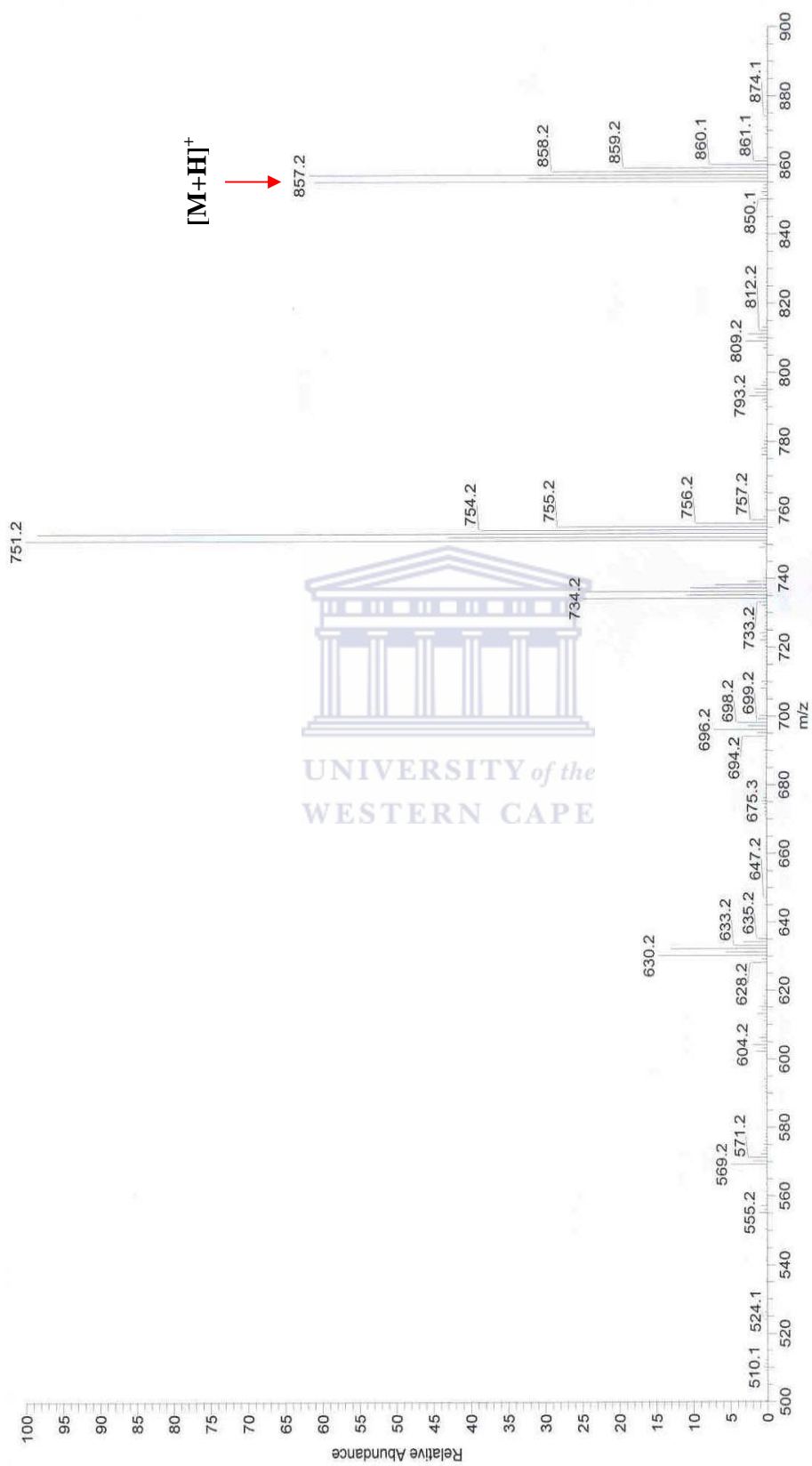*DL⁴.*

Infrared spectrum of G1 cobalt(II) metallodendrimer **19**.

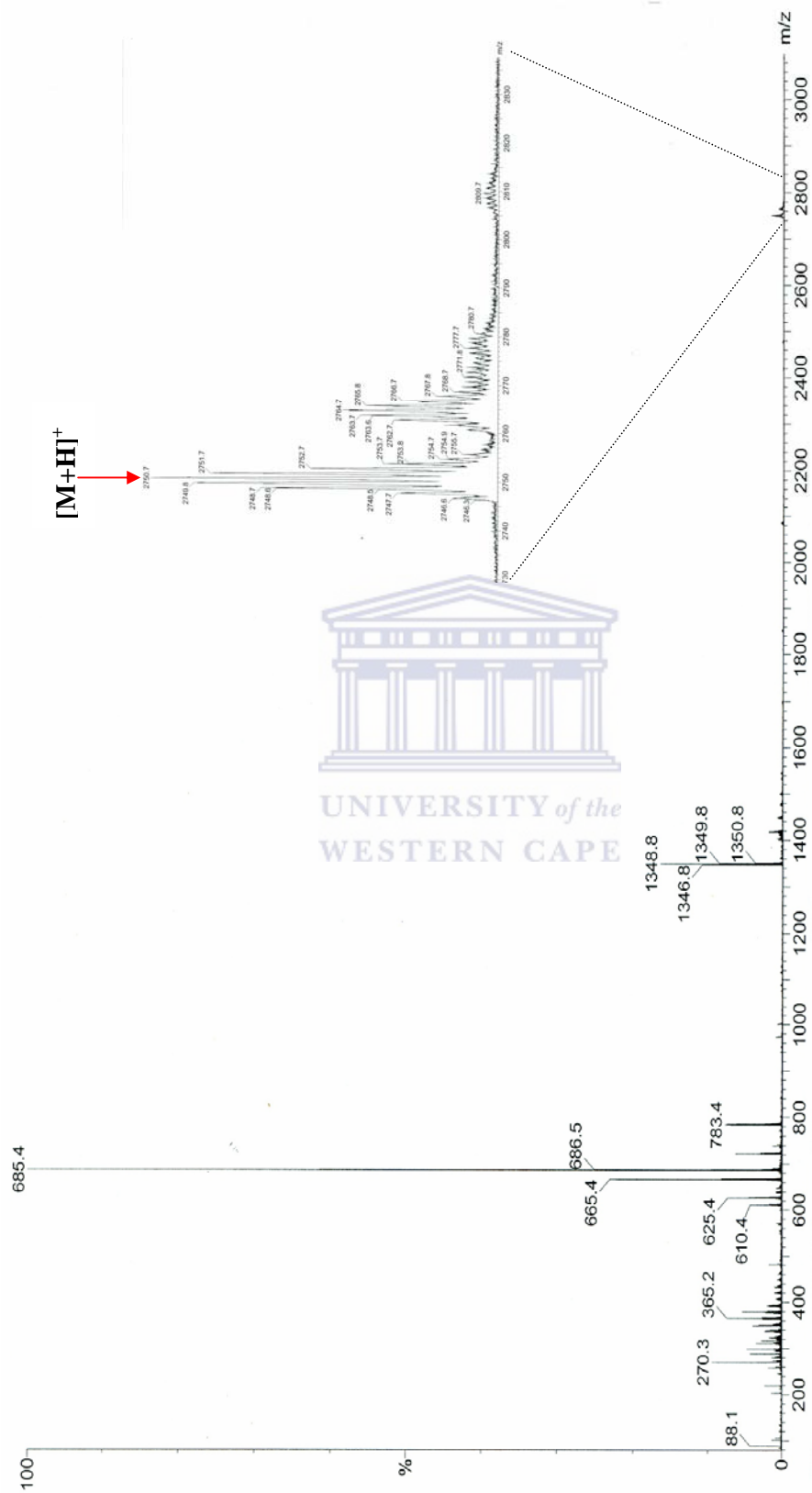*Infrared spectrum of G2 cobalt metallodendrimer* **23**.

*UV-Vis spectra of G1 (**DL^1**) and G2 (**DL^3**) salicylaldimine functionalized poly(propyleneimine) dendrimers.*

*UV-Vis spectra of G1 (**17**) and G2 (**21**) copper(II) metallodendrimers.*

ESI Mass spectrum of G1 copper(II) metallodendrimer 16.

ESI Mass spectrum of G2 copper(II) metallodendrimer 21.